Title

B cell receptor signaling is a critical regulator of IgE responses

Author

Wade-Vallance, Adam Kevin

Publication Date

2023

Peer reviewed|Thesis/dissertation

B cell receptor signaling is a critical regulator of IgE responses

by
Adam Wade-Vallance

DISSERTATION
Submitted in partial satisfaction of the requirements for degree of
DOCTOR OF PHILOSOPHY

in

Biomedical Sciences

in the

GRADUATE DIVISION
of the
UNIVERSITY OF CALIFORNIA, SAN FRANCISCO

Approved:

DocuSigned by:
Jason Cyster
5FFFC327038A40D...

Jason Cyster
Chair

DocuSigned by:
Christopher Allen
DocuSigned by:
K. Mark Ansel
DocuSigned by:
JULIE ZIKHERMAN
D967968925C2437...

CHRISTOPHER ALLEN
K. Mark Ansel
JULIE ZIKHERMAN

Committee Members

Acknowledgements

First, I want to thank Christopher Allen, who has been the most incredible mentor to me throughout my PhD experience. Time and time again, Chris went above and beyond to support me in my career. Whether it was rolling up his sleeves to help me with a massive mouse experiment, or editing my manuscript through to the early hours of the morning, Chris regularly exercised his tremendous work ethic to my direct benefit. Through it all, Chris showed me trust and empathy. He made sure I felt my opinions were valued and allowed me to set my own objectives and timelines. These things together gave me a strong sense of agency, building my confidence and scientific identity. Chris also invested in my scientific skillset. An example of this was in the preparation of our first manuscripts together, where we went back and forth over dozens of drafts as Chris painstakingly taught me the ins and outs of writing an Introduction, or a Discussion, things I had not experienced before. I also enjoyed our many, lengthy conversations. These held innumerable learning moments for me, but were also remarkable in that no matter how pessimistic I might have been feeling heading into them (because of a failed experiment, tricky protocol, or any number of other snags), I always emerged with a renewed sense of hope and direction. I am deeply fortunate to have found my way into Chris' lab.

I also want to thank my earlier scientific mentors who set me on the path towards graduate school. In my first research position at UBC, CK Wong was a superb role model. His work ethic, independence, and absolute scientific rigor impressed and inspired me. Dr. William Gibson, our PI, shared wisdom that remains with me to this day, including such things as "the narrative potential of the human genome" and "stop fidgeting!". At McMaster, I got my first taste of immunology research in Dr. Manel Jordana's lab where I worked closely with Joshua Koenig, who

is now a PI himself. Manel challenged me to invest myself in my work and indulge my interest in science to the fullest. Josh and I connected both over B cells and League of Legends, and he remains my mentor and close friend today. Josh's relentless enthusiasm and unabashed ambition to pursue the most compelling scientific questions continue to inspire me. Both CK and Josh taught me a lot about mentorship and I carried these lessons forward to my own mentees.

Mentoring Rachel Woody, Emily Matcham, Ananya Krishnapura, and Jeremy Libang has been one of the great joys of my PhD. All of them are intensely bright, hard-working individuals and it was impressive to witness the rapidity of their growth. Rachel, Emily and Ananya all came to the lab as undergraduates from UC Berkeley, and assisted me and James with various projects. They each brought a fresh perspective and I enjoyed the challenge of parsing out my thoughts and plans to them in a comprehensible manner. I'm also thankful that they were such good sports with an often-distracted mentor who was really hoping to submit his paper done before they showed up for that first summer and, of course, didn't. Over the course of their second summers in lab, Emily and Ananya grew into truly capable scientific teammates and both made impressive contributions. We were lucky to have Ananya return to the lab following her graduation as a postbac, where her talents and contributions have continued to accelerate.

Of all the members of the Allen Lab, Jeremy was the most directly involved in my experiments. When it was crunch time for my IgE PC JEM paper, Jeremy dropped everything as I put him through a crash course in my cell culture system. He then put in an extreme effort to get critical pieces of my manuscript to the finish line. As an example of the fruits of his efforts, his data makes up a significant part of Figure 3.5 of this dissertation. Those days were a daunting time in my

graduate school career, and I am very fortunate to have had in Jeremy a brother-in-arms. Even as he transitioned towards pursuing his own project, Jeremy was always there to catch any ball that I dropped, and as lab manager he continued to be a tremendous asset to my scientific progress.

I also want to thank all of the other members of the Allen Lab over the years. First James Jung, who is exactly the kind of colleague one wishes to have. He was always friendly and ready with a laugh, but also engaged meaningfully in my work and asked deep questions. I regularly took advantage of his scientific and technical knowledge, especially at the beginning of my PhD but even at the end when he got me up to speed on RT-qPCR and helped me with cell trace violet experiments in Figure 2.3 of this dissertation. At times, we also had similar struggles and successes. We seemed to make similar experimental mistakes which we could share a laugh about and commiserate over. Meanwhile, we both got married during my time in the lab, and so we shared the stories of our ring-hunting, proposal, and wedding-planning journeys.

Although our time together was shorter, I feel lucky to have had the opportunity to work with Karen Chan and Lieselotte Kreuk. Karen's mentorship was instrumental in getting my labwork off the ground, as in my first months she schooled me in cell culture techniques that would become central to my experimental endeavors. While Lies and I did not work as directly together, as a postdoc she was a role model to me and provided me with excellent advice and feedback, including years after she left the lab when she advised me on my postdoc applications. I overlapped with Zhiyong Yang and Marcus Robinson even less and not at all, respectively, but I am grateful to them both for breaking ground on the topics that I would investigate throughout my PhD. Their data and ideas gave me a headstart.

Beyond the Allen Lab, I would be remiss not to thank the broader scientific community in UCSF's Biomedical Science (BMS) PhD program. First of all, my supportive and dedicated thesis committee members Jason Cyster, Julie Zikherman, and Mark Ansel who I always looked forward to presenting to, and who, each time, brought fresh ideas and perspectives that revitalized my experimental directions. These individuals are each emblematic of the friendly and helpful nature of UCSF's BMS faculty, who together create a fantastic and supportive environment for graduate education. I have had too many positive interactions with various BMS faculty to name.

I am also privileged to have worked alongside fantastic and talented cohorts of my peers, who, similar to the faculty they worked under, provided me with excellent feedback, encouragement, and role models. In particular, I am thankful to the individuals in the SABRE and ImmunoX communities who listened to my presentations, took the time to engage with my work, and shared their own fascinating stories. On this note, I am grateful to all of those who gave me the opportunity to speak at meetings. Retreats and conferences, especially those I got to present at, were some of the most enjoyable and scientifically stimulating experiences of my PhD. At multiple important moments these meetings reminded me of the things I love about science.

Of my peers, I am especially grateful to those who became my friends. Although I won't mention them all, I particularly want to thank Raymond Dai who, when asked by a stranger on interview weekend if he'd like to move in together, said yes, and was my fast friend from then on. Relatedly, I want to thank my friends Mark Kelly and Fiona Raymond-Cox, who welcomed me into their home for my first week of rental-hunting in San Francisco and who have hosted me and Idara many times since then.

No doubt the greatest friend I made during my years at UCSF is my now-wife Idara Akpandak. I said all that there is to say about how thankful I am for her earlier this year at our wedding in Vancouver; suffice to say here that she has been my greatest source of support, comfort, and encouragement. I am so lucky to be united with her in Baltimore for the next stage of our careers.

I also want to thank my friends and family scattered around the world who, in their many different ways, worked to maintain our connection across great distances. First, of course, my parents, who I spoke with sometimes daily, especially as I walked or shuttled to/from lab. It was a favourite game to guess whether I was coming or going, as there was often little correlation to the time of day. I also want to thank my brother, Jacob, who regularly reminds me how proud he is of my efforts and who I am tremendously proud of in turn. My late grandfather and Aunt Wendy for many games of Hearts online, and my entire extended family for all of the quality time gathered at Shabbat dinner or Riptide Lagoon Minigolf. Ross, Philip, Sean, Jack, Darwin, Evan, Thomas, Sam, and many more for all of the hours playing online games, and Drew, Grace, Ryan, Cambria and many others including those at UCSF's Board Games Club for all of the hours of board games. I love games, and time spent playing them with good people kept me sane.

These years at UCSF have been simultaneously some of the most challenging and happiest of my life. While the difficulty was inevitable, the happiness was not, and I will never forget the people who worked day-by-day to keep me excited about science, brighten my mood, or provide sober advice. Thank you.

Contributions

1. Wade-Vallance, A. K. & Allen, C. D. C. Intrinsic and extrinsic regulation of IgE B cell responses. *Curr Opin Immunol* **72**, 221–229 (2021).

Author contributions: A.K. Wade-Vallance and C.D.C. Allen wrote and edited the manuscript as well as designed and edited the figures. C.D.C. Allen supervised the work.

Usage in this dissertation: Much of Chapter 1, including Figures 1.1 and 1.2, has been revised from this paper.[1]

2. Wade-Vallance, A. K. *et al.* B cell receptor ligation induces IgE plasma cell elimination. *J Exp Med* **220**, e20220964 (2023).

Author contributions: A.K. Wade-Vallance, Z. Yang, and C.D.C. Allen designed the experiments. Z. Yang performed initial phosflow and apoptosis experiments. J.B. Libang performed most inhibitor experiments and assisted with several other experiments. A.K. Wade-Vallance performed the remainder of the experiments. M.J. Robinson characterized the BLTcre mice and grew the R1E4 hybridoma. D.M. Tarlinton supervised the generation of the BLTcre mice. C.D.C. Allen supervised the research. A.K. Wade-Vallance and C.D.C. Allen analyzed the data and wrote the paper.

Usage in this dissertation: Chapter 3 has been reproduced in its entirety from this paper.[2] Furthermore, I used this paper as a starting point to prepare the Chapter 2 Methods section.

B cell receptor signaling is a critical regulator of IgE responses

Adam Wade-Vallance

Abstract

The cause of allergic disease has been an enigma for millennia. Likely due to its rarity, IgE was the final antibody isotype to be discovered when it was identified as a potent inducer of allergic reactivity. Recent work from our lab and others has revealed that the IgE B lymphocyte program is markedly different from that of other isotypes, being constrained in its generation and longevity. These constraints likely impede the development of allergy, and therefore regulatory breakdown represents a key candidate for how allergy might emerge. Previous work identified T_{FH}-derived cytokines as well as antigen-independent signaling of the IgE BCR as important regulators of IgE responses. However, our studies revealed that these factors cannot completely explain the extent to which IgE antibody production is actively suppressed. Here, we investigated the role of antigen-driven BCR signaling, both in preventing class-switch recombination to IgE and in eliminating class-switched IgE-secreting plasma cells (PCs, this term is used throughout to encompass all antibody-secreting cells including plasmablasts). The bulk of this investigation was carried out with a variety of murine primary B cell culture assays, including experiments using cell trace violet, CRISPR, pharmacologic inhibitors, cell sorting, and Ca^{2+}-sensitive dyes. Critical observations were validated in human B cell cultures or intact mice. In Chapter 2, we show that BCR stimulation preferentially inhibits IgE class-switch recombination (CSR) in a cell division-independent fashion by reducing ε germline transcript (GLT; a prerequisite for CSR). We found that antigen affinity associates inversely with IgE *in vitro* and *in vivo* and that antigen positively associates with selectivity for inhibition of IgE versus IgG1 CSR. Dose-dependent and IL-21-

synergistic effects of BCR stimulation on IgE CSR were also observed in human cell culture. Meanwhile, in Chapter 3 we demonstrate that IgE and IgM, but not IgG, PCs activate intracellular signaling cascades following antigen exposure. Signaling through the BCR signalosome preferentially eliminates IgE PCs in an affinity-, avidity-, dose-, and time-dependent manner. Using a recently developed transgenic line, we show that selectively impairing BCR signaling in PCs increases IgE PCs *in vivo*. Conversely, BCR ligation by injection of αIgE or cognate antigen acutely eliminates IgE PCs. Overall, these findings establish a new layer of IgE regulation by antigen-driven BCR signaling, providing a mechanism for constraining IgE responses especially towards high-affinity or prevalent antigens.

Table of Contents

List of Figures

List of Tables

Chapter 1: Introduction

In the first century A.D., the Roman philosopher Lucretius observed an enigma that "what is food to one man is bitter poison to others." From then until the first scientific descriptions of hay fever in the 1800s and the first use of the word "allergy" in 1906,[3] little progress was made towards understanding this variable disease. The isolation and discovery of immunoglobulin E (IgE) reported in 1966 began a new era of research into allergic disease.[3] Now, we understand the general mechanics of allergic reactions: most (those within the subset known as type-I hypersensitivities) occur when IgE antibodies, bound on the surface of mast cells and/or basophils by the high-affinity IgE receptor (FcεR1), recognize their cognate antigen. This recognition transduces intracellular signals, resulting in the release of inflammatory mediators, including histamine, which produce the various symptoms of allergic disease ranging from mild (e.g. rhinitis and pruritis) to life-threatening (e.g. airway constriction and anaphylaxis). An incredible feature of this response is its potency: minute quantities of IgE antibodies can sensitize individuals to react to vanishing doses of cognate antigen. Progress has been made in the clinical management of allergic conditions with anti-histamines, epinephrine, allergen immunotherapy, therapeutic antibodies (e.g. dupilomab [anti-IL-4rα] and omalizumab [anti-IgE]), and corticosteroids to name a few. However, no curative therapies for allergic diseases exist. Our inability to develop such therapies may stem from our failure to explain Lucretius' fundamental observation of how some individuals develop allergy while others do not.

A major obstacle to gathering evidence in pursuit of root causes of allergy has been the rarity of IgE antibodies and IgE-producing cells. In particular, IgE-producing cells are so few as to be difficult to reliably detect, not only in healthy humans or mice but even in sensitized ones. Prior

work in the Allen Lab has made possible the specific and reproducible detection of IgE-expressing cells. This advance enabled careful studies which revealed that the IgE B cell response is hamstrung by regulation. CSR to IgE is rare, IgE B cells compete poorly in the germinal center (GC, a site for efficient antibody affinity maturation and the generation of long-lived PCs [LLPCs] and memory B cells [MBCs]), and IgE MBCs and LLPCs have not been reliably detected, underlining the limited longevity of IgE-expressing B lymphocytes. Individual variation in the extent of IgE regulation could determine susceptibility to allergic disease, so by better understanding the mechanisms that constrain the IgE response we may finally begin to build a mechanistic understanding of the pathogenesis of allergy.

T_{FH} as the major direct extrinsic regulators of IgE responses

The emergence of an IgE response begins with B cell activation and CSR to IgE, but this process is tightly controlled, leading to the generation of only small numbers of IgE lymphocytes.[4] IL-4 has long been appreciated as critical to IgE responses.[5] In classical studies of CD4 T cell differentiation in cell culture, T_H1 cells and T_H2 cells were found to produce IFN-γ versus IL-4, which inhibited or promoted IgE production, respectively.[6] For many years thereafter it was thought that T_H2 cells interacted with B cells and were the cellular source of IL-4 that induced IgE CSR. However, over the past two decades, T follicular helper cells (T_{FH}) have emerged as the major subset of T cells that provide help to B cells.[7] Contemporaneously, early IL-4 reporter studies found that IL-4 production in the lymph node was almost exclusive to T_{FH}.[8,9] It was later found that eliminating T_{FH}-derived IL-4 abolished IgE production whereas deletion of the T_H2 master transcription factor GATA3 had a negligible impact on IgE production.[10,11] More recently, an impressive division of labor between T_H2 and T_{FH} cells was revealed in mouse models of

allergic airway inflammation.[12] T_H2 cells were positioned in the lung and produced local IL-4, IL-5, and IL-13, while T_{FH} localized to the mediastinal lymph node where they drove IgE antibody production. Together, this work has established T_{FH} as the major cellular source of IL-4 for IgE CSR.

Recent work highlights that T_{FH} are also critical negative regulators of IgE CSR. Although IFN-γ was considered to inhibit IgE responses, minimal changes in IgE responses were observed in *Ifng* gene-targeted mice.[13] Instead, the cytokine IL-21 appears to be a critical negative regulator of IgE in a broad range of immune responses in mice.[13] T_{FH}-derived IL-21 inhibits IgE CSR by binding to the IL-21 receptor on B cells which then transduces signals through the phosphorylation of STAT3[13] (**Figure 1.1**). This finding is consistent with the early studies of IL-21 receptor (IL-21R)-deficient mice,[14] the observation of high serum IgE in IL-21-deficient and IL-21R-deficient patients,[15] and the detection of *STAT3* mutations in a significant fraction of human patients with hyper-IgE syndrome (HIES).[16] However, these findings were in contrast to some previous human cell culture studies, in which IL-21 augmented IgE production.[17] These studies measured secreted IgE as a proxy for IgE CSR, but IgE secretion would also be affected by B cell proliferation and PC differentiation. Indeed, IL-21 potently stimulates both proliferation and PC differentiation of human B cells.[17] Recent studies of both mouse and human B cells additionally found that the effect of IL-21 on IgE CSR depended on the relative strength of CD40 ligation.[13] In particular, IL-21 inhibited IgE CSR in the context of limiting amounts of CD40 stimulation, whereas this effect was abrogated in the context of strong CD40 stimulation (**Figure 1.1**).[13] These results suggest that past discordant findings on the inhibitory effects of IL-21 on IgE class-switching are likely related to the strength of CD40 stimulation. In addition to the role of CD40, the relative balance of IL-4 and

IL-21 was recently found to be an important determinant of IgE versus IgG1 CSR in both mouse and human B cells.[13]

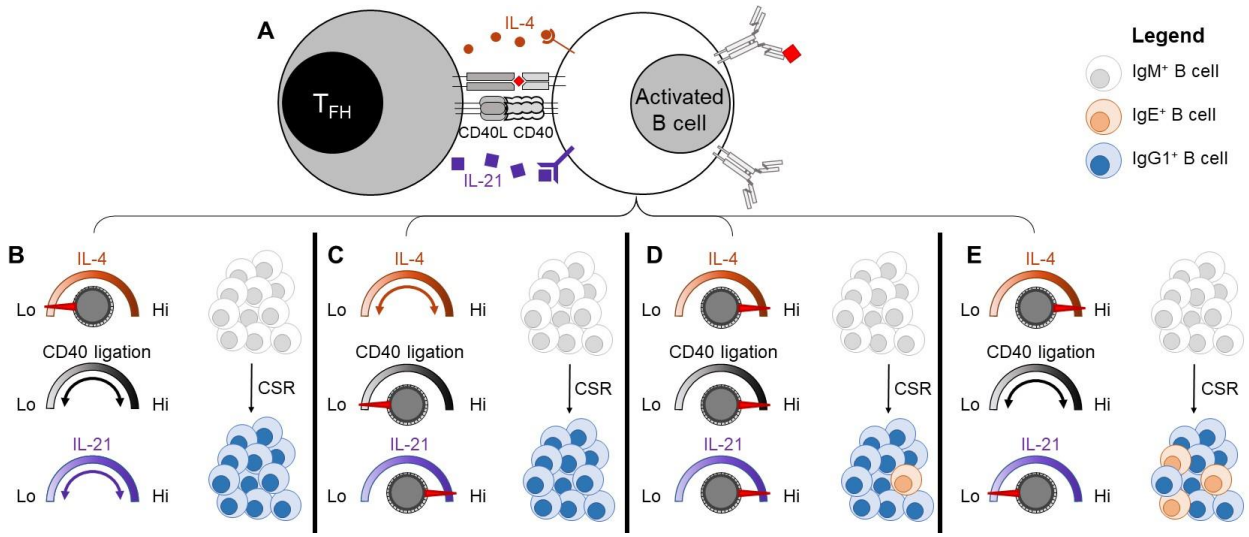

Figure 1.1 The opposing effects of IL-4 and IL-21 on IgE CSR are tuned by the strength of CD40 ligation. (A) Cognate interaction between a T follicular helper cell (T_{FH}) and an activated B cell. The B cell has presented antigen to the T cell and is receiving T cell help in the form of IL-4, CD40 ligation, and IL-21. B-E represent potential outcomes of the T-B interaction. (B) IgE CSR is disfavored in the context of low amounts of IL-4, regardless of the strength of CD40 ligation and the amount of IL-21. (C) IgE CSR is disfavored in the context of high amounts of IL-21 when CD40 ligation is weak, regardless of the amount of IL-4 present. (D) Some IgE CSR may occur despite high amounts of IL-21 in the context of high amounts of IL-4 and strong CD40 ligation. (E) IgE CSR is strongly promoted in the context of high amounts of IL-4 and minimal amounts of IL-21, across a range of the strength of CD40 ligation.

Recent work has identified a specialized subset of T_{FH} cells that, in contrast to most T_{FH}, are capable of expressing the cytokine IL-13.[18–20] These cells have been variably referred to as $T_{FH}2$ or $T_{FH}13$ to denote similarities to T_H2 cells or signify IL-13 production. A portion of this IL-13-competent subset was found to co-express GATA3 and Bcl-6 while also producing IL-4.[18–20] One group reported that the presence of this subset was positively associated with high-affinity IgE titers as detected by ELISA.[18] While intriguing, the interpretation of these findings is complicated by the lack of data on the ratio of high-affinity to total antigen-binding antibody for each sample, as is standard practice. In addition, ELISA measurements of antigen-binding IgE can be

significantly impacted by competition with antigen-binding IgG, which is much more abundant.[21] Thus, these assays are sensitive to differences in the amount of antigen-binding IgG in addition to the amount of antigen-binding IgE.[21] The absence of $T_{FH}13$ cells in *Il13*^{Cre} *Bcl6*$^{flox/flox}$ mice was associated with reduced detection of high-affinity IgE by ELISA and reduced passive cutaneous anaphylaxis.[18] This was provided as evidence for a critical role for $T_{FH}13$ cells and supported the conclusion that IL-13 is involved in high affinity IgE production.[18] Alternatively, these results could also reflect the loss of T_{FH} that were derived from T cells that previously produced IL-13 (e.g. former T_H2 cells), or could be related to the finding that the $T_{FH}13$ cells exhibited reduced production of IL-21 compared with other T_{FH} cells.[18] Notably, IL-21 suppressed sequential CSR of IgG1 GC B cells to IgE *ex vivo*[22] and immunized IgG1-deficient mice have normal IgE levels but impaired IgE affinity.[23] Further work is needed to determine the precise contributions of IL-13, IL-21, and $T_{FH}2$/$T_{FH}13$ cells to IgE production and affinity in allergic immune responses. Future studies would also benefit from Ig variable region sequencing to determine the frequency of high affinity somatic mutations.

In addition to T_{FH}, other T cell subsets regulate IgE production. FoxP3-expressing T regulatory cells (T_{reg}) are also important contributors to the control of IgE responses.[24,25] In general, T follicular regulatory (T_{FR}) cells that co-express Bcl-6 and FoxP3 have been shown to regulate B cell responses.[7] Genetic strategies to deplete T_{FR} cells based on the co-expression of these molecules have paradoxically been reported to result in both augmented and reduced IgE responses.[19,26,27] Interestingly IL-10 made by T_{FR} cells was reported to promote peanut-specific IgE and IgG1 production,[26] yet another study found that IL-10-deficiency had a negligible impact upon IgE levels.[13] Meanwhile, in human tonsils, the abundance of an IL-10-producing $CD25^+$

follicular T cell subset was found to inversely correlate with circulating IgE levels, whereas the abundance of FoxP3+ follicular T cells was found to positively correlate with circulating IgE levels.[28] Yet, recent work suggests T_{FR} cells also produce neuritin, a neuropeptide, that inhibits IgE production.[27] An improved understanding of the interacting partners of follicular T cell subsets and the molecular mechanism by which the molecules produced by these cells augment/inhibit IgE CSR may help to reconcile these conflicting findings.

Antigen-independent signaling of the IgE B cell receptor drives premature PC differentiation of IgE B cells

Early studies of rare IgE lymphocytes in murine primary immune responses reported that IgE B cells appeared in small numbers and only transiently in GCs.[22,29–31] Meanwhile, an abnormally high proportion of IgE B lymphocytes had differentiated into IgE PCs, the majority of which were short-lived.[22,29–31] Increased numbers of IgE GC B cells were observed in mice deficient for the master regulator of PC differentiation, Blimp-1, suggesting that normally a PC fate predisposition contributes to the reduced representation of IgE B cells in the GC.[29]

Cell culture studies revealed that the predisposition of IgE B cells for PC differentiation was driven by intrinsic signals from the IgE BCR. Initially, it was observed that when purified murine naïve B cells were cultured with stimuli that mimic T cell help (ligation of CD40 and IL-4) to induce CSR to IgE, a large proportion of the IgE cells that formed exhibited a PC phenotype.[29,32,33] Culture studies of human tonsil B cells also showed a higher frequency of PCs among IgE cells compared to IgG1 cells.[34] While these observations could have been due to increased IgE CSR in cells already poised to undergo PC differentiation, or conversely increased PC differentiation in cells

poised to undergo IgE CSR, recent studies found that the expression of the IgE BCR itself predisposes IgE B cells for PC fate.[32,33] Specifically, ectopic expression of the IgE BCR in activated B cells drove PC differentiation, whereas the ectopic expression of BCRs of most other isotypes, such as IgG1, did not, with a partial effect observed for IgA. A recent CRISPR screen in cell culture[35] further highlighted the contribution of BCR signaling components to IgE PC differentiation without antigen. Typically, antigen-induced BCR signaling promotes PC differentiation,[36] making it remarkable that ectopic expression of the IgE BCR promoted PC differentiation in an antigen-independent manner.

The above findings suggested that the IgE BCR exhibits autonomous signaling that differs from the tonic signaling of other BCRs. Indeed, evidence was obtained for increased phosphorylation of proximal signaling adapters and increased expression of genes induced by BCR signaling, such as *Nur77*, in B cells expressing the IgE BCR.[32,33] Notably, however, the antigen-independent signaling from the IgE BCR was substantially weaker than when the BCR was stimulated with antigen.[33] In addition, although expression of the IgE BCR promoted PC differentiation in activated B cells,[32,33] it did not do so in naïve B cells.[37] We propose that chronic weak signaling from the IgE BCR synergizes with extrinsic activation signals, such as from T cell help, to promote increased PC differentiation. Consistent with autonomous signaling from the IgE BCR promoting PC differentiation, genetic and pharmacological disruption of a variety of proximal signaling adapters led to reduced IgE PC differentiation in cultured B cells.[32,33] Interestingly, heterozygous mutations in *Syk* or *Cd19* resulted in substantial reductions in IgE PC differentiation, indicating that small changes in the magnitude of BCR signaling can have significant functional consequences.

Tendency towards apoptosis in IgE lymphocytes and the transience of IgE responses

In addition to its role in promoting PC differentiation, the IgE BCR has been implicated in IgE B cell apoptosis, although this remains controversial.[31–33,38] *In vitro*-differentiated mouse IgE B cells were observed to be more apoptotic than IgG1 B cells in some cell culture assays.[32,38] The ectopic expression of the IgE BCR in cultured primary B cells and a cell line was also reported to promote apoptosis.[32,38] However, in another study of mouse B cells, these findings could not be reproduced.[33] Specifically, similar rates of apoptosis were observed in IgE and IgG1 B cells differentiated *in vitro,* or after ectopic expression of the IgE versus IgG1 BCRs in primary B cells and cell lines. In addition, a recent study of cultured human tonsil B cells also concluded that IgE and IgG1 B cells exhibited similar rates of apoptosis.[39]

The reasons for these discrepancies in findings remain unclear, but may be related to technical details of the assays. One approach used in cell culture studies was to induce apoptosis by withdrawing pro-survival signals, including CD40 stimulation, IL-4, and in some cases BAFF.[32,33,38] In this context, antigen-independent signaling of the IgE BCR through the Syk→BLNK→JNK/p38 axis, or alternatively the sequestration of Hax1 from the mitochondria by the IgE BCR intracellular tail, was proposed to promote apoptosis.[32,38] One possibility is that antigen-independent signaling of the IgE BCR mimics stimulation of the IgM BCR, which induces apoptosis in the absence of other signals such as ligation of CD40.[40,41] However, the antigen-independent signaling of the IgE BCR is substantially weaker than direct BCR stimulation and may more closely reflect the chronic stimulation of the BCR in autoreactive B cells. An alternative model is that rather than being a stronger source of pro-apoptotic signals the IgE BCR is a deficient source of pro-survival signals. B cells require membrane BCR expression and resulting tonic

signaling via PI3K for survival.[42] The IgE BCR may be deficient in producing these survival signals, either due to its low surface expression (reviewed in depth below) or due to qualitative impairments in its pro-survival signaling. We speculate that specific differences in the culture conditions and the nature of the cell lines used in the above studies may be responsible for the different outcomes observed regarding the IgE BCR and apoptosis. It is unclear the degree to which these findings in cell culture are applicable to IgE B cells *in vivo*, where a milieu of complex signals are present. One attempt to address this question has been through the analysis of GC B cells *ex vivo*, however again conflicting findings have emerged. Specifically, one group found that IgE GC B cells exhibited higher rates of apoptosis than IgG1 GC B cells,[31] whereas another group could not reproduce these findings.[33] Nevertheless, the low amount of apoptosis of GC B cells detected *ex vivo* in these studies is a tiny fraction of the apoptosis that occurs *in vivo*, where it is thought that up to half of all GC B cells undergo apoptosis every 6 h.[43] Thus, more studies are needed to determine the extent to which the IgE BCR may promote the apoptosis of IgE B cells *in vivo* versus promoting their differentiation into short-lived PCs or otherwise rendering them less competitive within the GC, as we discuss further below.

Although conflicting evidence has been obtained regarding the predisposition of IgE B cells towards apoptosis, greater consensus has been achieved regarding the short lifespan of the majority of IgE PCs. For instance, in a model of IgE and IgG1 hypergammaglobulinemia, the overwhelming majority of IgE PCs were proliferating, unlike other PCs, suggesting that the IgE PCs were predominantly short-lived plasmablasts.[38] Indeed, markedly increased numbers of IgE PCs relative to IgG1 PCs were observed in *Bcl2* transgenic mice after immunization, indicating that IgE PCs are normally restrained by poor survival.[29] Less data exists on human IgE PCs, but culture studies

of human tonsil B cells also showed elevated rates of apoptosis among IgE PCs.[39] More research is needed to understand how IgE PCs are constrained to short-lived fates and what drives their apoptosis, as well as how long-lived IgE PCs might arise pathologically in allergy. Notably, no prior work has evaluated the potential for direct regulation of IgE PC longevity by BCR signaling.

Altered surface expression of the IgE BCR

Another unusual feature of the IgE BCR is its low surface expression on GC B cells (**Figure 1.2**).[31,33] IgE GC B cells exhibited reduced antigen-dependent BCR signaling compared with IgG1 GC B cells when stimulated *ex vivo*.[32] *In vivo*, IgE GC B cells captured, processed, and presented fewer antigen peptide MHC complexes compared with IgG1 GC B cells.[33] As a result, IgE GC B cells may compete poorly for T cell help in the GC, which is critical for selection. Consistent with this model, IgE GC B cells progressed more slowly through the cell cycle than IgG1 GC B cells.[33] Other evidence of enfeebled function of the IgE BCR comes from studies of mice whose B cells were pre-class-switched to either IgE ($IgH^{\varepsilon/\varepsilon}$) or IgG1 ($IgH^{\gamma1/\gamma1}$) before development.[37] In the context of a pre-rearranged light chain, $IgH^{\varepsilon/\varepsilon}$ B cells had massively reduced surface BCR expression and failed to mount an antigen-specific B cell response when immunized, whereas their $IgH^{\gamma1/\gamma1}$ counterparts did.[37]

There are multiple non-mutually exclusive models that might explain the low surface BCR expression in IgE GC B cells (**Figure 1.2**). One model is that these cells have low expression of transcripts encoding the IgE BCR. Surface and membrane forms of each Ig isotype are expressed through alternative splicing and polyadenylation. IgG1 B cells primarily express the membrane form of the BCR (mIgG1) whereas IgG1 PCs primarily express the secreted form (sIgG1). IgE B

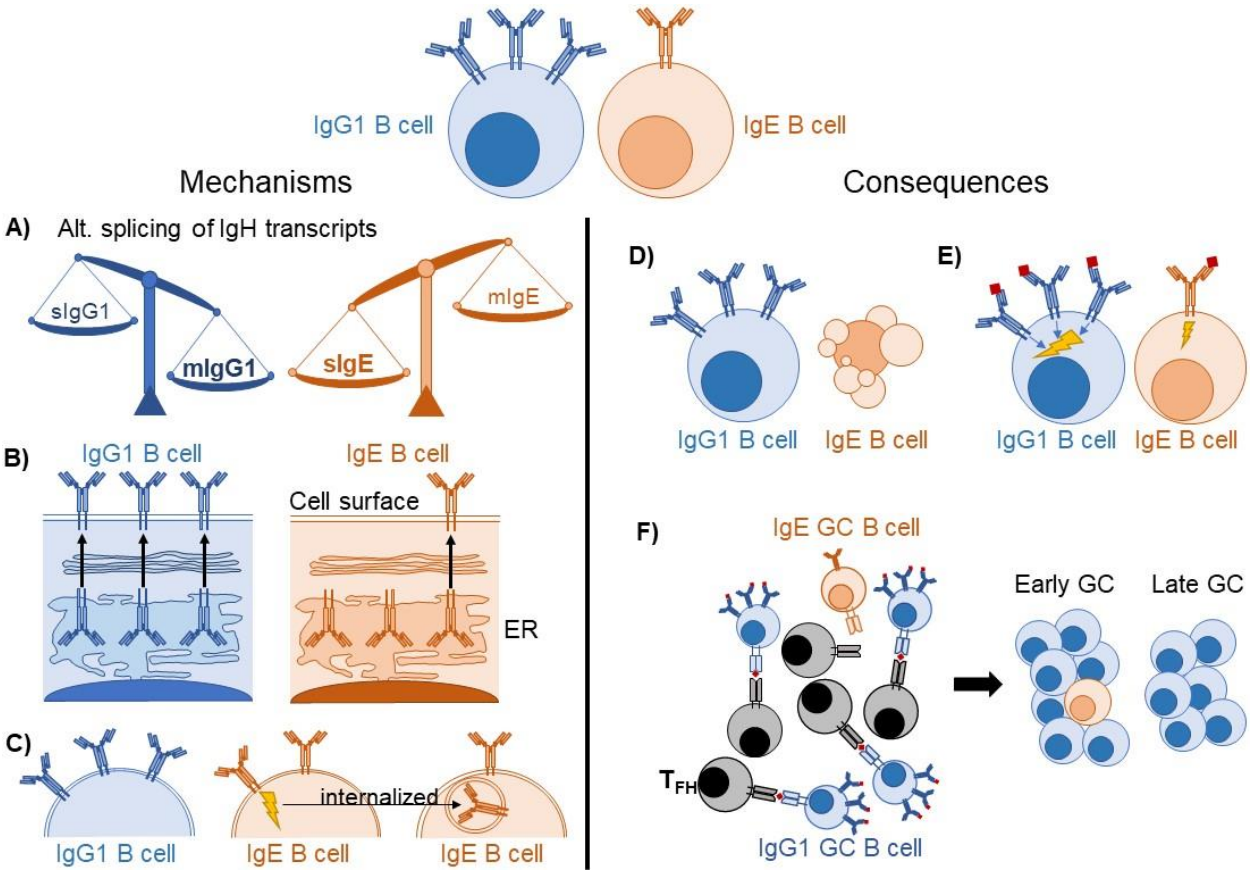

Figure 1.2 Proposed mechanisms and consequences of low surface BCR expression on IgE B cells (A-C) Potential mechanisms explaining low IgE BCR surface expression. (A) IgG1 B cells favor the mIg spliceoform of IgH, whereas IgE B cells favor the sIg spliceoform, resulting in fewer mIgE transcripts available for the translation of IgE BCR molecules. (B) The IgE BCR is retained in the ER after translation rather than being exported to the cell surface. (C) Antigen-independent signaling of the IgE BCR leads to its internalization, reducing surface BCR levels. (D-F) Putative consequences of low BCR expression on IgE B cells. (D) IgE B cells undergo apoptosis due to insufficient BCR expression. (E) IgE B cells have weaker antigen-dependent BCR signaling than IgG1 B cells. (F) IgE GC B cells are less able to capture and present antigens to GC TFH, causing them to be progressively out-competed over time.

cells, however, are unusual in that they express relatively higher amounts of sIgE than mIgE, and both sIgE and mIgE are greatly upregulated in IgE PCs.[29,37,44] The poor expression of mIgE in IgE B cells may in part be due to an inefficient polyadenylation sequence downstream of the M2 exon,[44] although a more classical polyadenylation sequence is located further downstream.

A second model is that mIgE is retained in the endoplasmic reticulum (ER). IgE, unlike IgG1, requires assembly with Igα/β to reach the cell surface,[33,45] which could be limiting in some contexts. Recent structural analysis revealed the mIg isotype-specific (migis) segment, a region unique to each isotype of BCR that protrudes from the plasma membrane into the extracellular space, was a critical determinant of whether the BCR must associate with Igα/β to reach the cell surface.[33] The IgE migis region was also found to be critical for the antigen-independent signaling activity of the IgE BCR,[32,33] leading us to speculate that some characteristics of its association with Igα/β mimic an antigen-binding state. The migis of IgE was also reported to promote enhanced interaction with CD19.[32] Interestingly, humans and primates have two splice variants of the IgE BCR, one isoform of which encodes a longer M1' segment of the extracellular membrane proximal domain (EMPD) that includes the migis. This long isoform was associated with retention of the IgE BCR in the ER.[46] Changes in the relative expression of the long versus short isoforms have been reported during IgE PC differentiation in human tonsil B cell cultures.[34]

A third possible model to explain low surface IgE BCR expression is that constitutive, antigen-independent signaling induces its internalization, analogous to the downmodulation of surface IgM in autoreactive B cells.[47] Evidence for increased internalization of mIgE was provided by incubating cells with fluorescently-labeled antibodies at different temperatures followed by flow cytometric analysis.[38] Taken together, multiple mechanisms may result in low surface BCR expression on IgE B cells, leading to functional consequences (**Figure 1.2**) that impair the ability of these cells to compete in GCs.

Contrasting with IgG PCs, IgE PCs greatly upregulate not only sIgE but also mIgE relative to their B cell counterparts.[29,31,39] This raises the question of whether the mechanisms that serve to constrain mIg in IgE B cells are disabled in IgE PCs. Alternatively, they may be overcome by altered regulation of alternative splicing of Ig transcripts in IgE PCs combined with the extreme Ig expression characteristic of PCs relative to B cells. Interestingly, high mIg expression has also been observed on IgM and IgA PCs, and these BCRs were signaling competent.[48,49] However, it remained to be determined whether the BCR on IgE PCs was functional.

The incomplete model of IgE regulation by BCR signaling and possible explanations

Based on the observations in cell culture discussed above and previous *in vivo* observations suggesting that premature PC differentiation hindered IgE GC B cell responses, it was predicted that perturbations of BCR signaling would lead to reduced IgE PC differentiation and enhanced IgE GC B cell responses *in vivo*. An increase in IgE GC B cells was indeed observed in mice with perturbations of various BCR signaling pathways.[32,33] The effect of these perturbations on *in vivo* IgE PC responses, however, was less clear, as both decreases and increases in the absolute number of IgE PCs were reported.[32,33] Specifically, one group found that in *Blnk*-deficient mice, early IgE PC responses were reduced, yet later IgE PC responses were increased and sustained IgE production was observed up to 100 days after immunization.[32] Ig variable region sequencing four weeks after immunization showed similar somatic mutations and selection in IgE and IgG1 PCs.[32] These findings suggest that *Blnk*-deficiency led to elevated IgE GC B cell responses that in turn resulted in the increased export of long-lived IgE PCs at later timepoints. However, in another study, an increase in the absolute number of IgE PCs was observed early in the immune response in mice with mutations in *Blnk*, *Cd19*, or *Syk*.[33] Analysis of *Syk* heterozygous cells indicated that

the majority of early IgE PCs were not somatically mutated, in contrast to co-isolated IgE GC B cells.[33] These data suggest that early increases in IgE PCs observed in the context of BCR signaling perturbations did not originate from the GC, but rather represented unexplained increases in extrafollicular IgE PC responses. These studies did not determine how BCR signaling might regulate the magnitude of the extrafollicular IgE PC response. This dissertation explores two non-mutually-exclusive mechanisms for IgE regulation by BCR signaling: direct inhibition of CSR to IgE (Chapter 2) and restriction of IgE PC survival (Chapter 3).

Conclusion

The research contained in this dissertation seeks to elucidate the overall importance of antigen-driven BCR signaling to the regulation of IgE responses by answering four questions:

1) Does BCR stimulation preferentially inhibit CSR to IgE relative to IgG1?
2) Do BCR ligation and IL-21 synergistically impair IgE CSR?
3) Is mIg on IgE PCs signaling-competent?
4) What is the outcome of IgE PC mIg stimulation relative to PCs of other isotypes?

Chapter 2: BCR ligation inhibits IgE CSR in mice and humans

Abstract

Mechanisms that restrict CSR to IgE limit the production of IgE antibodies and the development of allergic disease. Mice with even moderately impaired BCR signaling have significantly increased IgE, consistent with a role for BCR signaling in IgE regulation. While prior work focused on antigen-independent signaling in IgE B cells to explain these findings, it is known that strong BCR signaling can reduce CSR. These observations raise the possibility that IgE CSR might be particularly sensitive to inhibition by BCR signaling. Here, we found that immunization with higher affinity antigen lessened the representation of IgE-expressing cells among germinal center B cells and plasma cells. Mechanistic experiments in cell culture demonstrated that selective IgE CSR inhibition was a primary outcome of BCR stimulation rather than being secondary to effects on proliferation. BCR ligands inhibited IgE CSR in a dose-, affinity-, and avidity-dependent manner. We used chemical inhibitors to show that signaling via Syk was required for the inhibition of IgE CSR following BCR stimulation. While a partial contribution was observed for CD19-PI3K signaling, specific inhibition of p110δ increased IgE CSR similarly regardless of the presence or absence of BCR ligands. Next, we determined that BCR stimulation and IL-21 synergize to more greatly reduce IgE CSR. Finally, we provide evidence to newly support that BCR ligation inhibits CSR to IgE in human tonsillar B cells, and that this inhibition is compounded by the presence of IL-21. These findings establish that IgE CSR is uniquely susceptible to inhibition by BCR signaling, with important implications for how allergic disease might emerge or be treated.

Introduction

Diseases of type-1 hypersensitivity, such as allergy, emerge when IgE antibodies are produced against environmental antigens. Normally, the production of IgE is tightly controlled and the abundance of IgE in serum is orders of magnitude less than that of IgG. Moreso than other isotypes, IgE B cells readily differentiate into PCs, and therefore the main control point for IgE production is at the stage of CSR rather than PC differentiation. Indeed, IgE CSR is strongly suppressed *in vivo*, importantly including by IL-21.[13] However, mounting evidence suggests that IgE CSR may be constrained by yet further mechanisms.

Stimulation of the BCR can broadly inhibit class-switching,[50–53] and if IgE CSR was especially sensitive to this effect then relaxation of this regulation in the context of BCR signaling impairment could produce increases in IgE GC B cells and extrafollicular PCs. Indeed, prior studies from our lab and others have found increased IgE responses in mice with impairments in BCR signaling. Although this previous work focused on how IgE responses in these mice might be increased due to alterations in antigen-independent signaling of the IgE BCR in IgE B cells,[32,33] another possibility is that IgE CSR is especially susceptible to inhibition by BCR signaling, and thus BCR signaling impairment dis-inhibits IgE CSR. There is mixed evidence for whether BCR stimulation might selectively effect IgE CSR.[52,54]

B cell antigen encounter initiates a complex array of BCR signaling pathways that coordinate a variety of responses. The incipient events of BCR signaling include the formation of the "BCR signalosome" through a series of (often phosphorylation-induced) interactions between spleen tyrosine kinase (Syk), B cell linker protein (BLNK), Bruton's tyrosine kinase (Btk), and

phospholipase C γ 2 (PLCγ2), among others. This process is reinforced through the co-receptor CD19, which activates phosphoinositide-3-kinase (PI3K; composed of p110 catalytic and p85 regulatory subunits) to produce phospholipids that recruit several BCR signalosome components and other molecules to the plasma membrane.[55]

Mice with a heterozygous mutation in *Cd19* or disrupted p110δ (the highest expressed p110 isoform in B cells) signaling produce exaggerated IgE responses to type-2 immunizations.[32,33,56] These observations may relate to effects on IgE CSR, as CSR is broadly inhibited in mice with enhanced PI3K activity, while PI3K inhibitors broadly increase CSR.[50,57–59] Increased IgE responses have also been reported in mice with heterozygous mutations in Syk, homozygous mutations in BLNK, and pharmacologic inhibition of Btk.[33] However, the importance of these molecules (CD19, Syk, BLNK, and Btk) to antigen-independent signaling of the IgE BCR and the lack of prior evidence of their contribution to CSR inhibition by BCR stimulation makes it unclear if their role in reducing IgE involves effects on IgE CSR.

Here, we demonstrate that immunization with higher-affinity antigen lessens the representation of IgE cells in the GC and among extrafollicular PCs. We also support earlier work with new evidence that impairing BCR signaling elevates IgE in these same compartments. In cell culture, we show that BCR stimulation with anti-BCR antibodies or cognate antigen selectively inhibits IgE CSR. IgE CSR inhibition by BCR stimulation is dose-dependent, and in several cases IgE CSR was strongly inhibited even when IgG1 CSR was unaffected or increased. The stronger effect of BCR stimulation on IgE results from a sustained decrease in the fraction of cells that switch to IgE at every cell division number, whereas BCR stimulation delays IgG1 CSR but ultimately does not

impair IgG1 CSR frequency at later cell divisions. Contrasting with prior work, we identify a selective effect of BCR stimulation on ε germline transcripts rather than *Aicda* transcripts, providing a potential transcriptional mechanism for IgE CSR inhibition by BCR stimulation. Our experiments with CD19-deficient cells and pan-PI3K/mTOR inhibition suggest a partial contribution of CD19-PI3K signaling to IgE CSR inhibition following BCR stimulation. However, this contribution did not include a role for p110δ, which repressed IgE CSR independently of BCR stimulation. Conversely, Syk-dependent signaling did not play a major role in IgE CSR regulation in the absence of BCR stimulation, but upon BCR stimulation Syk-dependent signals were critical to inhibit CSR to IgE. Further, we used PMA and ionomycin to show that protein kinase C activation, and to a lesser extent Ca^{2+} flux, are sufficient to inhibit IgE CSR even without activating other BCR signaling pathways. Finally, we reveal that the selective, individual inhibitions of IgE CSR by BCR stimulation and IL-21 combine synergistically to almost completely eliminate IgE CSR in both mouse and human cells.

Results

BCR stimulation strength inversely correlates with switched IgE cells

To begin to untangle whether BCR signaling might selectively regulate IgE CSR *in vivo* we transferred Hy10 B cells with a fixed VDJ conferring specificity for avian egg lysozyme into congenic recipients and immunized those recipients with low- or high-affinity cognate antigen (duck egg lysozyme [DEL] or hen egg lysozyme [HEL], respectively) in alum adjuvant and compared the representation of IgE cells in the GC and PC compartments of the draining lymph node (dLN) one week later. IgE-expressing cells were more frequent among both GC B cells and PCs in recipients immunized with DEL compared to HEL, whereas the frequency of IgG1 cells was comparable or increased (Figure 2.1A). We also expanded upon prior findings that weakening BCR signaling results in greater IgE responses[32,33] by immunizing WT and Igα$^{+/-}$ (aka CD79a / Mb1) mice and comparing the frequencies of IgE and IgG1 cells within their GC and PC compartments. Igα is one of two ITAM-containing accessory proteins to the BCR thought to be responsible for the majority of signal transduction, and Igα-heterozygous mice had increased frequencies of IgE cells within both the GC and PC compartments (Figure 2.1B). Interestingly, these mice had a subtle increase in IgG1 GCBCs and decrease in IgG1 PCs, consistent with previously described roles for BCR signaling in PC differentiation.[60,61] Overall, these data are consistent with the hypothesis that IgE CSR is especially susceptible to inhibition by BCR ligation.

To dissect the effect of BCR ligation on IgE CSR in greater detail we turned to our previously described purified B cell culture system.[2,33] First, we tested the effect of stimulation with an anti-BCR antibody (goat anti-mouse IgD [αIgD]) vs control (goat gamma globulin [GGG]) on the frequency of IgE and IgG1 cells at culture endpoint. BCR stimulation greatly reduced the

frequency of IgE cells in the culture with a lesser reduction in IgG1 (Figure S2.1A-B). As BCR stimulation reduced overall class-switching in the culture (Figure S2.1C-D), we examined the frequency of IgE cells among class-switched cells and found that BCR stimulation greatly reduced

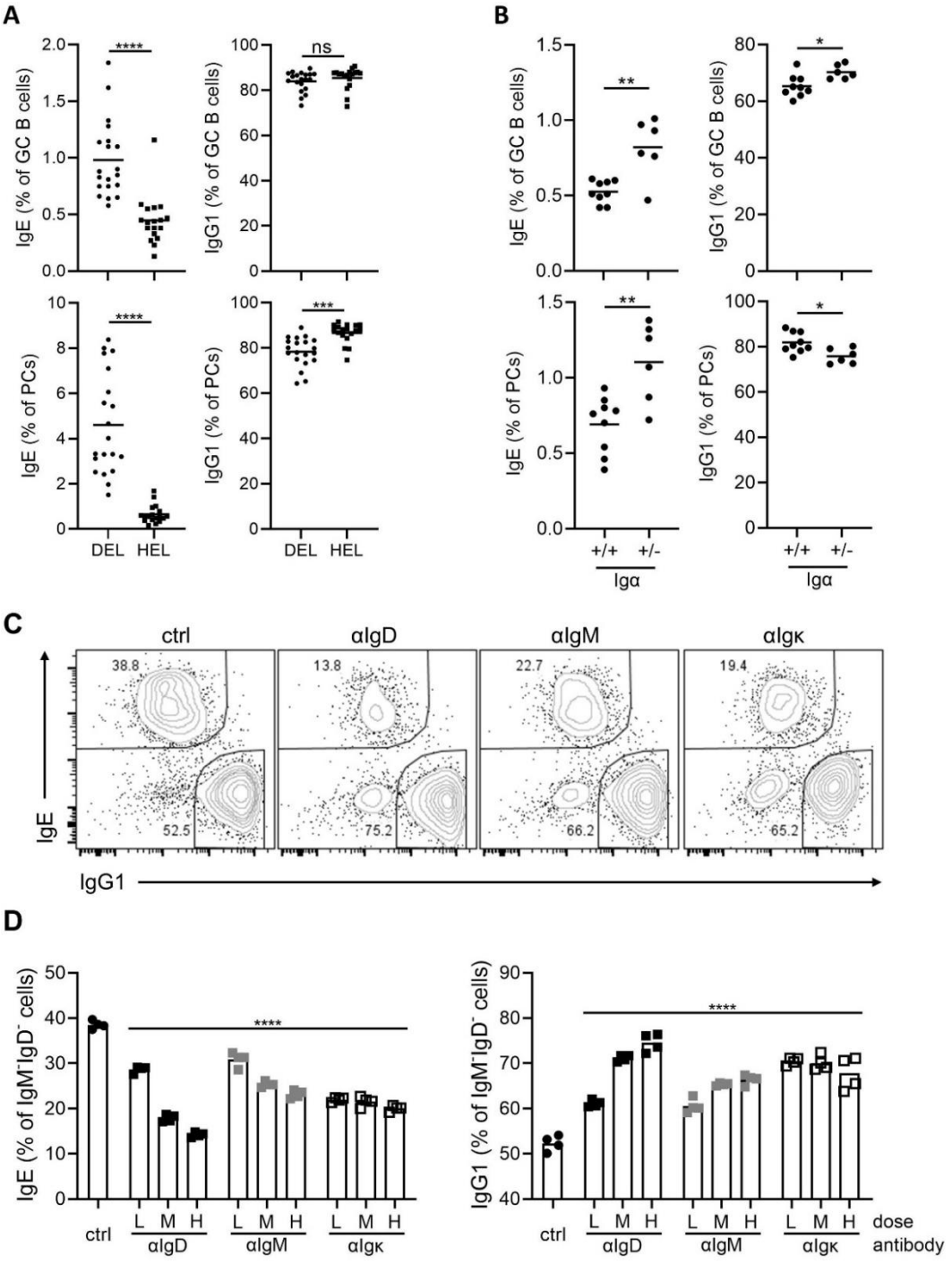

Figure 2.1 BCR stimulation reduces the representation of IgE cells *in vivo* and *in vitro*.
(A) Hy10 B cells were adoptively transferred into (Figure caption continued on the next page.)

(Figure caption continued from the previous page.) congenically-marked recipients that were then immunized with duck egg lysosome (DEL) or hen egg lysozyme (HEL) conjugated to ovalbumin. Shown are the fractional representation of IgE (left column) and IgG1 (right column) cells within the GC (top row) and PC (bottom row) compartments of transferred cells in the dLN at d7, quantified by flow cytometry. (B) Wildtype and Ig$\alpha^{+/-}$ mice were immunized with NP-CGG and the resultant immune response in the dLN at d7 was analyzed by flow cytometry. Plots are laid out as described for panel A. (C-D) B cells were cultured for 4 days with the indicated treatments prior to analysis by flow cytometry. (C) Representative flow cytometry plots of IgE and IgG1 staining among $IgM^{-}IgD^{-}$ cells according to treatment condition (from left to right; ctrl, αIgD, αIgM, αIgκ; all at 1μg/mL). (D) Quantification of the effects of treatment with low (L; 100ng/mL), medium (M; 300ng/mL), or high (H; 1μg/mL) doses of αIgD (black squares), αIgM (grey squares), αIgκ (white squares), or ctrl (1μg/mL; black circles) antibodies on the fractional representation of IgE (left) and IgG1 (right) cells among class-switched cells. (A-B, D) Dots represent samples from individual mice and bars represent the mean values. ns, not significant; *, $P < 0.05$; **, $P < 0.01$; ***, $P < 0.001$; ****, $P < 0.0001$ (unpaired t test [A-B], one-way repeated measures ANOVA [D] with Dunnett's post-test comparing each group to the control with the Holm-Sidak correction for multiple comparisons). Results are pooled from three (A) or two (B, D) independent experiments or are representative of two independent experiments (C).

the representation of IgE cells within the class-switched compartment, meanwhile the representation of IgG1 cells was increased (Figure S2.1E-F). These data suggest that BCR stimulation has a selective negative impact on IgE CSR.

We next asked whether these findings were generalizable to different anti-BCR antibodies as well as cognate antigen. While αIgD treatment resulted in the greatest dose-dependent reduction in IgE of anti-BCR antibodies we measured, both goat anti-mouse IgM (αIgM) and goat anti-mouse Ig kappa light chain (αIgκ) produced significant reductions in IgE (Figure 2.1 C-D). To investigate the impact of cognate antigen on IgE CSR, we purified and cultured Igλ light chain-expressing cells from $IgH^{B1\text{-}8i/+}$ (hereafter referred to as B1-8) mice.[62] B1-8 mice have a fixed heavy chain that endows most B cells expressing λ light chains with binding specificity towards the hapten 4-hydroxy-3-nitrophenyl (NP) and with 10-fold higher binding strength towards the hapten 4-hydroxy-3-iodo-5-nitrophenyl (NIP). By treating purified B cell cultures with different doses of

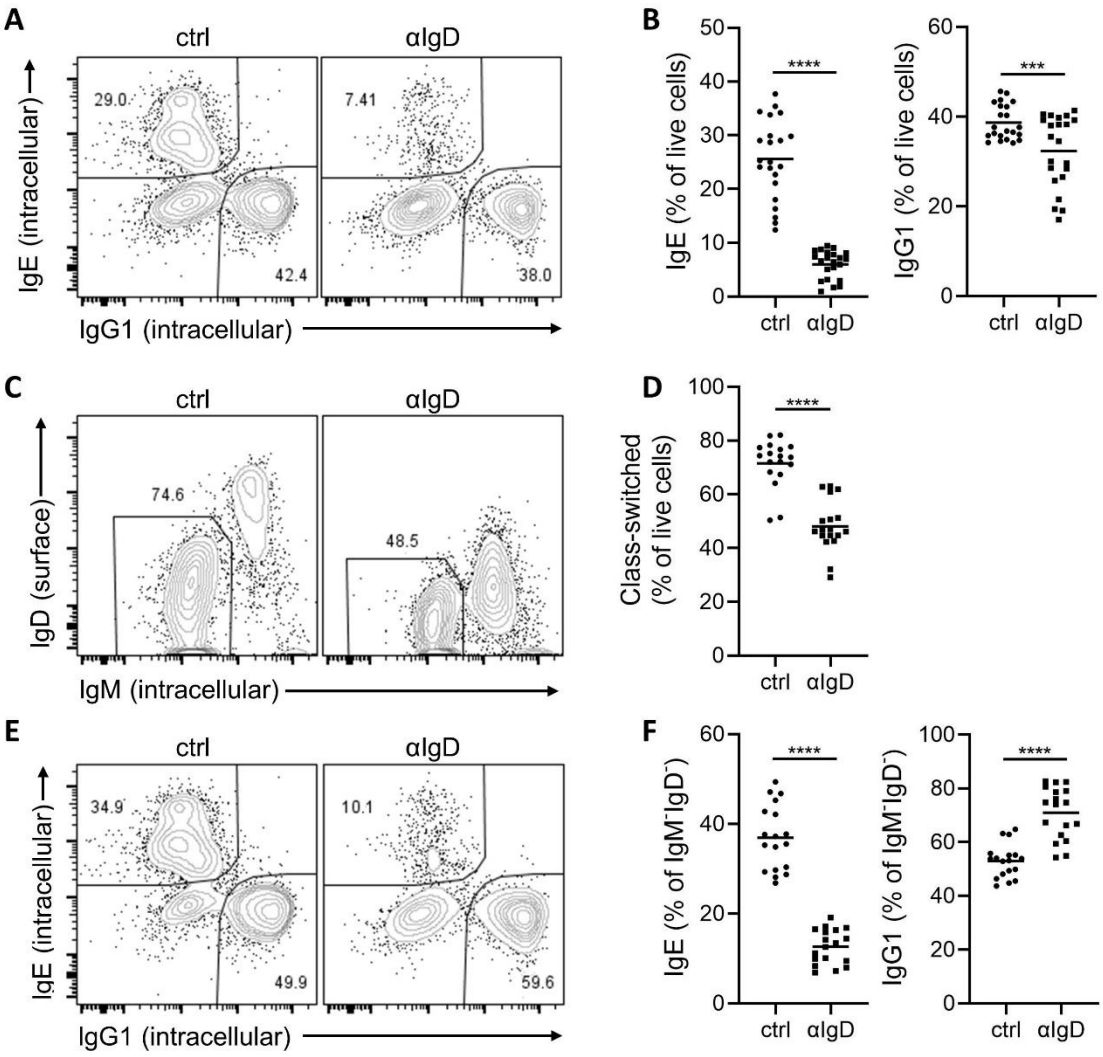

Figure S2.1 Supporting data for Figure 2.1 (A-F) B cells were cultured for 4 days prior to analysis by flow cytometry with control (goat gamma globulin, 3μg/mL) or αIgD (3ug/mL) antibodies. (A, E) Representative flow cytometry plots of IgE and IgG1 gating from live cells (A) or class-switched cells (E). (B, F) Quantification of the fractional representation of IgE (left) or IgG1 (right) cells among live B cells (B) or class-switched B cells (E). (C) Representative gating of class-switched B cells. (D) Quantification of rates of class-switching with control or αIgD treatment. (B, D, F) Dots represent samples from individual mice and bars represent the mean values. ***, $P < 0.001$; ****, $P < 0.0001$ (paired t test). Results are representative of six (A) or five (C, E), or are pooled from six (B) or five (D, F), independent experiments.

highly haptenated low-affinity antigen ($NP_{25}BSA$), lowly haptenated low affinity antigen (NP_4BSA), or highly haptenated high-affinity antigen ($NIP_{24}BSA$) we could assess the impact of cognate antigen dose and binding avidity on IgE CSR. All three cognate antigens dose-dependently

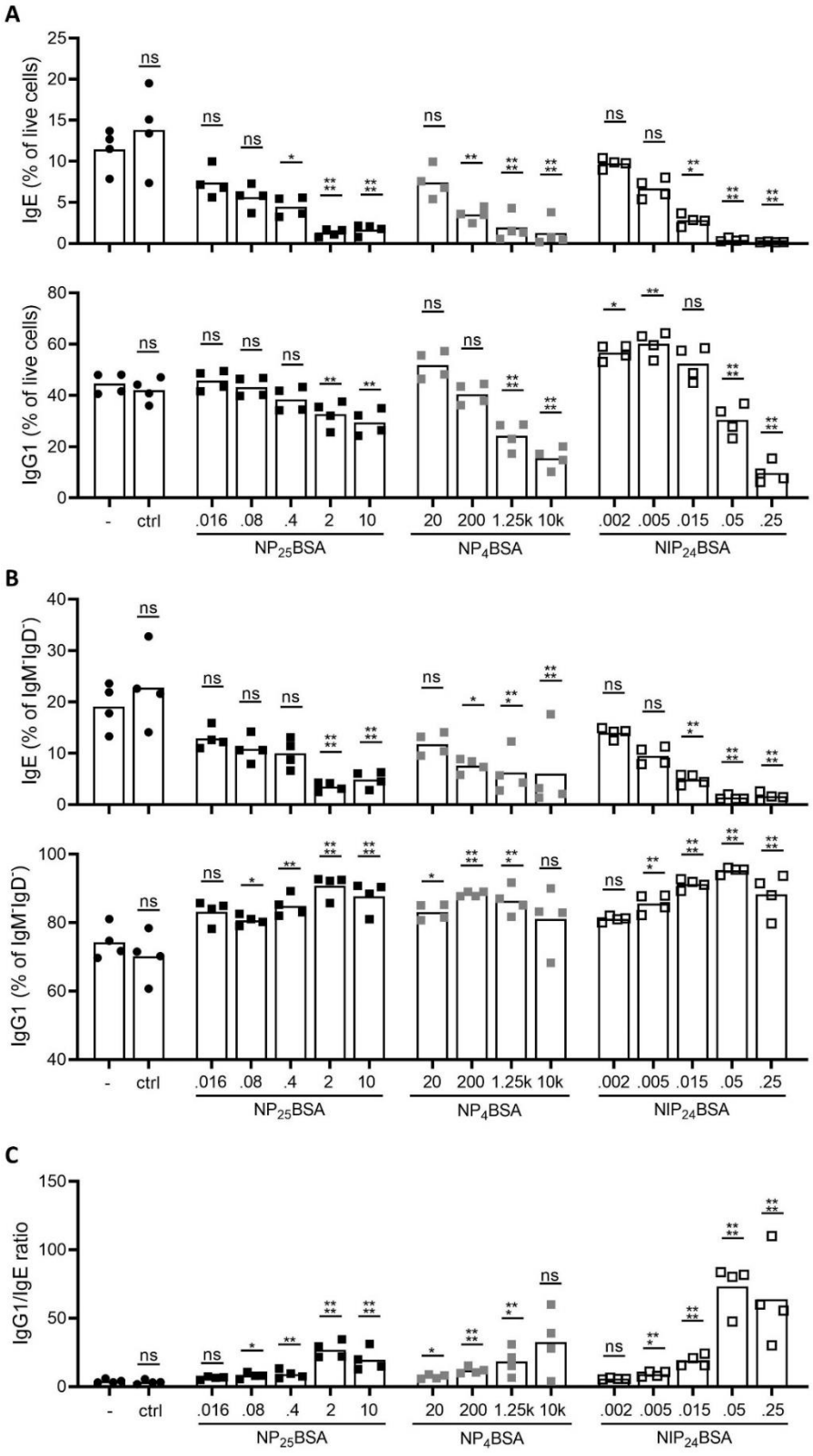

Figure 2.2 B cell culture with cognate antigen reduces yields of IgE cells. (A-C) Purified B1-8i B cells were cultured for 4 days with control (Figure caption continued on the next page.)

(Figure caption continued from the previous page.) ('-' is no treatment, 'ctrl' is BSA at 50ng/mL; black circles) or cognate antigen (NP_{25}BSA [black squares], NP_4BSA [grey squares], or NIP_{24}BSA [white squares] at doses given on the x-axes in ng/mL) prior to analysis by flow cytometry. (A-B) Quantification of the fractional representation of IgE (top) or IgG1 (bottom) cells among all live cells (A) or within the class-switched (IgM^-IgD^-) compartment (B) as assessed by flow cytometry. (C) Determination of the ratio of IgG1 : IgE cells according to treatment condition. (A-C) Dots represent samples from individual mice and bars represent the mean values. *, $P < 0.05$; **, $P < 0.01$; ***, $P < 0.001$; ****, $P < 0.0001$ (one-way repeated measures ANOVA with Dunnett's post-test comparing each group to the untreated control with the Holm-Sidak correction for multiple comparisons). Results are representative of two independent experiments.

reduced the representation of IgE- and IgG1-expressing cells among NP-binding B cells (Figure 2.2A). While all antigens inhibited CSR at some dose, the amount of antigen required to achieve similar effects varied over orders of magnitude. As both IgE and IgG1 CSR was affected, we examined the representation of IgE and IgG1 cells within the class-switched compartment to determine if there was a selectively stronger impact on IgE. Indeed, all cognate antigens dose-dependently reduced the representation of IgE cells and either did not change or increased the representation of IgG1 cells (Figure 2.2B). To determine whether cognate antigens with different binding strengths differed in their ability to selectively inhibit IgE versus IgG1, we quantified the ratio of IgG1 : IgE cells. At just 50pg/mL, NIP_{24}BSA produced the strongest inhibition of IgE relative to IgG1, suggesting that the most potent BCR ligands may have the greatest capacity to selectively inhibit IgE (Figure 2.2C).

BCR stimulation inhibits IgE CSR independently of proliferation by downmodulating ε germline transcription

There are multiple ways that a higher-affinity antigen could lead to reduced numbers of IgE cells. As class-switching is linked to cell division and IgE requires more cell divisions to emerge relative to IgG1,[63] one possibility is that the stronger BCR signal produced by encounter with higher-

affinity antigen results in reduced proliferation, limiting the opportunity for CSR overall but especially so for IgE CSR. To distinguish potential effects on proliferation versus CSR we loaded B cells with cell trace violet (CTV) and examined at each division number whether BCR stimulation affected the fraction of IgE or IgG1 cells. CTV fluorescence is reduced 2-fold with each cell division, and after four days of culture, we were able to visualize 7 distinct populations of B cells based on the intensity of their CTV staining (Figure 2.3A). Whereas IgG1 cells were first detectable after three divisions, IgE cells remained absent until 5 divisions, consistent with prior work (Figure 2.3B-C).[63] BCR stimulation reduced the fraction of IgE cells across all cell divisions at which they were present (Figure 2.3B), whereas the effect of BCR stimulation on IgG1 cells was to somewhat delay CSR, as the fraction of IgG1-switched cells was modestly reduced at divisions 3 through 6 but normalized and trended towards being increased at division 7 (Figure 2.3C). These results are consistent with the notion that the primary mechanism by which BCR stimulation reduces IgE is through the inhibition of IgE CSR rather than effects on proliferation. To gain further insight in the mechanism of IgE CSR inhibition, we compared ε and γ_1 germline and post-switch transcripts (GLT and PST, respectively) as well as *Aicda* transcripts between RNA extracted from BCR-stimulated or control B cell cultures. GLTs are transcribed from the I (e.g. I_ε or $I_{\gamma 1}$) region upstream of the switch region for all class-switched antibody isotypes and their production is a pre-requisite for a B cell to undergo CSR to that isotype. It is thought that this is due to their importance in 'opening up' local chromatin. Meanwhile, PSTs are transcribed from I_μ through a recombined isotype following CSR. BCR stimulation reduced εGLT ~2-fold at D2, but increased γ_1GLT. At D3, εPST was strongly reduced by BCR stimulation whereas there was a minor (~20%) impact on γ_1PST (Figure 2.3D). *Aicda* transcripts were equivalent at D2, but at D3 there was a subtle reduction in the αIgD condition. These data indicate that BCR stimulation can

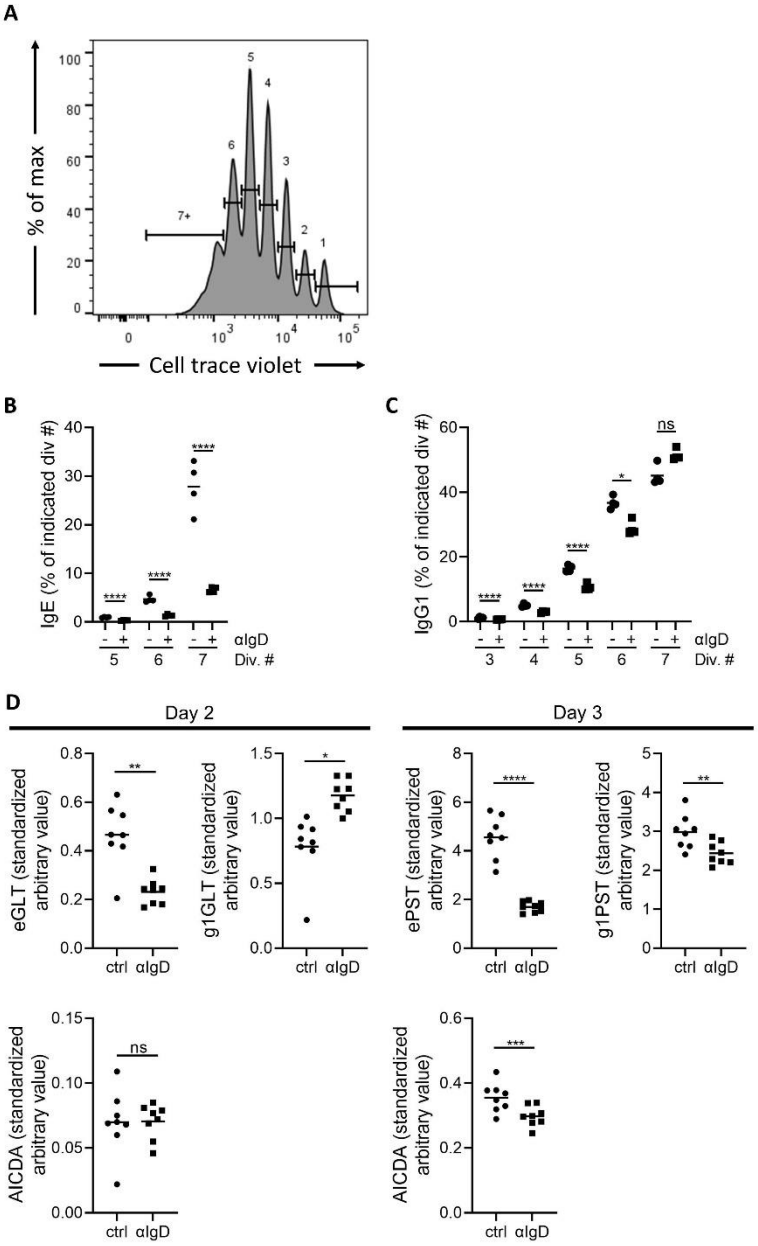

Figure 2.3 BCR stimulation inhibits IgE CSR. (A-C) Purified naïve B cells were loaded with cell trace violet (see Methods) and then cultured for 4 days prior to analysis by flow cytometry. (A) Representative histogram from the control-treated condition showing cell trace violet staining and cell division number gating. (B-C) Quantification of the fractional representation of IgE (B) and IgG1 (C) cells among live cells within each cell division (gated as shown in panel A) for control-treated (-; GGG at 3μg/mL; black circles) and αIgD-treated (+; 3μg/mL; black squares) conditions. Dots represent samples from individual mice (n=4) and bars represent the mean values. (D) Purified naïve B cells were cultured for two (left) or three (right) days prior to quantification of the indicated transcripts by RT-qPCR, using the standard curve method. Dots represent samples from individual mice (n=8) and bars represent the mean values. (A-C) *, $P < 0.05$; **, $P < 0.01$; ****, $P < 0.0001$ (paired t test [C]). Results are representative of five similar experiments (A-C) or are pooled from two independent experiments (D).

directly inhibit CSR and have an especially profound impact on IgE CSR, likely related to a reduction in εGLT.

IgE CSR inhibition by BCR stimulation is principally mediated by Syk

As discussed earlier in this dissertation, substantial prior literature has focused on the role of PI3K signaling in CSR.[50,53,56,57,59,64] Therefore, we set out to determine the importance PI3Kδ, the main PI3K isoform expressed in B cells, to the inhibition of IgE CSR by BCR stimulation. Consistent with prior work, the PI3Kδ inhibitor nemiralisib dose-dependently increased IgE (Figure 2.4A). However, regardless of the dose of inhibitor, IgE CSR remained strongly susceptible to inhibition by BCR stimulation (Figure 2.4A). To determine if the effects of PI3Kδ inhibition on IgE CSR were truly independent of the inhibition of IgE CSR by BCR stimulation it was necessary to normalize the fraction of IgE-switched cells in the αIgD-treated conditions against the fraction of IgE-switched cells in the non-αIgD-treated conditions treated with the same dose of inhibitor. This analysis revealed that, although the inhibitor dose-dependently increased the fraction of IgE-switched cells, this fraction was reduced by ~80% in all cases when αIgD was added to culture (Figure 2.4B). These results validated the known role for PI3Kδ in regulating IgE CSR,[56,64] but also demonstrated that the inhibition of IgE CSR by BCR stimulation did not require signaling through PI3Kδ. To more broadly investigate the CD19-PI3K axis, we compared the inhibition of IgE CSR in wildtype cells versus mice heterozygous (het) or deficient (KO) for *Cd19*. IgE CSR was strongly susceptible to inhibition relative to IgG1 CSR by BCR stimulation in wildtype and *Cd19*-het cells, however *Cd19*-KO cells were substantially resistant (Figure 2.4C). We considered two possible explanations for these results. Firstly, it was possible that there was redundancy between various p110 isoforms and that a complete blockade of CD19-PI3K signaling (only

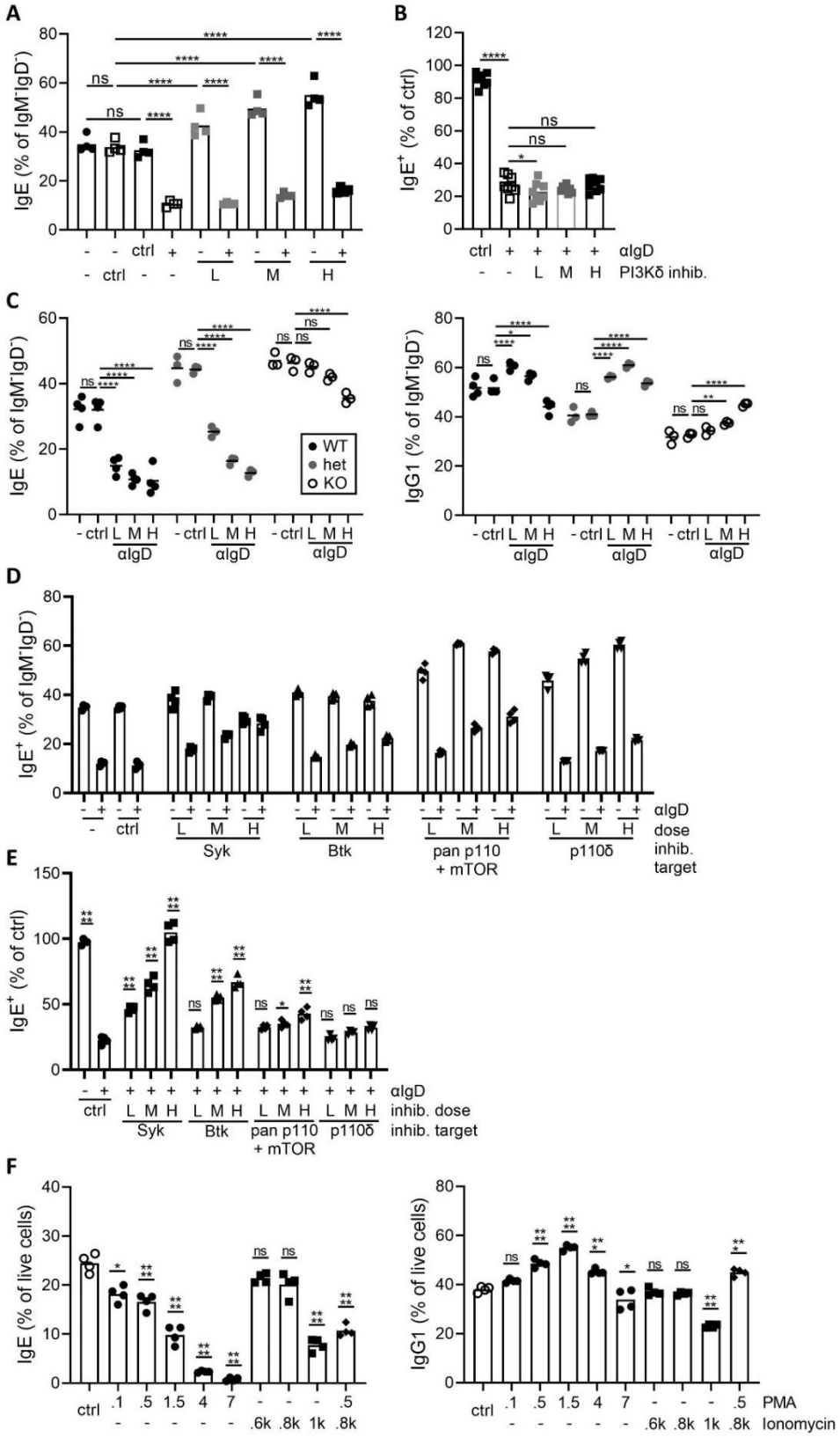

Figure 2.4 BCR stimulation represses IgE CSR via Syk-dependent rather than p110δ-dependent signaling. (A-D) Purified B cells were (Figure caption continued on the next page.)

(Figure caption continued from the previous page.) cultured for 4 days under various conditions of stimulation and/or inhibitor treatment (see labelling of x axes) prior to analysis by flow cytometry. (A) Quantification of the fractional representation of IgE cells among class-switched cells according to treatment with BCR stimulation or control (αIgD or GGG at 1μg/mL) as well as nemiralisib treatment or ctrl (L – 25nM, M – 100nM, H – 250nM; or DMSO). (B) Determination of the % change in IgE cells as a fraction of live cells following stimulation with αIgD (3μg/mL) or control (GGG; 1μg/mL) antibodies for each dose of nemiralisib or the no-treatment control. (C) Quantification of the fractional representation of IgE (left) and IgG1 (right) cells among class-switched B cells from WT (black circle), *Cd19*-heterozygous (grey circle), or *Cd19*-deficient (white circle) mice according to treatment group (-, no treatment; ctrl, GGG at 3μg/mL; L – 300ng/mL αIgD, M – 1μg/mL αIgD, or H – 3μg/mL αIgD). (D) Quantification of the fractional representation of IgE cells among live cells treated with αIgD (1μg/mL) or control (no treatment) and vehicle (DMSO) or one of three doses of inhibitors of Syk (PRT062607, L – 0.4μM, M - 1μM, H – 2.5μM), Btk (ibrutinib; L – 1nM, M – 10nM, H – 50nM), all p110 isoforms and mTOR (GSK2126458; L – 1nM, M – 5nM, H – 10nM), or p110δ (idelalisib/S2226; L – 10nM, M – 50nM, H – 250nM). (E) As in B except for the inhibitors described in D. (F) Quantification of the fractional representation of IgE (left) or IgG1 (right) cells within the class-switched compartment following treatment with the indicated doses of PMA and/or Ionomycin (given in ng/mL). Dots represent samples from individual mice and bars represent the mean values. *, $P < 0.05$; **, $P < 0.01$; ***, $P < 0.001$; ****, $P < 0.0001$ (one-way repeated measures ANOVA [A-F] with Dunnett's post-test comparing the indicated pairs of conditions [A-C], the conditions specified in Table 2.1 [D], the αIgD-treated condition [E], or the vehicle control [F] using the Holm-Sidak correction for multiple comparisons). Results are representative (A, C-F) or pooled from (B) two independent experiments.

achieved in *Cd19*-KO cells and not with inhibition of only the δ isoform of p110) was required to rescue IgE CSR from inhibition by αIgD. A second possibility was that a non-CD19-PI3K pathway was primarily responsible for inhibiting IgE CSR.

To test these possibilities, we performed further experiments with different inhibitors. We selected inhibitors of spleen tyrosine kinase (Syk; PRT062607) and Bruton's tyrosine kinase (Btk; ibrutinib) to assess alternative pathways by which BCR stimulation might inhibit IgE CSR, as well as a second p110δ inhibitor (idelalisib) to validate our earlier results and one pan-p110 + mTOR (mammalian target of rapamycin; GSK2126458) to assess if a more complete blockade of p110 signaling could interfere with the inhibition of IgE CSR by BCR stimulation. Interestingly, in the absence of a BCR ligand both Syk and Btk inhibition left IgE CSR mostly unaffected, whereas

both p110 inhibitors increased IgE CSR (Figure 2.4D, see Table 2.1 for statistical comparisons). Strikingly, both Btk and Syk dose-dependently rescued IgE CSR in the presence of BCR ligand. To control for the impacts of p110 inhibition on CSR independent of BCR stimulation and precisely quantify, the degree of IgE rescue achieved, we again normalized our analysis. Viewing the percentage change in IgE confirmed that the highest dose of Syk inhibitor achieved a complete rescue of IgE CSR from inhibition by BCR stimulation, while maximal Btk inhibition achieved a partial but substantial rescue (Figure 2.4E). Interestingly, whereas the p110δ inhibitor idelalisib achieved no significant rescue of IgE CSR, confirming our earlier result, the pan-p110 + mTOR inhibitor achieved a ~2-fold rescue at its maximal dose, suggesting a modest contribution of PI3K-mTOR to IgE CSR inhibition by BCR stimulation. These data provide strong evidence that p110δ signaling is not required for IgE CSR inhibition by BCR stimulation whereas Syk is required.

To determine if Syk-dependent signaling was sufficient for IgE CSR inhibition we sought to selectively activate different arms of the BCR signaling pathway using phorbol myristate acetate (PMA; a diacylglycerol analog that activates protein kinase C (PKC)) and/or ionomycin (induces Ca^{2+} flux). PMA strongly and dose-dependently reduced the representation of IgE cells, while, at all but the highest dose tested, IgG1 was either unaffected or increased (Figure 2.4F). Meanwhile, the highest dose of ionomycin reduced both IgE and IgG1, with a somewhat stronger effect for IgE. The combined effect of PMA and ionomycin together seemed mostly similar to the effect of stimulation with PMA alone. Overall, these data suggest that Syk-dependent signaling downstream of BCR stimulation, especially including PKC activation but with a minor role for Ca^{2+} flux, is sufficient to inhibit IgE CSR.

Table 2.1 Statistical Testing for Figure 2.4D

Šídák's multiple comparisons test	Summary	Adjusted P Value
neg vs. neg + aIgD	****	<0.0001
ctrl vs. ctrl + aIgD	****	<0.0001
Ibrutinib (50nM) vs. Ibrutinib (50nM) + aIgD	****	<0.0001
Ibrutinib (10nM) vs. Ibrutinib (10nM) + aIgD	****	<0.0001
Ibrutinib (1nM) vs. Ibrutinib (1nM) + aIgD	****	<0.0001
PRT062607 (4uM) vs. PRT062607 (4uM) + aIgD	ns	>0.9999
PRT062607 (2.5uM) vs. PRT062607 (2.5uM) + aIgD	ns	>0.9999
PRT062607 (1uM) vs. PRT062607 (1uM) + aIgD	****	<0.0001
PRT062607 (.4uM) vs. PRT062607 (.4uM) + aIgD	****	<0.0001
GSK2126458 (10nM) vs. GSK2126458 (10nM) + aIgD	****	<0.0001
GSK2126458 (5nM) vs. GSK2126458 (5nM) + aIgD	****	<0.0001
GSK2126458 (1nM) vs. GSK2126458 (1nM) + aIgD	****	<0.0001
S2226 (250nM)0 vs. S2226 (250nM)0 + aIgD	****	<0.0001
S2226 (5nM)0 vs. S2226 (5nM)0 + aIgD	****	<0.0001
S2226 (10nM) vs. S2226 (10nM) + aIgD	****	<0.0001
neg vs. ctrl	ns	>0.9999
ctrl vs. Ibrutinib (50nM)	ns	0.9968
ctrl vs. Ibrutinib (10nM)	ns	0.416
ctrl vs. Ibrutinib (1nM)	*	0.0455
ctrl vs. PRT062607 (4uM)	****	<0.0001
ctrl vs. PRT062607 (2.5uM)	ns	0.0671
ctrl vs. PRT062607 (1uM)	ns	0.5302
ctrl vs. PRT062607 (.4uM)	ns	0.9692
ctrl vs. GSK2126458 (10nM)	****	<0.0001
ctrl vs. GSK2126458 (5nM)	****	<0.0001
ctrl vs. GSK2126458 (1nM)	****	<0.0001
ctrl vs. S2226 (250nM)0	****	<0.0001
ctrl vs. S2226 (5nM)0	****	<0.0001
ctrl vs. S2226 (10nM)	****	<0.0001
neg + aIgD vs. ctrl + aIgD	ns	0.9966
neg + aIgD vs. Ibrutinib (50nM) + aIgD	****	<0.0001
neg + aIgD vs. Ibrutinib (10nM) + aIgD	****	<0.0001
neg + aIgD vs. Ibrutinib (1nM) + aIgD	**	0.0023
neg + aIgD vs. PRT062607 (4uM) + aIgD	****	<0.0001
neg + aIgD vs. PRT062607 (2.5uM) + aIgD	****	<0.0001
neg + aIgD vs. PRT062607 (1uM) + aIgD	****	<0.0001
neg + aIgD vs. PRT062607 (.4uM) + aIgD	****	<0.0001
neg + aIgD vs. GSK2126458 (10nM) + aIgD	****	<0.0001
neg + aIgD vs. GSK2126458 (5nM) + aIgD	****	<0.0001
neg + aIgD vs. GSK2126458 (1nM) + aIgD	****	<0.0001
neg + aIgD vs. S2226 (250nM)0 + aIgD	****	<0.0001
neg + aIgD vs. S2226 (5nM)0 + aIgD	****	<0.0001
neg + aIgD vs. S2226 (10nM) + aIgD	ns	0.9994

IL-21 and BCR stimulation synergize to abrogate IgE CSR

Having established that BCR signaling can substantially inhibit IgE CSR, we sought to determine if its effects were synergistic with IL-21, which our lab previously identified as a critical negative regulator of IgE *in vivo*.[13,16] To this end we cultured B1-8 B cells with cognate antigen and IL-21 (or controls) alone or in combination and measured the effects on IgE and IgG1 CSR. Cognate antigen and IL-21 each produced a strong inhibition of IgE CSR alone, but together resulted in an almost complete absence of IgE cells (Figure 2.5A-B). In contrast, while cognate antigen produced a mild reduction in IgG1 cells as a fraction of live cells (Figure 2.5A), when IL-21 was added alone or in combination IgG1 CSR was increased (Figure 2.5A-B).

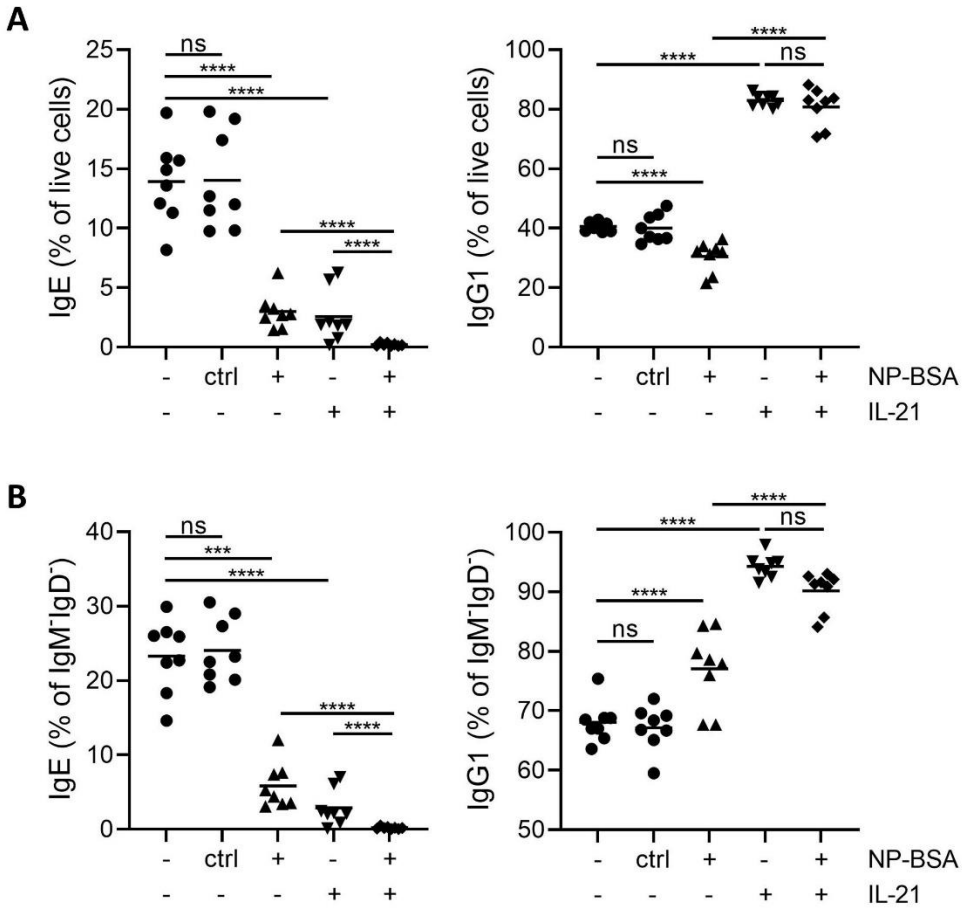

Figure 2.5 B cell receptor stimulation and IL-21 act synergistically to inhibit IgE class switching. (A-B) Quantification by flow cytometry of the frequency of IgE^+ cells from live cells (A) or class-switched cells (B) at D4 of B cell culture (Figure caption continued on the next page.)

(Figure caption continued from the previous page.) with or without control (BSA – 10ng/mL) or cognate (NP_{25}BSA – 10ng/mL) antigen and IL-21 (25ng/mL). (A-B) Dots represent samples from individual mice and bars represent the mean. ns, not significant; ***, $p < 0.001$; ****, $P < 0.0001$ (one-way repeated measures ANOVA with Dunnett's post-test comparing the indicated pairs of conditions with the Holm-Sidak correction for multiple comparisons). Results are pooled from two independent experiments.

BCR ligation inhibits IgE in human cell culture

Finally, we sought to translate our findings to humans by investigating the inhibition of IgE CSR by BCR stimulation of tonsillar B cells cultured in conditions that promote CSR to IgE, IgG1, and IgG4. We observed that, similar to our results in mouse cell culture, αIgM dose-dependently reduced the representation of IgE, but not IgG1 or IgG4, cells among class-switched cells (Figure 2.6A). Next, we investigated the synergism between BCR stimulation and IL-21 treatment of human B cells and found that, as with mouse B cells, BCR stimulation and IL-21 together achieved a greater reduction in IgE than either alone (Figure 2.6B). Also similar to our results in mouse cell culture, IL-21 seemed to increase IgG1 CSR. Neither BCR stimulation nor IL-21, along or together, had a clear effect on IgG4. These findings support the notion that BCR stimulation is a conserved inhibitor of IgE CSR in mice and humans.

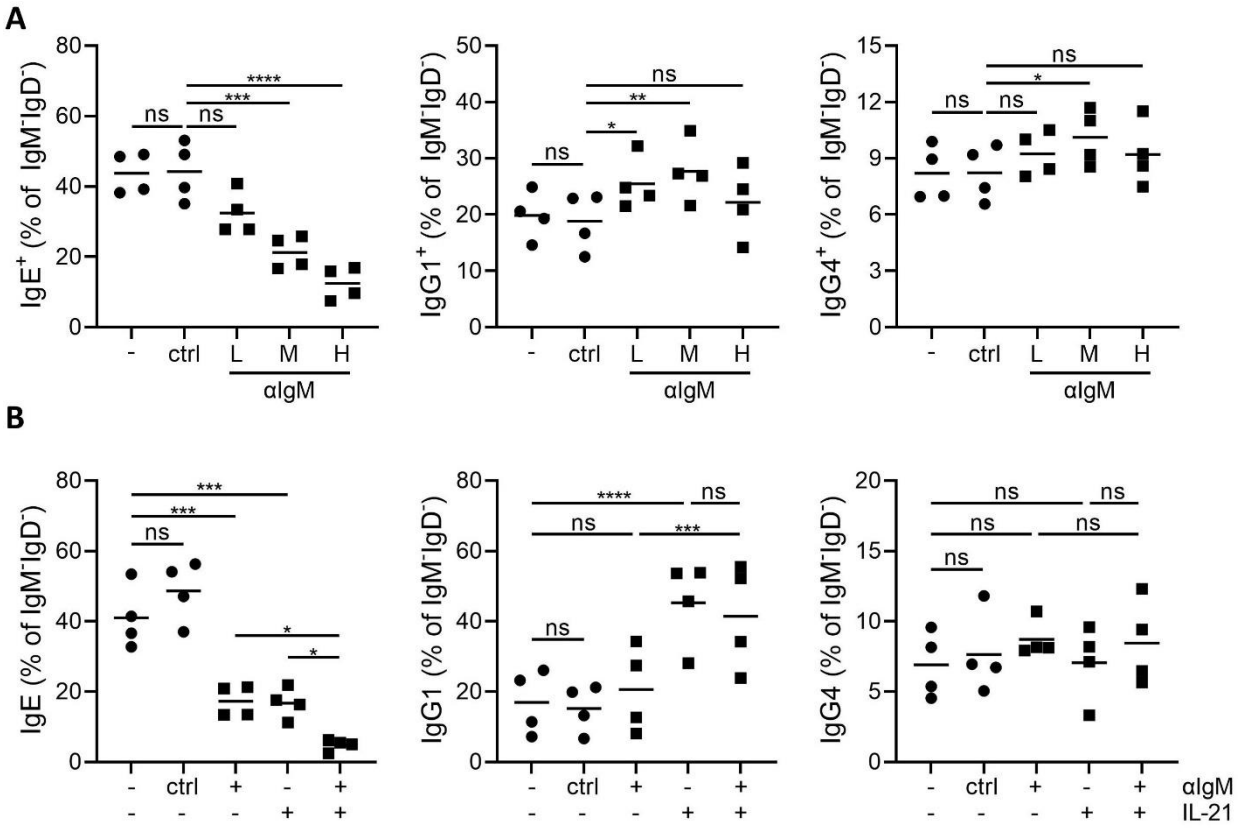

Figure 2.6 BCR stimulation inhibits IgE CSR in human B cells. (A-B) Purified tonsillar naïve B cells were cultured in the indicated treatment conditions (see x axes) for 8 days prior to analysis by flow cytometry. Quantified is the fractional representation of IgE (left), IgG1 (center), and IgG4 (right) within the class-switched (IgM^-IgD^-) compartment. (A) Treatment doses were: GGG (ctrl) – 3μg/mL; αIgM – 0.1/0.3/3μg/mL for low (L) / medium (M) / high (H) doses, respectively. (B) treatment doses were: GGG (ctrl) – 300ng/mL or 2μg/mL, αIgM – 300ng/mL or 2μg/mL, IL-21 (5-10ng/mL). (A-B) Dots represent samples from individual tonsil donors and bars represent the mean. ns, not significant; *, $P < 0.05$; **, $P < 0.01$; ***, $P < 0.001$; ****, $P < 0.0001$ (one-way repeated measures ANOVA with Dunnett's post-test comparing the indicated pairs of conditions and the Holm-Sidak correction for multiple comparisons. Results are pooled from two experiments.

Discussion

Here, we report that BCR stimulation selectively inhibits CSR to IgE in mouse and human B cells. Stronger antigen–BCR interactions reduced IgE more greatly in mouse and human cells *in vitro* as well as in intact mice while CSR to IgG isotypes was not similarly affected. Blocking signaling through Syk produced a full rescue of IgE CSR, while bypassing the BCR using PMA and/or ionomycin was sufficient to inhibit IgE CSR. BCR stimulation acted synergistically with IL-21 to eradicate IgE CSR and this and other key findings were replicated in human tonsillar B cells. These observations establish that IgE CSR is uniquely susceptible to inhibition by BCR signaling.

The present work extends our understanding of the inhibition of IgE CSR by BCR stimulation in several important ways. Firstly, prior work generally found that BCR stimulation broadly inhibited CSR, and did not conclude selective effects of BCR signaling on IgE CSR.[52,53] One study that did find an additional effect of BCR stimulation on IgE proposed that it was due to inhibition of sequential CSR from IgG1,[54] but in our study we performed experiments with αIgD and αIgM targeting non-class-switched BCRs, both of which more strongly inhibited IgE CSR than IgG1 CSR (Figure 2.1C-D and Figure S2.1). These data indicate that the additional effect of BCR stimulation on IgE CSR relative to IgG1 CSR was not only due to the stimulation of the BCR on potential IgG1-expressing class-switch intermediaries.

While prior studies exclusively used antibodies to stimulate the BCR,[51–53,65] we additionally include data with cognate antigen *in vitro* and *in vivo*. These experiments allowed us to examine if different cognate antigens exhibited different selectivity for IgE versus IgG1 CSR inhibition. Indeed, low doses of high-affinity, high-valency antigen most selectively inhibited IgE CSR.

Our qPCR results indicate that a likely mechanism for the inhibition of IgE CSR by BCR stimulation is a reduction in εGLT. This finding contrasts with earlier work exploring the mechanism by which BCR stimulation inhibited CSR, which failed to identify effects on εGLT.[52] This discrepancy between studies could be due to the different culture techniques employed, as this prior work used IL-4 and lipopolysaccharide (LPS) and checked εGLT at D4 whereas we used IL-4 and αCD40 and checked at D2. This and other prior work instead focused on a temporary, BCR stimulation-induced reduction in *Aicda* transcripts as a potential mechanism for CSR inhibition.[52,53] A reduction in AID would represent a logical explanation for reduced CSR, and it might even be that IgE CSR is especially sensitive to AID levels. However, one of these studies ultimately found no effect of BCR stimulation on AID protein abundance or function (despite effects on transcripts),[52] while a series of studies from a different group[51,65] found that, while BCR stimulation reduced AID in a calmodulin-dependent fashion, this actually augmented IgE CSR. Further muddying this picture, other prior work found that BCR stimulation did not reduce *Aicda* transcripts in LPS + IL-4 B cell cultures and did reduce *Aicda* transcripts in CD40 + IL-4 B cell cultures.[53] Here, we found that *Aicda* transcripts were unchanged at D2 and only subtly reduced at D3 by BCR stimulation, suggesting that in our system differences in εGLT represent a more plausible explanation for reduced IgE CSR than differences in *Aicda*.

Using various inhibitors, we establish a Syk-dependent rather than p110δ-dependent signaling mechanism for the inhibition of IgE CSR. The weak rescue of IgE CSR we observed with the pan-p110/mTOR inhibitor in the face of BCR stimulation was unexpected given a prior report that a PI3Kα/δ/β inhibitor completely rescued IgG1 CSR from inhibition by BCR stimulation.[53] This difference in the extent of CSR rescue for IgE and IgG1 might indicate that BCR-dependent effects

on IgG1 CSR are exclusively driven by PI3K signaling, whereas we have shown that BCR-dependent effects on IgE CSR include additional Syk-dependent signaling pathways. This model might also help to explain the selectively enhanced impact of BCR stimulation on IgE switching relative to IgG1. In the future, it would be interesting to test if Syk-dependent signaling is also involved in the inhibition of IgG1 CSR by BCR stimulation, or if this pathway is exclusively important to the inhibition of IgE CSR. The modest rescue of IgE CSR from inhibition by BCR stimulation that we observed with pan-p110/mTOR inhibition is also surprising given the more substantial rescue we observed in the context of CD19 deficiency. This discrepancy could be due to broader effects of CD19 deficiency on BCR signaling as a whole.[66–68] Alternatively, this discrepancy could be due to limitations in the maximal achievable inhibition of PI3K due to the necessity of PI3K signaling for B cell survival.[42] It would be interesting to determine whether BCR ligation-induced tyrosine phosphorylation of Syk and Btk is impaired in CD19-deficient vs WT cells, or whether fixing Btk at the membrane eliminates the ability of CD19-deficiency to rescue IgE CSR from inhibition. Meanwhile, pan-Akt inhibitors could be used to assess the alternative hypothesis that molecules canonically downstream of CD19-PI3K are involved in IgE CSR inhibition by BCR stimulation.

Ours is also the first study, to our knowledge, to identify an effect of PKC activation (via PMA) and Ca^{2+} flux (via ionomycin) on IgE CSR by demonstrating that PKC activation and, to a lesser extent, Ca^{2+} signaling are sufficient to inhibit IgE CSR without the activation of other BCR stimulation-induced signaling pathways. It will be interesting in future work to determine the mechanisms linking PKC activity and Ca^{2+} flux to transcriptional regulation at the IgH locus. The role of PKC in particular was somewhat surprising given its importance to assembly of the CBM

complex (CARD11/Bcl10/Malt1) and subsequent NF-κB activation, with NF-κB activity being a critical requirement for IgE CSR.[70] While it initially seems unlikely that the IgE CSR inhibitory effects of PKC activity result from its activation of NF-κB, the hyper-IgE phenotype observed in patients with CBM mutations suggests it should not be ruled out.[71] Furthermore, activation of inhibitor of kappa kinase beta (IKKβ) (and resultant inhibitor of kappa B alpha [IκBα] phosphorylation) via the non-canonical pathway induced by CD40 ligation is not sensitive to deficiency for PKCβ,[72] indicating that impairing PKCβ-mediated activation of NF-κB downstream of BCR ligation likely would not compromise CD40-induced NF-κB activity and associated IgE CSR. Meanwhile, canonical NF-κB signaling can induce expression of NF-κB inhibitor alpha (IκBα) and p100,[73] indicating that, long-term, BCR stimulation might suppress CD40-induced NF-κB via negative feedback. To assess this possibility, it would be interesting in future work to determine the impact of ongoing BCR ligation on p100:RelB and p52:RelB complexes at D2 when we detected a decrease in εGLT with BCR stimulation. Alternatively, another pathway downstream of PKC, such as MAPK activation, could be responsible for IgE CSR inhibition, while BCR-driven NF-κB activation may simply be redundant with NF-κB activity already induced by CD40 signaling.[73] Inhibitors, such as U0126, could be used to investigate the role of MEK/ERK signaling in the inhibition of IgE CSR by BCR stimulation.

Our finding of synergy between BCR signaling and IL-21 for the inhibition of IgE CSR is potentially of particular relevance to the physiologic regulation of IgE. As discussed above, T_{FH} are a critical source of both IL-4, which promotes IgE CSR, as well as IL-21, which inhibits IgE CSR. The extent of T cell help received by a B cell is related to the amount of antigen presented, and therefore not only are BCR ligands likely present while B cell : T cell interactions are occurring

but also the affinity of the BCR will affect both the strength of the BCR signal received and the nature of the B : T interaction as a result of the quantity of gathered antigen. It will be interesting to examine how receiving these signals *in vivo* selectively regulates CSR to IgE or other isotypes.

Our finding that BCR stimulation also impaired human IgE CSR provides an important translation for this topic which until now was restricted to mouse studies. We found that αIgM produced similar inhibition of IgE CSR in human cells to that which we observed in mouse cells. Interestingly, prior work suggests that observations with p110 inhibitors increasing baseline switching to IgE[56] may not translate to humans, as inhibition of p110δ was reported to reduce IgE in cultured human B cells.[74] It will be interesting to determine in the future if the inhibition of IgE CSR by BCR stimulation in human cells is Syk-dependent, as we observed in mouse B cells.

Methods

Mice and immunizations

All mice used for experiments in this study were on a C57BL/6 (B6) background (backcrossed ≥10 generations). Mice for experiments were sex and age-matched between groups as much as possible and both male and female mice were used. For *in vivo* experimentation, mice were at least 6 weeks of age and for *in vitro* experimentation donor animals were at least 5 weeks of age. Mice were housed in specific-pathogen-free facilities. Mouse work was approved by the Institutional Animal Care and Use Committee (IACUC) of the University of California, San Francisco (UCSF). *IgH*$^{B1\text{-}8i}$ (012642; B6.129P2(C)-*Igh*^{tm2Cgn}/J), Boy/J (002014; B6.SJL-*Ptprc*^{a}*Pepc*^{b}/BoyJ), B6/J (000664; C57BL/6J), and B6 Thy1.1 (000406; B6.PL-*Thy1*^{a}/CyJ) mice were originally from The Jackson Laboratory and were maintained in our colony. B6/J, Boy/J, and B6 Thy1.1 mice were used as "WT" throughout. *Cd19*^{Cre} mice[75] were maintained in our colony on a B6 background. All immunizations consisted of NP conjugated to chicken gamma globulin (NP-CGG; Biosearch Technologies) dissolved in D-PBS at 1mg/mL and mixed 50:50 volumetrically with Alhydrogel (Accurate Chemical and Scientific). 20μL of this solution (10μg of NP-CGG) was delivered to each ear by subcutaneous injection and the facial LNs from each side were pooled for analysis at endpoint (d7) by flow cytometry.

HEL-OVA/DEL-OVA preparation

HEL/DEL-OVA conjugations were carried out as using maleimide thiol chemistry as described previously.[33] Correct product formation was verified with SDS-PAGE. Finally, products were separated from reactants by HPLC, enrichment was assessed using SDS-PAGE, and concentration was determined by A_{280}.

Mouse cell culture, in vitro BCR stimulation, and inhibitor treatments

All *in vitro* mouse cell culture experiments were performed with B cells purified by negative selection as described previously.[2] After purification, cells were resuspended in complete RPMI (cRPMI), components as described previously.[2] Purified B cells were seeded at a density of 2-10 * 10^3 cells per well and were cultured for 4 days prior to analysis by flow cytometry or for 2-3 days prior to analysis by RT-qPCR. Cells were plated in triplicate for each condition, except for some cell trace violet experiments where sextuplicates were used. In some cases, CD45-congenic B cells were co-plated to allow the combined assessment of cells from two different mice.

BCR stimulation with antibodies was performed using goat anti-mouse IgD (Sapphire North America), goat polyclonal F(ab')2 anti-mouse Igκ (LifeSpan Biosciences), goat polyclonal F(ab')2 anti-mouse IgM (αIgM; Jackson ImmunoResearch), or Chrompure Goat IgG (Jackson ImmunoResearch) as a control. BCR stimulation with cognate antigen was performed using NP(4)BSA (Biosearch Technologies), NP(25)BSA (Biosearch Technologies), NIP_{24}BSA (Biosearch Technologies), or BSA (Sigma-Aldrich) as a control. Stimulations were prepared in the culture medium at the doses indicated in figure legends. All inhibitors were diluted in DMSO. The concentration of DMSO in culture never exceeded 0.1% and was typically lower. The specific DMSO vehicle control concentration in each experiment was made to be equivalent to the highest concentration of DMSO in any inhibitor-treated well. See figure captions for specific inhibitors and concentrations used.

Cell trace violet labelling

Labelling with cell trace violet (CTV; Life Technologies Corporation) was performed as described

previously.[13] Briefly, cells were incubated with CTV at 1μM for 20 minutes in a 37ºC water bath and then washed twice with FBS (Life Technologies Corporation) underlaid in each wash step. When calculating seeding density, it was assumed that CTV labelling resulted in a 75% reduction in live B cells.

RNA extraction, cDNA conversion, and RT-qPCR amplification

Harvesting of nucleic acids, the preparation of cDNA, and RT-qPCR amplification, standard curve preparation, and analysis were performed as described previously.[13] The following specific primers were used for the qPCR assays:

ε GLT forward: 5'-TCGAATAAGAAC AGTCTGGCC-3'

ε GLT reverse: 5'-TCACAGGACCAGGGAAGTAG-3'

γ1 GLT forward: 5'-CAGGTTGAGAGAACCAAGGAAG-3'

γ1 GLT reverse: 5'-AGGGTCACCATGGAGTTAGT-3'

Aicda forward: 5' CCTAAGACTTTGAGGGAGTCAA-3'

Aicda reverse: 5'-CACGTAGCAGAGGTAGGTCTC-3'

Hprt (internal control) forward: 5'-TGACACTGGCAAAACAATGCA-3'

Hprt (internal control) reverse: 5'GGTCCTTTTCACCAGCAAGCT-3'

Human samples, B cell purification, and cell culture

Human B cells were purified from tonsils fractions obtained from UCSF pathology. Excess tissue collected following routine tonsillectomies was completely de-identified, allowing samples to not be classified as human subjects research according to the guidelines from the UCSF Institutional Review Board. Tonsillar tissue was dissociated, a single cell suspension was prepared and then

cells were cryopreserved as described previously.[76] Naive B cells were purified by magnetic bead depletion using the Mojosort Human Naive B Cell Isolation kit (BioLegend) according to manufacturer's instructions but with some additional modifications as previously described.[13] Following purifications, naïve human B cells were resuspended in complete Iscove's modified Dulbecco's medium (cIMDM), consisting of: IMDM supplemented with GlutaMAX™ (Gibco), 10 % FBS, 1X pencillin-streptomycin (UCSF Cell Culture Facility), 1X insulin-transferrin-selenium (ITS-G, Fiser Scientific), 0.25μg/mL Amphotericin B (Neta Scientific), and 100 IU/mL Nystatin (Neta Scientific).

A fraction of purified cells was analyzed by flow cytometry to verify purity. Cells were then cultured for 8 days with 100ng/mL anti-human CD40 antibody (clone G28.5; Bio-X-Cell), 25ng/mL recombinant human IL-4 (Peprotech), and 50ng/mL human IL-10 (Peprotech). Where indicated in the figure caption, 50ng/mL human IL-21 (Peprotech), goat anti-human IgM F(ab')2 fragments, or goat gamma globulin (control) was added in addition.

Flow cytometry

Processing of dLNs and downstream flow cytometric analysis was performed as previously described.[2] For both *in vivo* and *in vitro* experiments all incubations were 20 minutes on ice except for Fc block incubations (10 minutes) and antibody staining of fixed and permeabilized cells (45 minutes to 1 hour). For human experiments, excess mouse gamma globulin was used to block, as anti-human fluorochrome conjugates were mouse IgG antibodies. See Tables 2.3 and 2.4 for mouse and human flow cytometry reagents, respectively.

For both mouse and human experiments, we used our previously-established intracellular staining technique[29] to sensitively and specifically detect IgE-expressing cells. Briefly, to prevent the detection of IgE captured by non-IgE-expressing cells, surface IgE was blocked with a large excess of unconjugated αIgE (clone RME-1 for mouse experiments, clone MHE-18 for human experiments). IgE-expressing cells were then detected after fixation/permeabilization by staining with a low concentration of fluorescently-labelled αIgE of the same clone.

After staining, cells were collected on an LSRFortessa (BD). Data were analyzed using FlowJo v10. Counting beads were identified by their high SSC and extreme fluorescence and were used to determine the proportion of the cells plated for staining that had been collected on the flow cytometer for each sample. Cells were gated on FSC-W versus FSC-H and then SSC-W versus SSC-H gates to exclude doublets and as negative for the fixable viability dye eFluor780 and over a broad range of FSC-A to capture resting and blasting live lymphocytes. 2D plots were presented as contour plots with outliers shown as dots.

Statistical analysis

To achieve power to discern meaningful differences, experiments were performed with multiple biological replicates and/or multiple times, see figure legends. The number of samples chosen for each comparison was determined based on past similar experiments to gauge the expected magnitude of differences. GraphPad Prism v9 was used for statistical analyses. Data approximated a log-normal distribution and thus were log transformed for statistical tests. Statistical tests were selected by consulting the GraphPad Statistics Guide according to experimental design. All tests were two-tailed. Groups were assumed to have similar standard deviation for ANOVA analysis.

Table 2.2: Antibody-fluorochrome conjugates and other reagents used for flow cytometry in mouse experiments

Antibody target or reagent designation	Clone	Company	Conjugate	Dilution
B220	RA3-6B2	BD Biosciences	V500	1/100
		Life Technologies	Qdot 655	1/100-400 (varies by lot)
			APC	1/200
CD38	90	Life Technologies	Alexa Fluor 700	1/100
		BD Biosciences	Brilliant Violet 786	1/200
CD45.1	A20	BD Biosciences	Alexa Fluor 647	1/200
			Alexa Fluor 700	1/100
CD45.2	104	Biolegend	Biotin	1/400
			FITC	1/100
			Brilliant Violet 785	1/100
CD138	281-2	BD Biosciences	Brilliant Violet 711	1/175
Fixable Viability Dye eFluor 780	N/A	Life Technologies	N/A	1/600-1000
IgD	11-26c.2a	Biolegend	PerCP-Cy5.5	1/200
			Alexa Fluor 700	1/100
IgE	RME1	Biolegend	Unconjugated	1/15
			FITC	1/300-500
			PE	1/300-500
IgG1	A85-1	BD Biosciences	V450	1/300-400
			FITC	1/300-400
$Ig\lambda_{1,2,3}$	R26-46	BD Biosciences	FITC	1/200
IgM	II/41	Life Technologies	PE-Cy7	1/175-1/400
NP	N/A	Conjugated in-house as described.[33]	APC	1/750 of 0.1mg/mL stock
PNA (peanut agglutinin)	N/A	Vector Laboratories	Biotin	1/1000
			FITC	1/500
Streptavidin	N/A	Life Technologies	QDot 605	1/400
		BD Biosciences	Brilliant Violet 711	1/400
TruStain FcX (anti-mouse CD16/32)	93	Biolegend	Unconjugated	1/50

Table 2.3: Antibody-fluorochrome conjugates and other reagents used for flow cytometry in human experiments

Antibody target or reagent designation	Clone	Company	Conjugate	Dilution
CD20	2H7	Biolegend	Pacific Blue	1/200
CD27	O323	Biolegend	PE	1/50
CD38	HB-7	Biolegend	PE-Cy7	1/200
Fixable Viability Dye eFluor 780	N/A	Life Technologies	N/A	1/600-1000
IgD	IA6-2	Biolegend	PerCP-Cy5.5	1/50
IgE	MHE-18	Biolegend	Unconjugated	1/10
			APC	1/150-300
IgG1	IS11-12E4.23.30	Miltenyi Biotec	biotin	1/150-300
IgG4	HP6025	Southern Biotechnology	FITC	1/800
IgM	MHM-88	Biolegend	Brilliant Violet 605	1/125-1/200
Streptavidin	N/A	Life Technologies	QDot 605	1/400
		BD Biosciences	Brilliant Violet 711	1/400
Mouse gamma globulin	N/A	Jackson Immunoresearch	Unconjugated	1/100

Chapter 3: B cell receptor ligation eliminates IgE plasma cells

Abstract

The proper regulation of IgE production safeguards against allergic disease, highlighting the importance of mechanisms that restrict IgE plasma cell (PC) survival. IgE PCs have unusually high surface B cell receptor (BCR) expression, yet the functional consequences of ligating this receptor are unknown. Here, we found that BCR ligation induced BCR signaling in IgE PCs followed by their elimination. In cell culture, exposure of IgE PCs to cognate antigen or anti-BCR antibodies induced apoptosis. IgE PC depletion correlated with the affinity, avidity, amount, and duration of antigen exposure and required the BCR signalosome components Syk, BLNK, and PLCγ2. In mice with a PC-specific impairment of BCR signaling, the abundance of IgE PCs was selectively increased. Conversely, BCR ligation by injection of cognate antigen or anti-IgE depleted IgE PCs. These findings establish a mechanism for the elimination of IgE PCs through BCR ligation. This has important implications for allergen tolerance and immunotherapy as well as anti-IgE monoclonal antibody treatments.

Introduction

The production of IgE specific for environmental antigens is a critical driver of allergic disease. Normally, the production of IgE is tightly controlled and the abundance of IgE in serum is orders of magnitude less than that of IgG. In the past decade, technical advancements in the detection of rare IgE-expressing cells have rapidly expanded our knowledge of the mechanisms that limit IgE production.

IgE-expressing (IgE) B cell responses are constrained by multiple key regulatory mechanisms. The initial class-switch recombination to IgE requires adequate IL-4 and is profoundly inhibited by IL-21, leading to the generation of limited numbers of IgE B cells.[13,77–79] Once generated, IgE B cells exhibit a propensity to undergo rapid differentiation into IgE antibody-secreting cells (plasmablasts or plasma cells [PCs], which we collectively refer to hereafter as PCs for simplicity).[22,29] IgE B cells are rare within germinal centers (GCs) and their relative abundance there further diminishes over time.[29,31] In GCs, B cells undergo iterative cycles of Ig mutation and selection, resulting in antibody refinement and affinity maturation, and ultimately differentiate into long-lived PCs or memory B cells. In contrast, most IgE PCs are short-lived and are generated independently from GCs, while IgE memory B cells have not been reliably detected.[29,31,80,81]

The skewed cell fate trajectories of IgE B cells are driven by antigen-independent signaling of the IgE B cell receptor (BCR). When B cells were cultured in the absence of cognate antigen, the expression of membrane IgE (mIgE) resulted in enhanced PC differentiation compared with the expression of other BCR isotypes.[32,33] In addition, genetic deficiency or pharmacological inhibition of proteins involved in BCR signal transduction, such as Syk, Btk, BLNK, and CD19,

resulted in a decrease in the frequency of IgE PCs in cell culture without antigen.[32,33] A recent CRISPR screen in cell culture[35] further highlighted the contribution of BCR signaling components to IgE PC differentiation without antigen. Overall, these data are consistent with a model that the IgE BCR has antigen-independent activity that promotes PC differentiation.[32,33]

Based on this model, we predicted that mice with impaired BCR signal transduction would have reduced IgE PC differentiation, which would result in the enhanced differentiation and/or maintenance of IgE GC B cells. While these mice indeed had increased frequencies of IgE B cells in GCs, unexpectedly they also had increased numbers of IgE PCs.[32,33] Moreover, a recent mutagenesis screen in mice found that IgE production was increased when BCR signaling was impaired.[82] One possibility is that the increases in IgE PCs in the context of *in vivo* BCR signaling impairments were due to the enhanced IgE GC B cell responses. Indeed, in BLNK-deficient mice, a sustained increase in the abundance of IgE PCs was observed, and Ig sequencing four weeks after immunization showed somatic mutations consistent with a GC origin.[32] However, we also observed an increase in IgE PCs early after immunization of mice with BLNK-deficiency or with heterozygous mutations in *Syk*,[33] suggesting these PCs may be generated through the extrafollicular pathway, independently from GCs. We confirmed that most IgE PCs expressed unmutated, germline Ig sequences, consistent with a GC-independent origin, 9 days after immunization of mice with *Syk*-heterozygous activated B cells.[33] The mechanism by which impairments of BCR signal transduction led to increases in both GC-dependent and GC-independent IgE PC responses *in vivo* remains unclear.

One possibility to account for these findings is that BCR signaling has direct effects on differentiated IgE PCs rather than only their IgE B cell precursors. While the differentiation of B cells into PCs is often thought to coincide with a shift from the expression of membrane Ig (mIg) to secreted Ig (sIg), we and others previously reported that IgE PCs upregulated mIg expression compared with IgE B cells.[29,31,34] High mIg expression has also been observed on IgM and IgA PCs, and these BCRs were signaling-competent.[48,49] Whether the BCR on IgE PCs is functional has not been directly examined. In addition, while previous studies focused on antigen-independent signaling of the IgE BCR,[32,33] antigen stimulation of the BCR would be relevant to real-world immunizations, allergen exposures, allergen immunotherapies, and parasitic worm infections.

Here, we report that high surface mIg expression on IgE PCs corresponds with elevated phosphorylation of Syk, BLNK, and PLCγ2 after stimulation with antigen. Cell culture studies revealed that this BCR signaling depleted antigen-specific IgE PCs in a manner that corresponded to the strength and duration of BCR stimulation. Consistent with the induction of apoptosis in IgE PCs after cognate antigen exposure, BCR ligation led to caspase-3 activation in IgE PCs, followed by cell death, which was rescued by *Bcl2* overexpression. Antigen-induced IgE PC elimination was also blocked by inhibition of Syk or genetic deficiency in *Blnk* or *Plcg2*, highlighting the importance of the BCR signalosome to this process. *In vivo*, heterozygosity for *Syk* specifically in PCs resulted in an increase in the absolute number and relative frequency of IgE PCs. Conversely, ligating mIgE on IgE PCs with cognate antigen or a monoclonal antibody led to the robust depletion of IgE PCs. Based on these findings, we propose that IgE PCs are intrinsically regulated by BCR signaling-induced apoptosis.

Results

IgE PCs have heightened BCR expression and signaling

Previous studies in mice revealed that IgE PCs, in addition to expressing large amounts of sIg, have markedly elevated surface mIg expression compared with IgE GC B cells and IgG1 PCs.[29,31] However, the relative surface mIg abundance on IgE-expressing cells compared with IgM-expressing cells has not been reported. We therefore directly compared the surface BCR expression on IgE PCs to GC B cells and PCs of various isotypes *in vivo*. IgE-expressing cells were robustly identified by our intracellular staining approach (see Methods for details and Figure S3.1 for gating strategy). To control for possible effects of the Ig variable region on surface BCR expression, we utilized B cells from B1-8i (hereafter referred to as B1-8) mice.[62] These B cells express a knock-in heavy chain VDJ specific for the hapten 4-hydroxy-3-nitrophenyl (NP) when paired with Igλ light chains. To compare mIg expression *in vivo*, we adoptively transferred naïve Igλ-enriched B1-8 B cells into *Cd19*$^{-/-}$ recipients, immunized them with NP conjugated to chicken gamma globulin (NP-CGG) in alum adjuvant, and then analyzed the surface BCR expression on responding B1-8 cells in the draining lymph nodes (dLNs) by flow cytometry. For equivalent comparison of surface mIg expression, we stained the Ig light chain (LC) on cells with an antibody to Igλ. We observed that IgE PCs had the highest surface mIg expression among all isotypes of GC B cells and PCs examined, which was more than an order of magnitude higher than IgG1 PCs and IgE GC B cells and was slightly higher (1.5- to 2-fold) than IgM PCs and naïve B cells (Figure 3.1A).

We next tested whether ligation of mIg on IgE PCs would trigger an intracellular BCR signaling

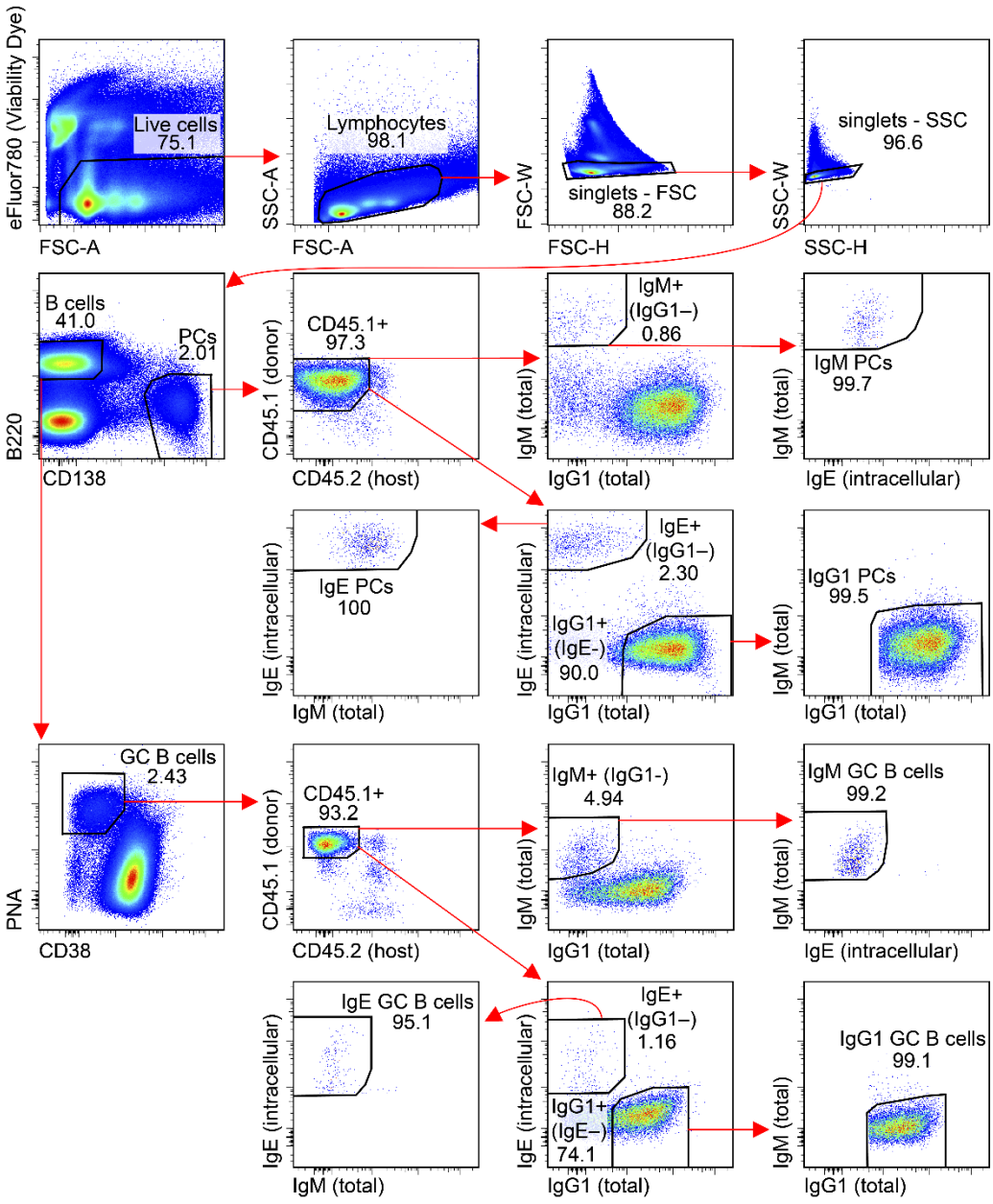

Figure S3.1: Representative flow cytometric analysis of cells from draining LNs. Cells were gated for viability, as lymphocytes based on their scatter characteristics, and then as singlets by pulse width versus height. Cells were then sub-divided into B cell and PC populations. In this particular representative gating strategy, cells were also gated on congenic markers ($CD45.1^+$ $CD45.2^-$) to isolate transferred cells. PCs were then gated as highly expressing intracellular Ig of the indicated isotype without expression of Ig of any other isotype by sequential gating. GC B cells were gated as $PNA^{hi}CD38^-$ and then by isotype, using a similar strategy as for PCs. All plots shown are from the same representative sample.

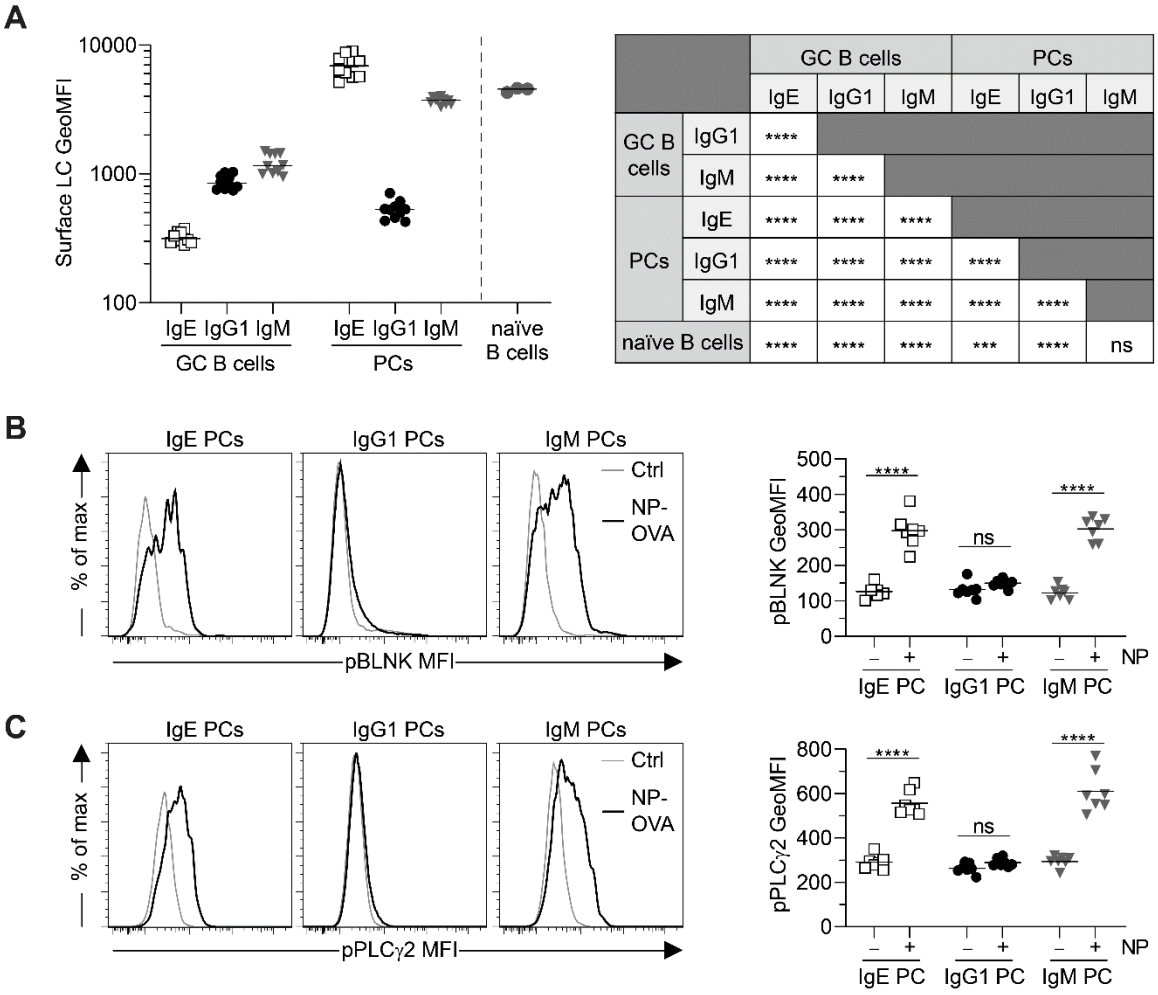

Figure 3.1: IgE PCs have high surface BCR expression and enhanced signaling in response to antigen in vivo. (A) Quantification of the surface expression of Igλ LC on the indicated cell types by flow cytometry. B1-8 B cells were adoptively transferred into $Cd19^{-/-}$ mice, which were then immunized subcutaneously with NP-CGG in alum adjuvant. dLNs were collected 6 d later. After gating on congenic markers to identify transferred B1-8 cells, GC B cells were gated as $B220^{hi}CD138^{-}PNA^{+}CD38^{-}IgD^{-}$ and PCs were gated as $B220^{int}CD138^{+}$ and negative for other isotypes; see Figure S3.1 for detailed gating strategy. Data for GC B cells and PCs are pooled from two independent experiments. For analysis of naive B cells, splenocytes were isolated from separate B1-8 mice at the time of analysis and cells were gated as $B220^{hi}CD38^{+}IgD^{+}$ $Ig\lambda^{+}$ and NP-binding. (B and C) Phosflow analysis of pBLNK (B) and pPLCγ2 (C) after in vivo BCR stimulation with representative histograms (left) and quantification (right). Mice were immunized subcutaneously with NP-CGG in alum adjuvant and then, 6.33–6.5 d later, were injected with NP-OVA 30 min prior to the collection of dLNs. PCs were gated as $B220^{int}CD138^{+}$ and negative for other isotypes. Data are pooled from three independent experiments. Dots represent samples from individual mice and bars represent the mean. ***, $P < 0.001$; ****, $P < 0.0001$ (one-way ANOVA with Tukey's post-test comparing the mean of each group with the mean of every other group [A, table], one-way ANOVA with Sidak's post-test comparing the means of pre-selected pairs of groups [B and C]). GeoMFI, geometric mean fluorescence intensity.

cascade as has been reported for IgM and IgA PCs.[48,49] We injected antigen *in vivo* and examined the activation of intracellular signaling proteins by phosflow 30 minutes later. IgE and IgM PCs exhibited robust phosphorylation of BLNK (Figure 3.1B) and PLCγ2 (Figure 3.1C), whereas IgG1 PCs did not, indicating that IgE and IgM PCs can sense and respond to antigen *in vivo*.

To further explore BCR signaling in IgE PCs, we turned to an *in vitro* cell culture system. B cells were cultured with anti-CD40 (αCD40) and IL-4 to induce class-switch recombination and PC differentiation. For studies of BCR expression, we cultured Igλ-enriched B1-8 cells and detected surface BCR expression by flow cytometry with an antibody to the Igλ LC. In cell culture, we observed that IgE and IgM PCs had similar BCR expression, which was higher than IgG1 PCs (Figure S3.2A). Surface BCR expression on IgE PCs was also higher than on IgE B cells, which had several-fold lower surface BCR expression than IgG1 and IgM B cells. Overall, these trends were similar to B1-8 cells differentiated in mice (Figure 3.1A), although we observed a further upregulation of surface BCR expression on IgE PCs generated *in vivo*.

To assess BCR signaling *in vitro*, we cultured polyclonal purified B cells, the vast majority of which express Igκ LC, and then ligated the BCRs with a polyclonal antibody to Igκ (αIgκ). Due to the increased numbers of IgE-expressing cells we were able to generate *in vitro*, we were able to assess the phosphorylation of Syk in addition to BLNK and PLCγ2. BCR ligation led to the phosphorylation of Syk (Figure S3.2B), BLNK (Figure S3.2C), and PLCγ2 (Figure S3.2D), which was more pronounced for IgE PCs and IgM PCs compared with IgG1 PCs, consistent with the relative amounts of surface BCR on these cells.

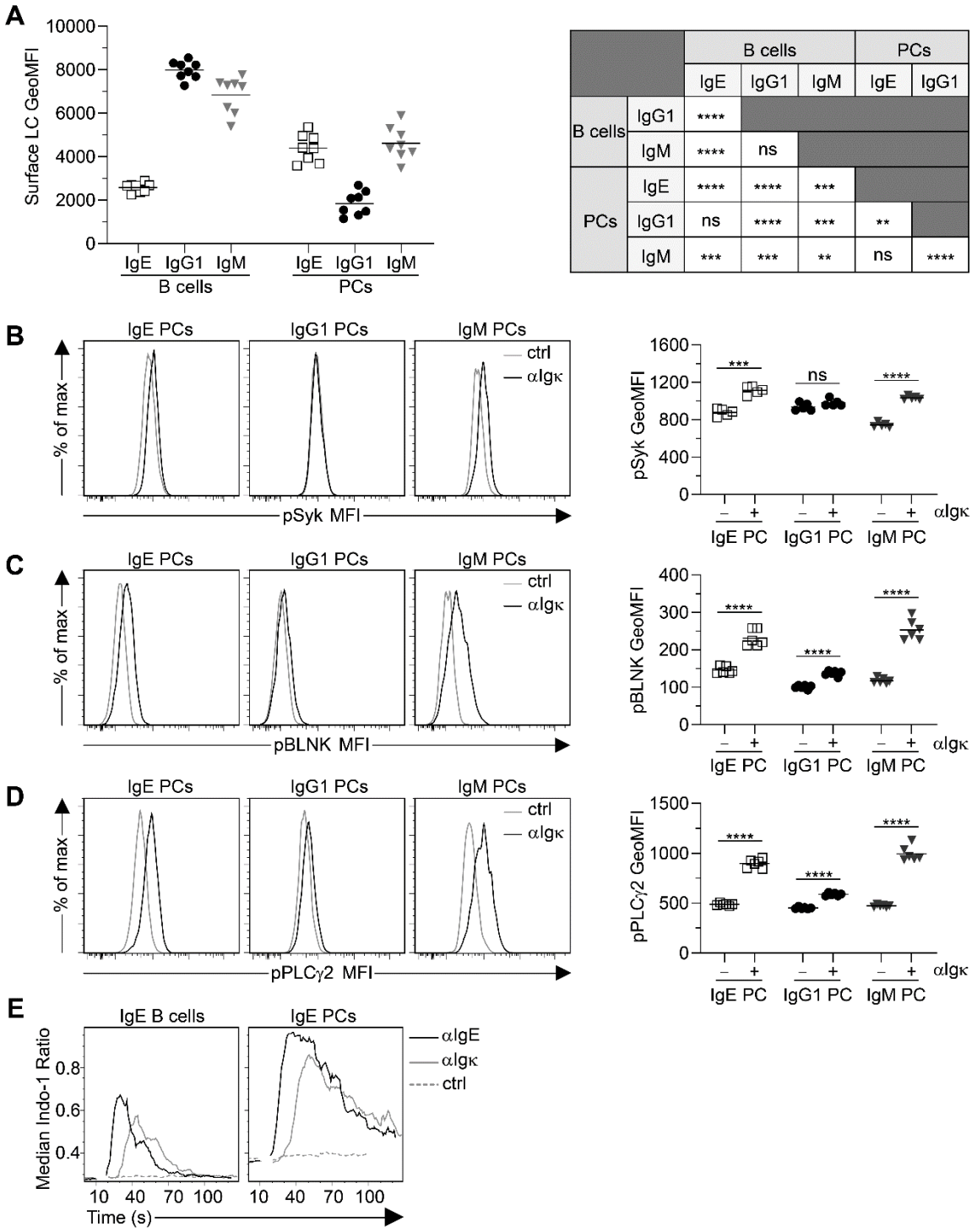

Figure S3.2: IgE PCs have high surface BCR expression and enhanced signaling in response to antigen in vitro. (A) Quantification of the surface Igλ LC expression on the indicated cell types by flow cytometry of Igλ-enriched B1-8 B cells cultured for 5.5 d ± 6 h. B cells were gated as $B220^{+}CD138^{-}IgD^{-}$ and PCs were gated as $B220^{int}CD138^{+}$. Residual $Ig\kappa^{+}$ B cells were excluded by gating on NP-binding cells. GeoMFI, geometric mean fluorescence intensity. (B–D) Phosflow analysis of pSyk (B), pBLNK (C), and pPLCγ2 (D) with representative histograms (left) and quantification (right). Purified B cells were cultured (Figure caption continued on the next page.)

(Figure caption continued from the previous page.) for 4.5 d then treated for 5 min with either polyclonal goat anti-Igκ F(ab)'2 antibody (αIgκ; "+") or goat IgG control ("–"). PCs were gated as $B220^{int}IgD^{-}CD138^{+}$ and negative for other PC isotypes. (E) Purified Verigem B cells were cultured for 4.5 d, after which cells were stained and loaded with Indo-1. Shown are plots of the median ratio of bound:unbound Indo-1 in IgE B cells (left; identified as $Venus^{lo}CD138^{-}$) and IgE PCs (right; identified as $Venus^{hi}CD138^{+}$) prior to and following administration of the indicated control or stimulating antibodies. Dots represent cells cultured from individual mice and bars represent the mean (A–D). **, $P < 0.01$; ***, $P < 0.001$; ****, $P < 0.0001$ (one-way ANOVA with Tukey's post-test comparing the mean of each group with the mean of every other group [A, table], one-way ANOVA with Sidak's post-test comparing the means of pre-selected pairs of groups [B–D]). Data are pooled from (quantification graphs and table) or representative of (histograms) two (A–D) or three (E) independent experiments.

To determine whether BCR stimulation induced Ca^{2+} flux in IgE PCs, we took advantage of Verigem IgE reporter mice in which IgE-switched B cells and PCs express the Venus yellow fluorescent protein.[29] Cultured Verigem B cells were loaded with the Ca^{2+}-sensitive, ratiometric dye Indo-1 and were then stimulated with anti-BCR antibodies. Both IgE PCs and IgE B cells fluxed Ca^{2+}, but IgE PCs exhibited stronger Ca^{2+} flux in response to BCR stimulation with either αIgE or αIgκ (Figure S3.2E). Together, these findings demonstrate that IgE PCs have elevated mIg which corresponds to increased signaling in response to BCR ligation.

IgE PCs are preferentially lost in response to cognate antigen

We next sought to determine the functional consequence of BCR signaling in IgE PCs. In our Igλ-enriched B1-8 B cell culture system, approximately 50-80% of PCs expressed NP-specific BCRs. This allowed us to assess the responsiveness of NP-specific and non-specific IgE PCs in the same culture. When IgE PCs reached peak numbers at day 4.5, we added cognate antigen (NP conjugated to bovine serum albumin, NP-BSA) for BCR stimulation or control antigen (BSA). We then detected NP-specific cells by flow cytometry with NP-APC staining after fixation and permeabilization; this approach allowed us to detect antigen-specific PCs due to their abundant intracellular Ig, even if NP-BSA treatment might have blocked their surface mIg. After 24 hours

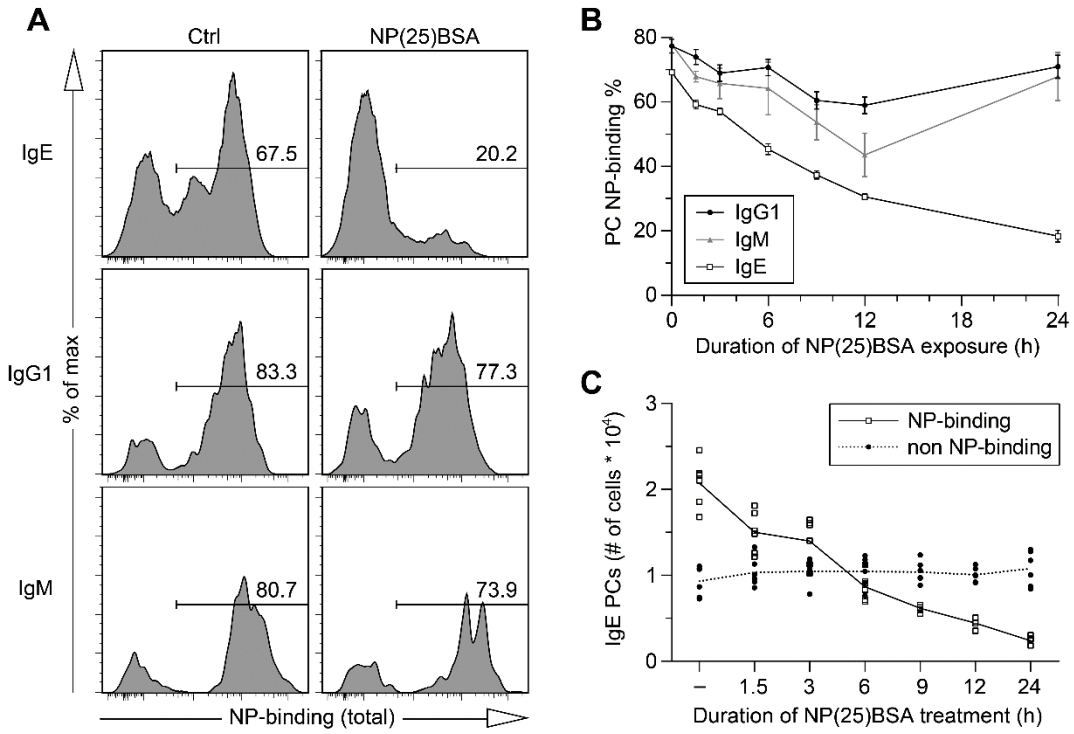

Figure 3.2 IgE PCs are preferentially depleted by cognate antigen over time. (A–C) Igλ-enriched B1-8 B cells were cultured for 5.5 d ± 6 h. (A) Representative flow cytometry histograms showing the proportion of PCs ($B220^{int}CD138^{+}$) of the indicated isotypes with total (surface + intracellular) binding to NP-APC after 24 ± 3 h of exposure to either NP(25)BSA (50 ng/ml) or control antigen (BSA; 50 ng/ml). (B and C) NP(25)BSA (50 ng/ml) was added at the indicated timepoints, compared with a no antigen control ("0 h" in B and "–" in C), prior to analysis by flow cytometry, as in A. (B) The proportion of PCs of each isotype that bound NP-APC is shown over time. Dots represent the mean of each group (cells from n = 6 mice) and error bars reflect standard error. (C) The number of IgE PCs that were either NP-binding (white squares) or non–NP-binding (black circles) is shown over time. Dots represent samples from individual mice. In B and C, lines are drawn connecting the mean values. Results are representative of >10 independent experiments (A) or are pooled from two independent experiments (B and C).

of stimulation, we observed a profound decrease in the proportion of IgE PCs that were NP-binding, whereas there was no change in the proportions of IgG1 or IgM PCs that were NP-binding (Figure 3.2A). This result indicated that antigen recognition selectively disfavored antigen-specific IgE PCs. In an extensive timecourse analysis, the proportion of IgE PCs that were NP-binding decreased over time to a greater extent than for IgM PCs and IgG1 PCs (Figure 3.2B). Notably, the proportion of IgM and IgG1 PCs that were NP-specific transiently decreased at intermediate

timepoints (6-12h), but by 24 hours had recovered. This phenomenon may have been due to antigen-induced BCR signaling in IgM and IgG1 B cells that promoted the differentiation of new IgM and IgG1 PCs, whereas IgE PC differentiation in cell culture is antigen-independent.[32,33] To further assess if the observed reduction in the proportion of NP-binding IgE PCs after NP-BSA treatment was due to a decrease in the number of NP-binding cells or an increase in the number of non-antigen-binding cells, we enumerated these cells over the timecourse. The number of non-antigen specific IgE PCs was constant, whereas the number of NP-specific IgE PCs declined steadily with increasing duration of NP-BSA exposure (Figure 3.2C). These findings indicate that antigen-mediated stimulation of the BCR on IgE PCs leads to their loss over time.

The loss of IgE PCs is proportional to the strength of BCR stimulation

We next investigated the relationship between the strength of BCR stimulation and the loss of IgE PCs in our B1-8 B cell culture system. BCR stimulation strength was modulated by altering the dose and valency of NP-BSA treatment for the final 24 hours of the culture and the proportion of IgE PCs that were NP-binding was determined by flow cytometry as above. The depletion of NP-specific IgE PCs was much more pronounced with high-valency NP(25)BSA than with low-valency NP(4)BSA and correlated with the amount of antigen added (Figure 3.3A). Since IgE PCs express higher surface BCR than IgG1 PCs, we reasoned that IgE PCs would be more sensitive to depletion following BCR stimulation. Therefore, we compared the NP-binding frequency of IgE, IgM, and IgG1 PCs following exposure to NP-BSA of varying doses and valency for 12 hours, a timepoint at which we had previously observed some reductions in PCs of all isotypes. Indeed, while all NP-specific PCs showed valency- and dose-dependent depletion, IgE PCs were depleted to a greater extent than IgG1 PCs, most notably with a high dose of low-valency NP(4)BSA or

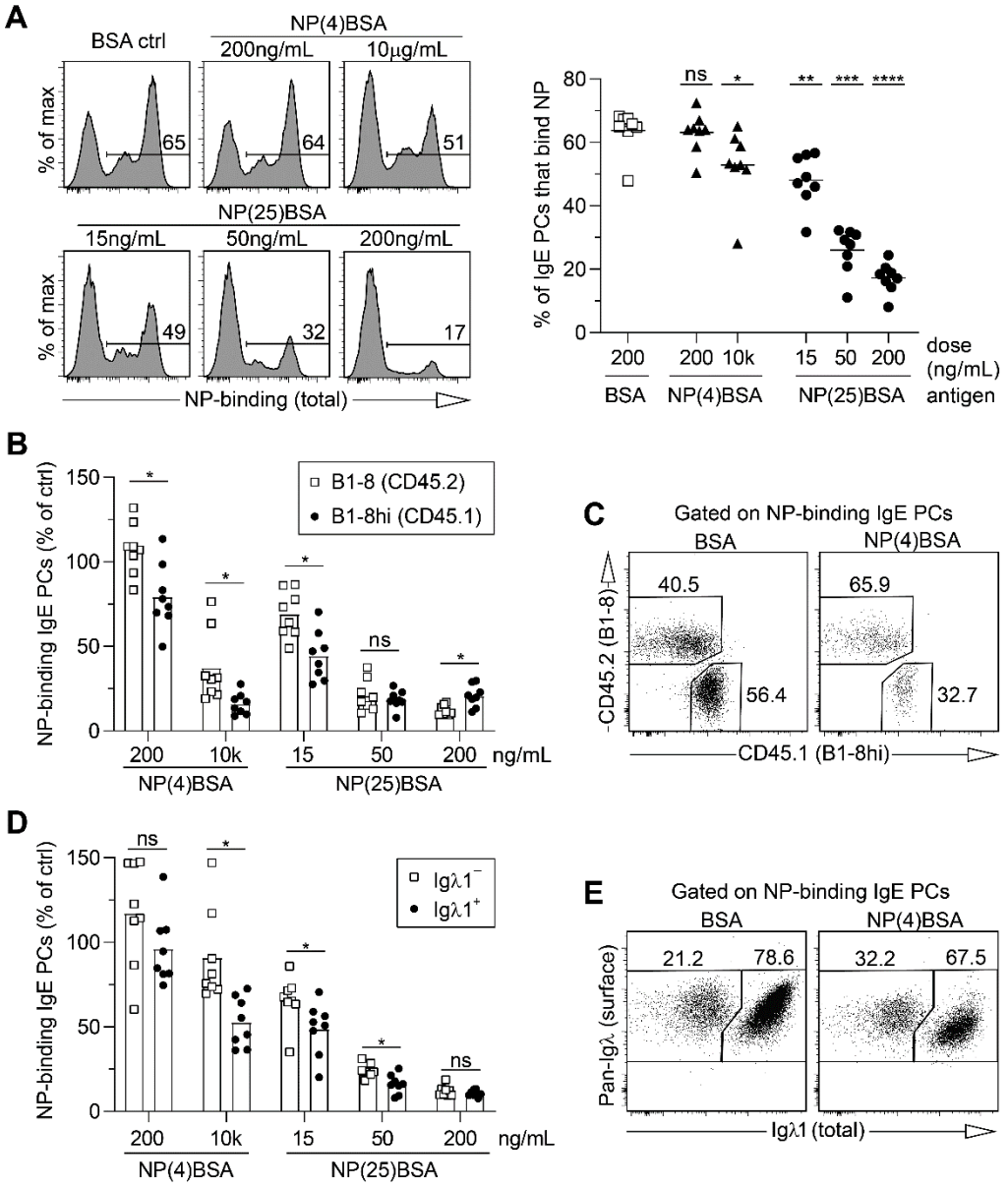

Figure 3.3 IgE PC depletion by cognate antigen is dose-dependent, affinity-dependent, and avidity-dependent. (A–E) Igλ-enriched B cells were cultured for 5.5 d ± 6 h. The indicated antigens were added to the cultures 24 ± 3 h prior to analysis by flow cytometry to determine the proportion of IgE PCs that bound to total (surface + intracellular) NP-APC. (A) Shown are representative histograms (left) and quantification (right) of the proportion of IgE PCs that were NP-binding after treatment with the indicated antigens. (B) Quantification of the number of NP-binding IgE PCs after incubation with the indicated antigens as a percentage of the number of NP-binding IgE PCs in control BSA-treated (200 ng/ml) wells. B cells were derived from B1-8 (white squares) and B1-8hi (black circles) mice and co-cultured, and then, as in C, were identified by CD45 congenic markers. (C) Representative flow cytometry dot plots showing the proportion of NP-binding IgE PCs that were derived from B1-8 (CD45.2) or B1-8hi (CD45.1) donors after treatment with BSA as a control (200 ng/ml) or with NP(4)BSA (10 μg/ml). (D) Similar to B, except that only B1-8 cells were cultured and NP-binding IgE PCs were categorized as staining negatively (white squares) or positively (black circles) (Figure caption continued on the next page.)

(Figure caption continued from the previous page.) for intracellular Igλ1. (E) Representative flow cytometry dot plots showing the proportion of NP-binding IgE PCs that were Igλ1$^-$ or Igλ1$^+$ after treatment with BSA or NP(4)BSA, as in C. IgE PCs were gated as B220^{int}CD138$^+$IgE$^+$. Dots in A, B, and D show data points derived from cells from individual mice. *, $P < 0.05$; **, $P < 0.01$; ***, $P < 0.001$; ****, $P < 0.0001$ (one-way repeated measures ANOVA with Dunnett's post-test comparing each group to the BSA control [A] or unpaired [B] or paired [D] t tests with the Holm-Sidak correction for multiple comparisons). Bars represent the mean. Data are representative of (A, left panels; C; E) or pooled from (A, right panel; B; D) two independent experiments.

with a low dose of high-valency NP(25)BSA (Figure S3.3A). As IgM PCs were less abundant under these culture conditions, their responses showed greater variability, but compared with IgE PCs, they were similarly sensitive to low-valency NP(4)BSA, but less sensitive to high-valency NP(25)BSA. Therefore, IgE PCs exhibited enhanced elimination following BCR stimulation compared with IgG1 PCs and in some cases with IgM PCs.

To determine how the affinity and avidity of antigen binding to the BCR affected cognate IgE PC depletion, we took advantage of a B1-8 line with a point mutation that confers 10-fold higher affinity to NP (B1-8hi).[83] We co-cultured Igλ-enriched cells from B1-8 and B1-8hi mice and then treated them with low- versus high-valency antigens at different doses as above for 24 hours. Low-valency or low-dose NP-BSA preferentially depleted B1-8hi IgE PCs (Figure 3.3B and C), indicating that the affinity of IgE PC mIg for antigen is most critical when antigens have low valency or are in low abundance.

As an additional affinity comparison, we took advantage of differences in Igλ LC expression among PCs in the B1-8 culture. A previous study identified two NP-binding populations of B1-8 cells that could be differentiated by their LC expression, one dominated by Igλ$_1$ and the other by Igλ$_2$.[84] We found that PCs derived from Igλ-enriched B1-8 B cells were divisible into three

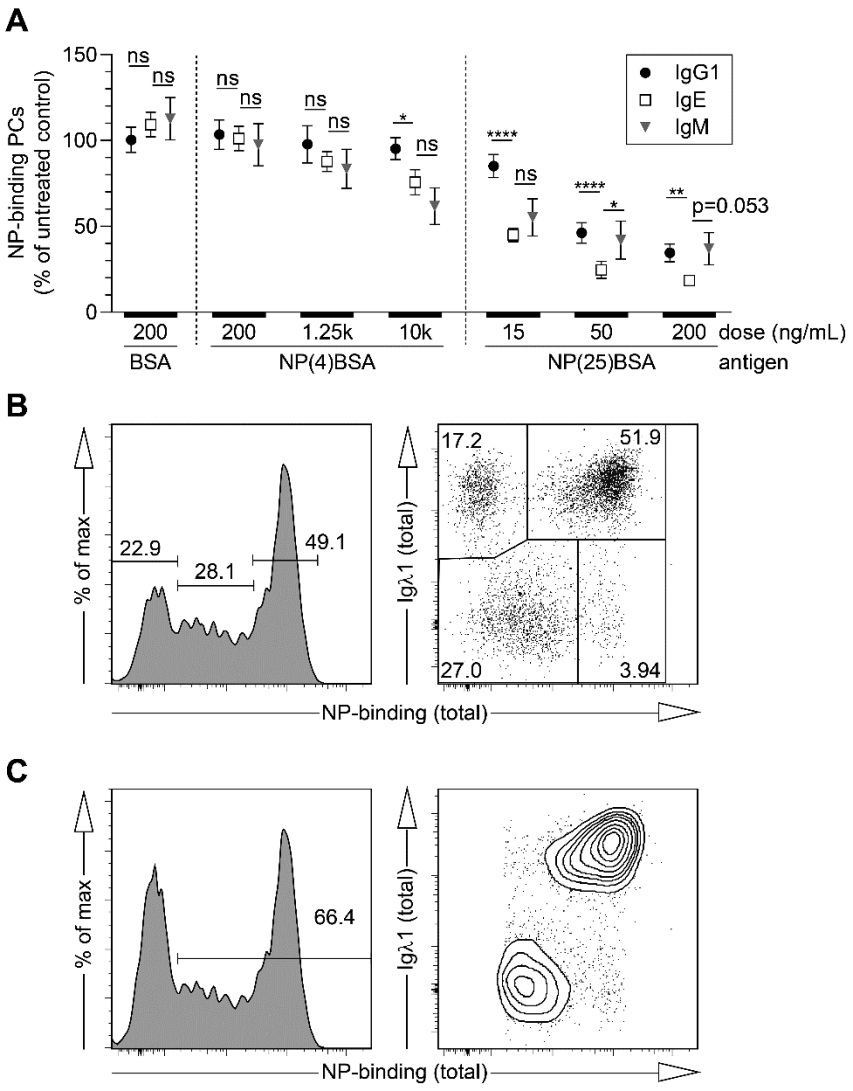

Figure S3.3 Analysis of PC depletion after 12 h and characterization of two distinct populations of NP-binding B1-8 IgE PCs. (A–C) Igλ-enriched B1-8 B cells were cultured for 5.25 d ± 7 h and then analyzed by flow cytometry. (A) After treatment with the indicated antigens for the final 12 ± 1 h of the culture, the number of NP-binding PCs of each isotype was quantified by flow cytometry and is shown as a percentage of the number of NP-binding PCs of the same isotype in untreated wells. Dots represent the mean and error bars reflect the standard error; cells from n = 14 mice. (B) Left, representative flow cytometry histogram of total (surface + intracellular) NP-APC staining of Igλ-expressing IgE PC divided into non-NP-binding, intermediate-NP-binding, and high-NP-binding gates. Right, representative flow cytometry dot plot of the same cells comparing NP-binding to $Ig\lambda_1$ staining. (C) Left, representative flow cytometry histogram of total NP-APC staining of IgE PC gated on all NP-binding cells (including both intermediate NP-binding + high NP-binding cells). Right, representative flow cytometry contour plot of IgE PCs gated as NP-binding (as shown in the left panel). (A–C) IgE PCs were gated as $B220^{int}CD138^{+}IgE^{+}$. *, $P < 0.05$; **, $P < 0.01$; ****, $P < 0.0001$ (two-way ANOVA with Dunnett's post-test comparing IgG1 and IgM to IgE [A]). We note that the comparison between IgE and IgM PCs treated with 200 ng/ml of NP(25)- (Figure caption continued on the next page.)

(Figure caption continued from the previous page.) BSA (A) was near our threshold for statistical significance (P = 0.053). Data are pooled from (A) or are representative of (B and C) three independent experiments.

populations with no NP-binding, low NP-binding, and high NP-binding (Figure S3.3B, left). $Ig\lambda_1^+$ cells were predominantly high NP-binding with a smaller subset that was non-NP-binding, whereas the $Ig\lambda_1^-$ (likely $Ig\lambda_2^+$) cells were almost entirely intermediate NP-binding (Figure S3.3B, right). Among NP-binding PCs (gated as shown in Figure S3.3C, left), $Ig\lambda_1^+$ staining clearly correlated with high NP-binding (Figure S3.3C, right), suggesting these cells would have increased sensitivity to cognate antigen. Indeed, low-valency or low-dose NP-BSA preferentially depleted $Ig\lambda_1^+$ compared with $Ig\lambda_1^-$ IgE PCs (Figure 3.3D and E), analogous to our results comparing higher-affinity B1-8hi to lower-affinity B1-8 IgE PCs. Taken together, these data provide evidence that the strength of BCR stimulation determines the extent of IgE PC depletion.

IgE PCs undergo apoptosis following BCR stimulation in a cell-intrinsic manner

Our data above were consistent with a model in which stimulation of the BCR on IgE PCs resulted in signal transduction leading to apoptosis. However, these data did not exclude the possibility of indirect effects; for example, BCR stimulation could potentially affect the PC differentiation of precursor B cells. To formally establish whether BCR stimulation led to IgE PC apoptosis, we isolated pure populations of IgE PCs, non-IgE PCs, IgE B cells, and non-IgE B cells by sorting live *in vitro*-differentiated Verigem B cells by Venus fluorescence and CD138 staining (Figure S3.4A, left). Although IgG1- and IgM-expressing cells were indistinguishable at sorting, they were disentangled at the final analysis by staining with anti-isotype antibodies. To determine the effects of BCR stimulation, the sorted cell populations were cultured with αIgκ or control antibody for 24 hours. IgE PCs were depleted 4-fold by BCR stimulation, whereas IgG1 and IgM PCs showed a more modest 2-fold depletion (Figure 3.4A). This difference was not due to the expression of the

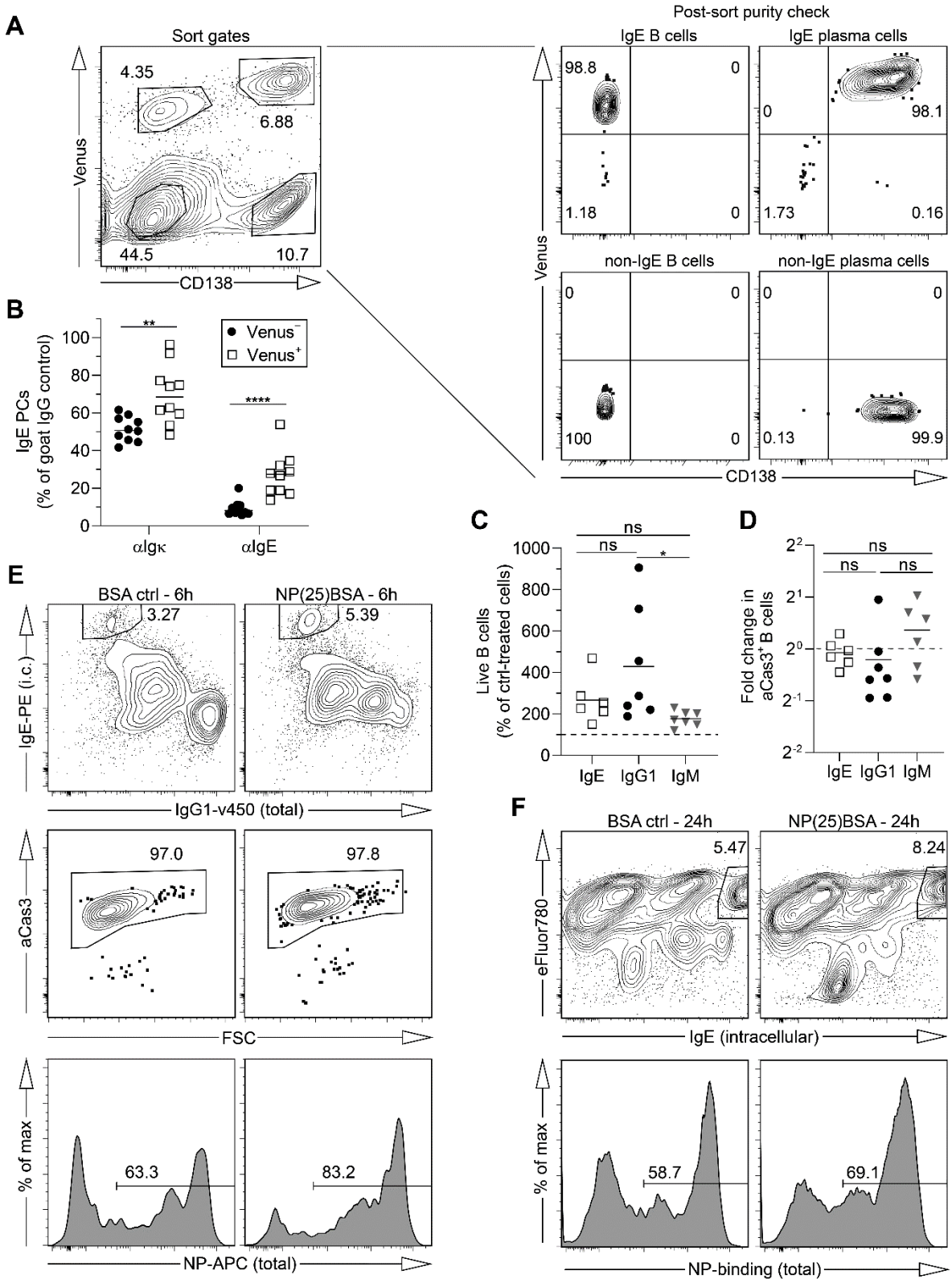

Figure S3.4: Representative flow cytometry gating schemes and validation for PC apoptosis experiments in Figure 3.4, with additional B cell survival data. (A) For the experiments shown in Figure 3.4, A–C, representative flow cytometry (Figure caption continued on the next page.)

(Figure caption continued from the previous page.) contour plots depict the gates used for cell sorting (left) and a confirmation of the purity of sorted cells (right). (B) B cells from Verigem heterozygous mice were purified and cultured for 5.5 d ± 6 h and then analyzed by flow cytometry. 24 ±3 h prior to analysis, cells were treated with goat IgG control, αIgκ, or αIgE. The relative number of IgE PCs ($B220^{int}CD138^{+}IgE^{+}$) after BCR stimulation is shown as a percentage of the number of IgE PCs after treatment with control IgG with the data segregated by whether the cells expressed the Verigem allele ($Venus^{+}$) or the WT allele ($Venus^{-}$). (C and D) Cells were sorted by flow cytometry as shown in A and cultured as described in Figure 3.4, A–C, and Materials and methods. Sorted cells were cultured separately and treated with either goat polyclonal IgG control or αIgκ antibody for 24 ± 3 h. (C) Quantification of the number of B cells after αIgκ treatment shown as a percentage of the number of B cells after control IgG treatment for each isotype. The dotted line represents no change from control. (D) The fold change in the proportion of B cells that were $aCas3^{+}$ after αIgκ treatment compared to control IgG treatment. The dotted line represents no change from control. (E) Representative flow cytometric analysis of cells from the time course analysis in Figure 3.4 F at 6 h. Cells were gated as$CD138^{-}$ and then sequentially from top to bottom showing the identification of $IgE^{hi}NP^{+}aCas3^{+}$ cells. (F) Representative flow cytometric analysis of cells from the timecourse analysis in Figure 3.4 G at 24 h. Cells were gated sequentially from top to bottom showing the identification of eFluor780 $(e780)^{+}IgE^{hi}NP^{+}$ cells. Dots represent data points derived from cells from individual mice. *, $P < 0.05$; **, $P < 0.01$; ****, $P < 0.0001$ (paired t tests with the Holm-Sidak correction for multiple comparisons [A], one-way unmatched ANOVA with Tukey's post-test comparing each group to each other group [C and D]). Bars represent the mean. Results are representative of three (A) or two (E and F) independent experiments or are pooled from three (B and C) or two (D) independent experiments.

Verigem reporter in IgE cells: in cultures of Verigem-heterozygous cells, the expression of mIgE from the Verigem allele did not promote, and in fact was slightly protective against, IgE PC elimination compared with the expression of mIgE from the wild-type allele (Figure S3.4B). We hypothesized that IgE PCs were undergoing apoptosis and sought to determine whether BCR stimulation led to increased caspase-3 activation. Indeed, we observed a 2-fold increase in active Caspase-3 (aCas3) staining among sorted IgE PCs treated with αIgκ (Figure 3.4B) but not among IgG1 or IgM PCs. Notably, BCR stimulation improved the survival of sorted IgE, IgG1, and IgM B cells and did not increase caspase-3 activation in these cells (Figure S3.4C and D), highlighting the different outcomes of BCR stimulation of IgE B cells versus IgE PCs. Taken together, these data provide evidence that BCR stimulation of IgE PCs results in caspase-3 activation and apoptosis.

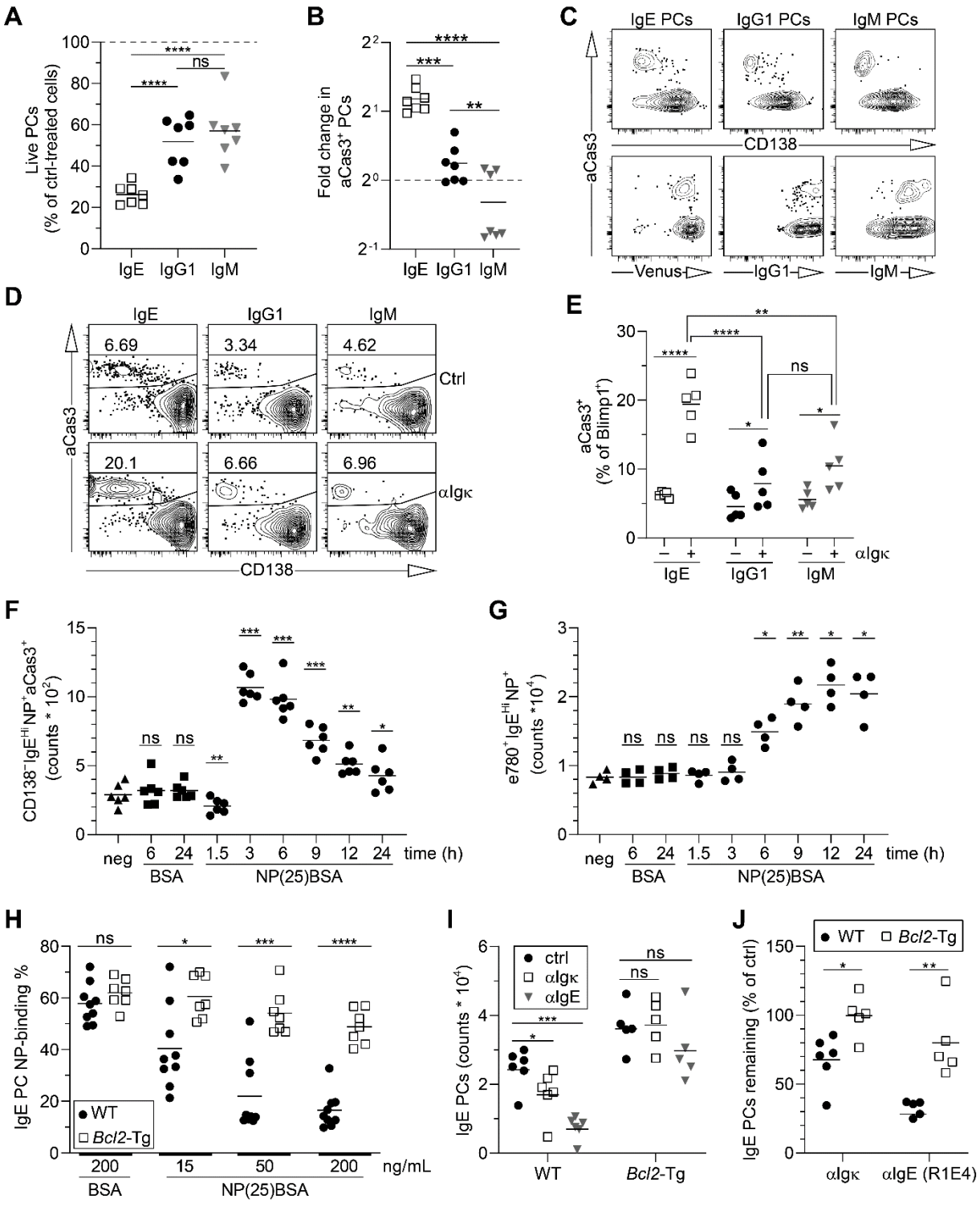

Figure 3.4: BCR stimulation results in IgE PC apoptosis. (A–C) Purified Verigem B cells were cultured for 4.5 d ± 6 h, sorted by flow cytometry (see Figure S3.4 A), returned to culture, treated with goat polyclonal IgG control or αIgκ antibody for 24 ± 3 h, and then analyzed by flow cytometry. (A) Quantification of the number of live PCs after αIgκ treatment as a percentage of the number of live PCs after control IgG treatment for (Figure caption continued on the next page.)

(Figure caption continued from the previous page.) each isotype. The dotted line represents no change from control. (B) Quantification of the fold change in the proportion aCas3$^+$ PCs after αIgκ treatment compared with control IgG treatment for each isotype. The dotted line represents no change from control. (C) Representative flow cytometry contour plots of aCas3 versus CD138 staining (top) or aCas3 versus fluorescence/isotype staining (bottom) for the indicated isotypes of PCs treated with αIgκ. (D and E) Purified B cells from Blimp1-YFP mice were cultured for 4.5 d and then treated with αIgκ (+) or goat IgG as a control ("ctrl" or "–") for 6 h prior to analysis by flow cytometry. (D) Representative flow cytometry contour plots of aCas3 versus CD138 staining for YFP+ cells of the indicated isotypes. (E) Quantification of the proportion of YFP+ cells of the indicated isotypes that were aCas3$^+$. (F and G) Purified B cells from B1-8 mice were cultured for 5.5 d ± 6 h. Cells were cultured with BSA (control) or NP(25)BSA at the indicated timepoints prior to analysis by flow cytometry, similar to Figure 3.2, B and C. The number of CD138$^–$ IgE^{hi}NP$^+$aCas3$^+$ cells (F) and eFluor780 (e780)$^+$IgE^{hi}NP$^+$ cells (G) are shown. Cells were gated as shown in Figure S3.4, panels E and F. (H) Quantification of the proportion of IgE PCs that were NP-binding after antigen treatment. Igλ-enriched B1-8 B cells from Bcl2-Tg (white squares) or control (WT, black circles) littermates were cultured for 5.5 d ± 6 h and the indicated antigens were added for the final 24 ± 3 h prior to analysis by flow cytometry. (I and J) Polyclonal B cells from Bcl2-Tg or WT littermates were purified and cultured for 5.5 d ± 6 h. At D4.5 ± 6 h, cells were treated with either αIgκ or αIgE for BCR stimulation, compared with control (goat IgG) treatment. Quantification of the absolute number of IgE PCs (I) or the relative percentage of IgE PCs remaining compared to control (J) after treatment as indicated. Dots represent data points derived from cells from individual mice. *, $P < 0.05$; **, $P < 0.01$; ***, $P < 0.001$; ****, $P < 0.0001$ (one-way ANOVA with Tukey's post-test comparing each group to each other group [A and B], one-way matched ANOVA with the Sidak post-test comparing the indicated pairs of groups [E], one-way matched ANOVA with Dunnett's post-test comparing the mean of each group to the negative control [F and G], paired t tests with the Holm-Sidak correction for multiple comparisons [H and J], and two-way ANOVA matched within each genotype with the Sidak post-test comparing the mean of each group to the control for each genotype [I]). IgE PCs were gated as B220^{int}CD138$^+$IgE$^+$ (H–J). Bars represent the mean. Data are pooled from three (A and B), two (E–G), or four (H–J) independent experiments or are representative of three (C) or two (D) independent experiments.

Our studies of sorted PCs showed that apoptotic (aCas3$^+$) PCs of all isotypes lost expression of CD138 (Figure 3.4C, top). These CD138$^–$ aCas3$^+$ cells were not contaminating B cells, because they retained similarly high intracellular antibody staining as live PCs (Figure 3.4C, bottom) and our post-sort purity routinely exceeded 99% (Figure S3.4A, right). Therefore, we identify CD138 downregulation as a general feature of PC apoptosis.

To further characterize PC apoptosis after BCR stimulation without cell sorting, we cultured cells from Blimp1-YFP-transgenic mice, in which YFP expression correlates with Blimp-1 expression

and is therefore a marker of PC differentiation. The vast majority of YFP^+ cells were also marked by CD138 (Figure 3.4D), indicating PC identity, but a small proportion of YFP^+ cells was $CD138^–$ and stained for aCas3, consistent with our prior observations that surface CD138 is lost during PC apoptosis. Treatment with αIgκ but not control antibody induced a large (3-4-fold) increase in the proportion of IgE^+YFP^+ cells that stained for aCas3 (Figure 3.4D and E), whereas only a slight increase in aCas3 staining was observed among $IgG1^+YFP^+$ cells and IgM^+YFP^+ cells. These results were consistent with our findings using sorted cells and provided further evidence that IgE PCs are uniquely sensitive to undergo apoptosis following BCR stimulation.

These observations prompted us to return to our timecourse experiments to examine the kinetics of BCR ligation-induced IgE PC apoptosis. We found that the addition of NP-BSA expanded a population of $CD138^–IgE^{hi}$ cells which was overwhelmingly (>95%) $aCas3^+$ (Figure 3.4F and Figure S3.4E). This population spiked three hours after BCR stimulation and dwindled slowly thereafter. The proportion of these cells that were NP-binding was increased after NP-BSA treatment compared with control BSA treatment, consistent with the preferential induction of apoptosis in cognate antigen-specific IgE PCs (Figure S3.4E). Subsequent to the induction of aCas3, we observed an accumulation of $CD138^–$ IgE^{hi} IgE PCs that stained with the fixable dye we used to exclude non-viable cells, suggesting these cells had completed apoptosis (Figure 3.4G). The frequency of NP-binding among these dead cells also increased following NP-BSA treatment (Figure S3.4F). Overall, these findings depict a progression of antigen-specific IgE PCs from live, to apoptotic, to dead following cognate antigen exposure.

Based on our previous finding that mice with an anti-apoptotic *Bcl2* transgene expressed in the B cell lineage had markedly increased numbers of IgE PCs,[29] we sought to determine whether *Bcl2* overexpression could rescue IgE PCs from depletion after BCR stimulation. IgE PCs derived from *Bcl2*-Tg B1-8 B cells were strongly resistant to cognate antigen-induced elimination, at multiple doses of NP(25)BSA, relative to B1-8 IgE PCs derived from littermates lacking the *Bcl2* transgene (wildtype [WT]; Figure 3.4H). IgE PCs generated in cultures of polyclonal B cells from *Bcl2*-Tg mice without the B1-8 knock-in were also protected against elimination induced by αBCR antibodies relative to cells from WT littermates, showing no significant depletion even after exposure to αIgE, which depleted more than 75% of WT IgE PCs (Figure 3.4I and J). We note that our aforementioned intracellular staining approach ensured that our detection of IgE PCs was unimpaired by αIgE treatment. Therefore, these data further support the model that BCR ligation induces apoptosis in IgE PCs, leading to their elimination.

Antigen-induced IgE PC elimination requires the BCR signalosome

In Figure 1, we identified enhanced phosphorylation of BCR signalosome components following mIg stimulation of IgE PCs. Having observed that BCR stimulation led to IgE PC apoptosis, we next determined the contribution of BCR signalosome components to IgE PC elimination. First, we tested the role of Syk, an apical kinase in the BCR signaling phosphorylation cascade, and Btk, a kinase downstream of Syk, with the well-characterized pharmacological inhibitors PRT062607 and ibrutinib, respectively. Inhibition of either kinase dose-dependently rescued IgE PCs from BCR stimulation-induced elimination (Figure 3.5A and B). However, maximal Syk inhibition achieved a complete rescue, whereas maximal Btk inhibition had a partial effect. BLNK is an adaptor molecule critical for the activation of PLCγ2, which is important for Ca^{2+} flux and other

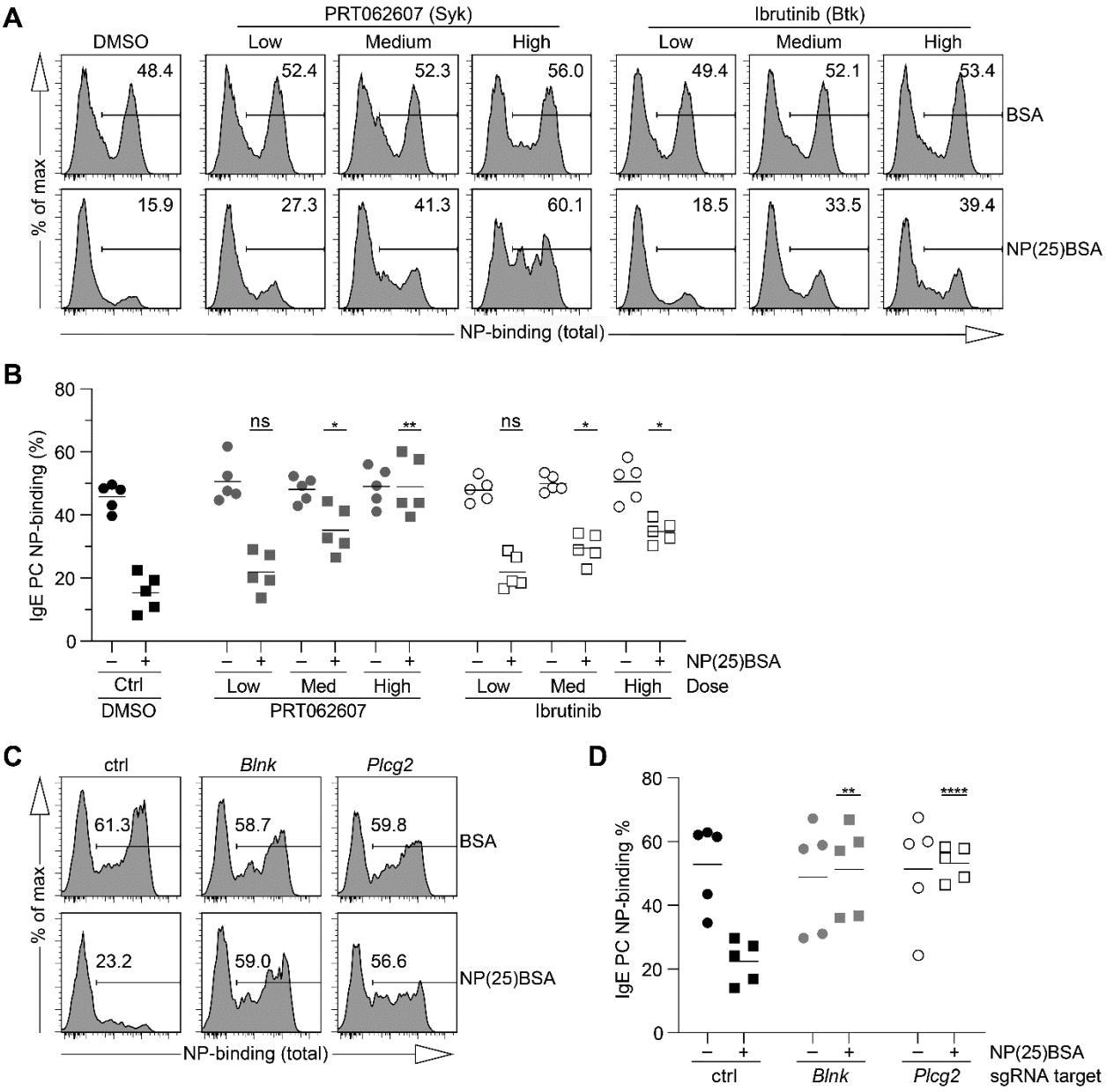

Figure 3.5: The BCR signalosome is required for mIg ligation-induced IgE PC elimination. (A and B) Igλ-enriched B1-8 B cells were cultured for 4.5 d ± 6 h and then treated with NP(25)BSA or BSA (50 ng/ml) for 24 ± 3 h prior to analysis. Shown are representative flow cytometry histograms (A) and quantification (B) of the proportion of IgE PCs that were NP-binding when cells were treated with the indicated inhibitors or vehicle control (DMSO) prior to incubation with antigen. See Table 3.1 for inhibitor concentrations. (C and D) Genes were targeted by electroporation with CRISPR-Cas9 ribonucleoproteins containing the indicated sgRNAs (or no sgRNA as a control) in cultured Igλ-enriched B1-8 B cells (see Methods and Table 3.2 for details). Representative flow cytometry histograms (C) and quantification (D) of the proportion of IgE PCs that were NP-binding after treatment with NP(25)BSA or BSA as a control (50–100 ng/ml) for 24 ± 3 h prior to analysis. IgE PCs were gated as B220intCD138+IgE+. Dots represent data points derived from cells from individual mice. *, $P < 0.05$; (Figure caption continued on the next page.)

(Figure caption continued from the previous page.) **, P < 0.01; ****, P < 0.0001 (one-way matched ANOVA with Dunnett's post-test comparing the mean of each NP(25)BSA-treated inhibitor condition to the NP(25)BSAtreated DMSO control [B] or each NP(25)BSA-treated sgRNA condition to the NP(25)BSA-treated no-sgRNA control [D]). Bars represent the mean. Data are representative of (A and C) or pooled from (B and D) two independent experiments.

downstream processes, and both BLNK and PLCγ2 were phosphorylated in IgE PCs following BCR stimulation (Figure 3.1). To test the contribution of these proteins to IgE PC depletion, we targeted the genes encoding these proteins by CRISPR-Cas9 ribonucleoprotein electroporation of B1-8 B cells. Targeting either *Blnk* or *Plcg2* completely blocked antigen-induced IgE PC elimination, whereas electroporation with Cas9 only (without a guide RNA) as a control did not (Figure 3.5C and D). We observed similar results with multiple independent guides targeting either *Blnk* or *Plcg2* compared to a non-targeting sgRNA control (Figure S3.5A and B). These findings indicate that the mIg ligation-induced elimination of IgE PCs depends upon the activation of the BCR signalosome, with critical contributions from Syk, BLNK, and PLCγ2.

Table 3.1: Inhibitors

Inhibitor name	**Company**	**Final concentration**		
		"Low"	"Medium"	"High"
Ibrutinib	Gift from Dr. Jack Taunton	500pM	2nM	20nM
PRT062607	Selleck Chemicals	250nM	1μM	4μM

Table 3.2: sgRNA sequences

Guide Target and Number (*gene*-#)	**sgRNA sequence**
Negative control	GCACUACCAGAGCUAACUCA
Blnk-1	GAUAUUAAGAACAAUGAAGG
Blnk-2	CCCUUCGAGGAACACUUGGA
Blnk-3	AAGAUAAUCGAUCCAGCCAG
Plcg2-1	GGUGUCCACGUUGACCAUGG
Plcg2-2	GAAGCCUUCAAUCUUGUCUG
Plcg2-3	AGAUAAAGGAAAUCCGUCCG

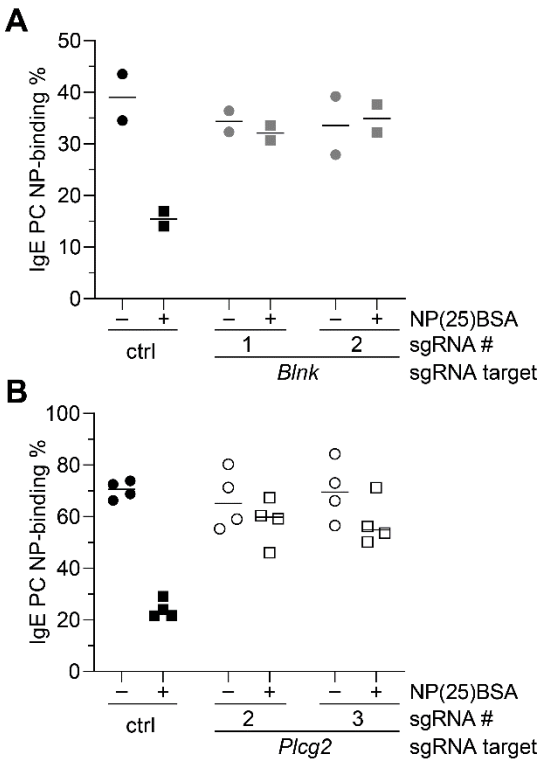

Figure S3.5: Validation of CRISPR gene targeting results in Figure 3.5 with additional guide RNAs. (A and B) Genes were targeted by electroporation with CRISPR-Cas9 ribonucleoproteins as described in Figure 3.5 and Materials and methods. The proportion of IgE PCs that were NP-binding was determined by flow cytometry. Control conditions either received no guide RNA (A) or a non-targeting sgRNA (B). IgE PCs were gated as $B220^{int}CD138^{+}IgE^{+}$. Dots represent data points derived from cells from individual mice. Bars represent the mean. Results are representative of two independent experiments.

IgE PCs are constrained by BCR signaling *in vivo*

Having established that activation of the BCR signalosome led to the elimination of IgE PCs *in vitro*, we sought to confirm the importance of BCR signaling in restraining IgE PCs *in vivo*. To this end, we developed a genetic system where BCR signaling could be conditionally impaired exclusively in PCs. Specifically, we bred mice carrying a PC-restricted, tamoxifen-inducible Cre (BLIMP1-tdTomato-inducible Cre; BLT_{cre})[85] and a single floxed *Syk* allele ($Syk^{flox/+}$)[86]. To ensure Cre activity was restricted to the hematopoietic lineage and to produce matched group sizes sufficient for analysis, we generated bone marrow chimeras using BLT_{cre} $Syk^{+/+}$ donors as controls. Following immunization and tamoxifen treatment, IgE PCs were selectively increased in

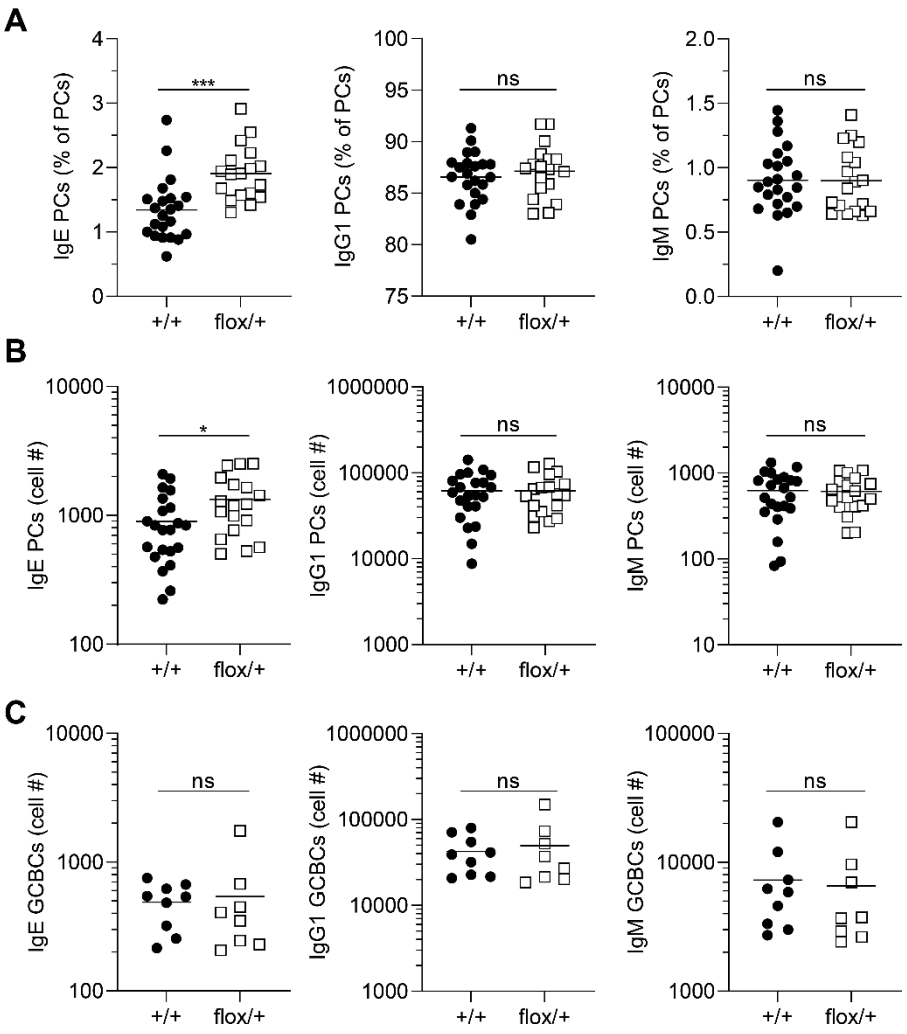

Figure 3.6: IgE PCs are constrained by BCR signaling in vivo. (A–C) Bone marrow chimeras were generated from BLTcre donors that were either $Syk^{flox/+}$ or $Syk^{+/+}$ and then immunized with NP-CGG in alum adjuvant after reconstitution. Quantification of the frequency (A) or number (B and C) of the indicated isotypes of PCs or GC B cells (GCBCs) in the dLN as determined by flow cytometry 9 d after immunization. Tamoxifen was administered to all mice 6, 7, and 8 d after immunization (see Materials and methods for details). PCs were gated as $B220^{int}CD138^{+}$ and negative for other isotypes, GC B cells were gated as $B220^{+}CD138^{-}PNA^{hi}CD38^{-}IgD^{-}$ and negative for other isotypes. Dots represent individual mice and bars represent the mean. *, $P < 0.05$; ***, $P < 0.001$ (unpaired t tests). Data are pooled from (A and B) or are representative of (C) three independent experiments.

frequency (Figure 3.6A) and cell number (Figure 3.6B) in the dLNs of chimeras derived from *Syk*$^{flox/+}$ donors compared with chimeras derived from *Syk*$^{+/+}$ donors, whereas other isotypes of PCs and of GC B cells were unchanged (Figure 3.6B-C). These findings provide evidence for the selective regulation of IgE PCs *in vivo* by BCR signaling.

BCR ligation depletes IgE PCs *in vivo*

Based on our earlier observation that the administration of cognate antigen induced BCR signaling in IgE PCs *in vivo*, we next sought to determine whether this signaling was followed by the depletion of IgE PCs, as we had observed *in vitro*. As for our *in vitro* experiments above, we used an intracellular staining approach to identify antigen-specific PCs. The subcutaneous injection of cognate antigen led to a reduction in the frequency of IgE PCs, but not IgG1 or IgM PCs, that bound cognate antigen (Figure 3.7A). This was due to a ~2-fold decrease in the number of antigen-specific IgE PCs, versus no change in the number of IgE PCs that were not antigen-specific (Figure 7B), mirroring our earlier *in vitro* results. We did not observe any change in the number of antigen-specific IgG1 or IgM PCs following antigen injection (Figure 7B). These data extend our *in vitro* results and provide evidence that IgE PCs are uniquely susceptible to depletion by cognate antigen *in vivo*.

To further test if directly ligating mIgE would be a useful strategy to acutely eliminate IgE PC *in vivo*, we took advantage of the unique properties of the R1E4 clone of αIgE that we had previously observed to induce Ca^{2+} flux (Figure S3.2E) and deplete IgE PCs in cell culture (Figure 4I-J and Figure S3.4B). This particular αIgE clone only recognizes IgE that is not bound to CD23 or FcεRI, mitigating the possibility that its activity upon IgE PCs could be related to the ligation of receptor-bound IgE.[87] Illustrating the potential therapeutic benefit of R1E4, a prior study revealed that recombinant single-chain R1E4 could suppress IgE production in mice.[88] Therefore, we sought to determine if R1E4 could acutely deplete IgE PCs *in vivo*. WT mice were immunized, and then, after the bulk of IgE PC differentiation had occurred, were administered a single injection of either control antibody, un-modified αIgE R1E4 (Fc-WT), or αIgE R1E4 with a mutated, non-functional

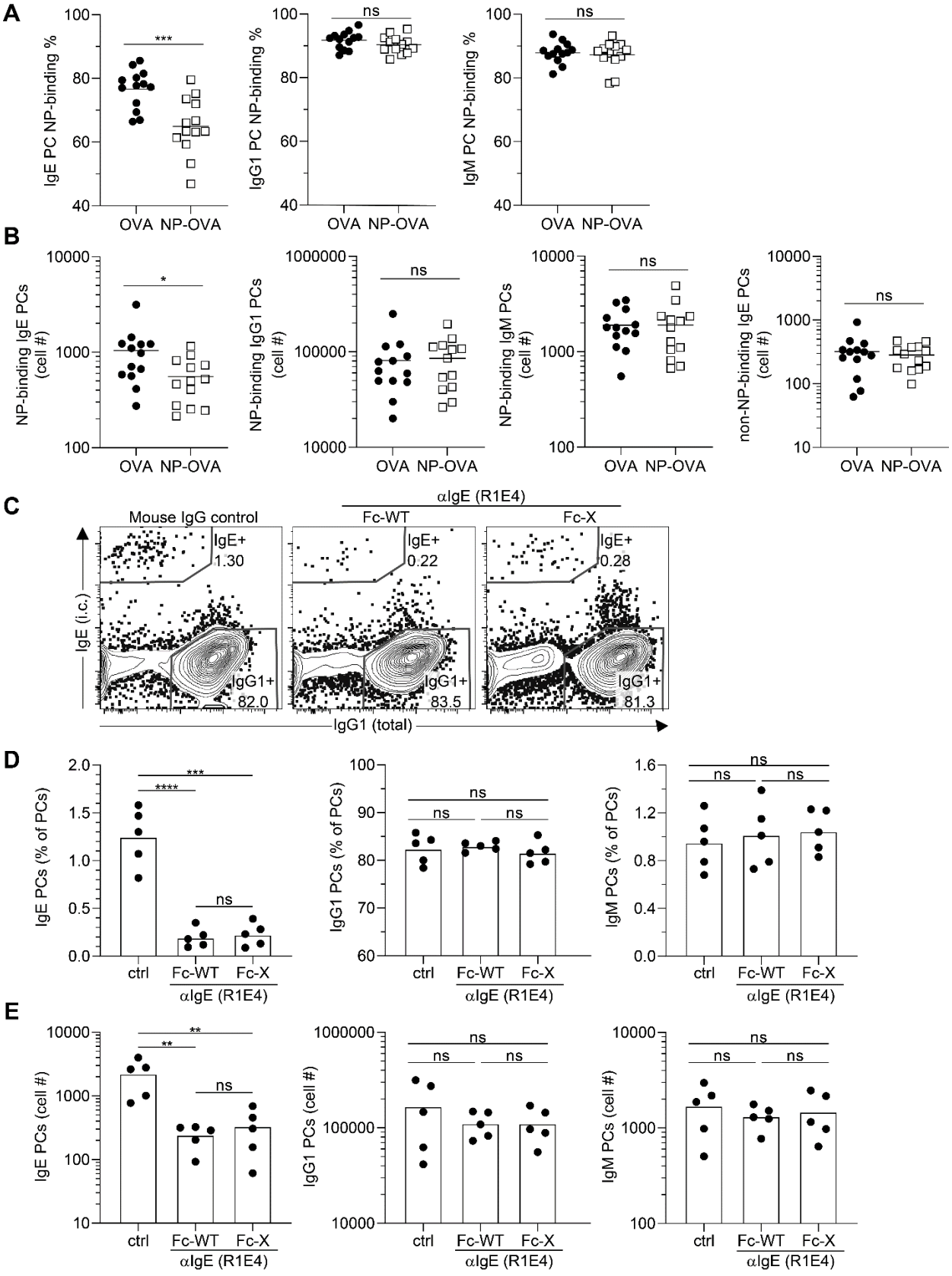

Figure 3.7: BCR ligation depletes IgE PCs in vivo. (Figure caption continued on the next page.)

(Figure caption continued from the previous page.) (A and B) Mice were immunized subcutaneously with NP-CGG in alum adjuvant and injected with control (OVA) or cognate antigen (NP-OVA) 6.33–6.5 d later. The proportion (A) and number (B) of PCs that were NP-binding were quantified by flow cytometry 16 h after antigen injection. The number of non-NP-binding IgE PCs is also shown (B). PCs were gated as $CD138^{+}B220^{int}$ and negative for other isotypes. (C–E) Mice were immunized with NP-CGG in alum adjuvant and then injected intravenously with αIgE R1E4 (with either a normal Fc region [Fc-WT] or with a mutated Fc region [Fc-X]) or control antibody at 7.33 d after immunization. dLNs were analyzed by flow cytometry 16 h later. Representative flow cytometry contour plots (C) and quantification of the frequency (D) and number (E) of PCs of the indicated isotypes in the dLN. PCs were gated as $CD138^{+}B220^{int}$ and negative for other isotypes. Dots represent individual mice and bars represent the mean. *, $P < 0.05$; **, $P < 0.01$; ***, $P < 0.001$; ****, $P < 0.0001$ (unpaired t tests [A and B], one-way unmatched ANOVA with Tukey's post-test comparing each group to each other group [C–E]). Antigen injection results (A and B) are pooled from two independent experiments while R1E4 Fc-WT versus control comparisons (C–E) are representative of three independent experiments.

Fcγ-receptor binding site (Fc-X). Sixteen hours later, PCs were enumerated in the dLN by flow cytometry. Injection of αIgE R1E4, but not of control antibody, induced a strong decrease in the frequency (Figure 7C-D) and absolute number (Figure 7E) of IgE PCs. As expected, PCs of other isotypes were unaffected by αIgE R1E4 injection (Figure 7E). The depletion of IgE PCs was equivalent between Fc-WT and Fc-X versions of αIgE R1E4, ruling out a contribution from antibody-dependent cell cytotoxicity (ADCC) or other BCR-independent mechanisms of IgE PC depletion involving Fcγ receptors. These findings demonstrate that ligation of the BCR on IgE PCs *in vivo* results in IgE PC elimination.

Methods

Mice and bone marrow chimeras

All mice used for experiments in this study were on a C57BL/6 (B6) background (backcrossed ≥10 generations). Mice for experiments were sex and age-matched between groups as much as possible and both male and female mice were used. For *in vivo* experimentation, mice were at least 6 weeks of age and for *in vitro* experimentation donor animals were at least 5 weeks of age.

BLT_{cre} mice,[85] *Cd19*^{Cre} mice,[75] *EμBcl2-22* (*Bcl2*)-Tg mice,[89] *Igh-J*^{tm1Dh} mice,[90] and Verigem mice[29] were maintained in our colony on a B6 background. *IgH*$^{B1\text{-}8i}$ mice (012642; B6.129P2(C)-*Igh*^{tm2Cgn}/J), *IgH*$^{B1\text{-}8hi}$ mice (007594; B6.129P2-*Ptprc*^{a}*Igh*^{tm1Mnz}/J), and *Syk*^{flox} mice (017309; B6.129P2-*Syk*$^{tm1.2Tara}$/J) were purchased from The Jackson Laboratory and then bred in our colony on a B6 background. The following five strains of mice were used as "WT" throughout the manuscript: Boy/J (002014; B6.SJL-*Ptprc*^{a}*Pepc*^{b}/BoyJ), NCI B6-Ly5.1/Cr (originally 01B96; B6-Ly5.2/Cr, later renamed to B6Ly5.1/Cr), B6/J (000664; C57BL/6J), NCI B6 (556; C57BL/6NCrl), and B6 Thy1.1 (000406; B6.PL-*Thy1*^{a}/CyJ). Boy/J, B6/J, and B6 Thy1.1 mice were originally from The Jackson Laboratory and were maintained in our colony, while NCI B6-Ly5.1/Cr and NCI B6 were purchased from Charles River.

Mice were housed in specific-pathogen-free facilities. Mouse work was approved by the Institutional Animal Care and Use Committee (IACUC) of the University of California, San Francisco (UCSF). Bone marrow chimeras were generated as described.[29] We allowed at least 6 weeks for full reconstitution of the chimeras before immunization.

Total B cell purification and Igλ B cell enrichment

All *in vitro* culture experiments were performed with B cells purified by negative selection. B cell purification was generally performed as described[91] but with the following modifications: Media used was DMEM (Fisher Scientific) containing 4.5 g/L of glucose, 2% fetal bovine serum (FBS, Life Technologies), and 10 mM HEPES (Life Technologies). Centrifugation steps were performed at 400g for 5 minutes. ACK lysis was not performed. αCD11c biotin (clone N418, Biolegend) was used at 1μL per 10^8 cells, and αTER-119 biotin (clone TER-119, Biolegend) was used at 10μL per 10^8 cells. 100μL of Dynabeads MyOne Streptavidin T1 (Life Technologies) were used per 10^8 cells. In the case of Igλ B cell enrichments, 10μL of αIgκ biotin (clone RMK-12, Biolegend) were added per 10^8 cells and 200μL of Dynabeads MyOne Streptavidin T1 were used per 10^8 cells. After purification, cells were resuspended in complete RPMI (cRPMI), composed of RPMI 1640 without L-glutamine (Fisher Scientific), 10% FBS, 10mM HEPES, 1X Penicillin Streptomycin L-Gluatmine (Fisher Scientific), and 50μM β-mercaptoethanol (Fisher Scientific). Final purity was assessed by flow cytometry. Total B cell purity routinely exceeded 98%. For Igλ-enriched purifications ~80% of B cells obtained were routinely $Ig\lambda^+$.

Mouse cell culture and in vitro BCR stimulation

All cell culture was performed in a humidified incubator with 5% CO_2 at 37ºC using cRPMI (see above for ingredients) supplemented with 150ng/mL αCD40 (clone FGK-45; Miltenyi Biotec) and 25ng/mL recombinant murine IL-4 (Peprotech) in 96-well Microtest U-bottom plates (BD Falcon) with a volume of 200μl per well. Purified B cells were cultured at a density of 10^4 cells per well, while Igλ-enriched B cells were cultured at 10^3 cells per well. Culture duration varied between experiments as described in figure legends. Cells were plated in triplicate for each condition,

except for some timecourse experiments where sextuplicates were used. In some cases, CD45-congenic B cells were co-plated to allow the combined assessment of cells from two different mice, such as in comparisons of B1-8 and B1-8hi B cells. Cell counts from such experiments were scaled up two-fold to account for each sample having had half of the normal cell input.

In vitro BCR stimulation with cognate antigen was performed by adding NP(4)BSA (Biosearch Technologies), NP(25)BSA (Biosearch Technologies), or BSA (Sigma-Aldrich) as a control directly to the culture supernatant without a media swap. See figure legends for timing and doses.

Media swap for in vitro experiments with anti-BCR antibodies

In some experiments, a media swap was performed to remove sIg from the culture which would otherwise block anti-BCR antibodies. First, the culture supernatant was removed. Then cells were washed once with pre-warmed cRPMI and resuspended in "swap" cRPMI. This "swap" cRPMI was not freshly prepared, but rather was an aliquot of the initial plating media which was maintained in the incubator throughout the culture period. This strategy ensured that the stimulatory environment of the cells did not change pre- and post-swap, obviating the burst of B cell activation that occurs if fresh stimulatory reagents are used as well as the drop off in viability which occurs if costimulatory signals are completely withdrawn. After the media swap, Goat polyclonal F(ab')2 anti-mouse Igκ (αIgκ; LifeSpan Biosciences), rat anti-mouse IgE clone R1E4, control Chrompure Goat IgG (Jackson ImmunoResearch), or control rat gamma globulin (Jackson ImmunoResearch) was added to achieve a final concentration of 2.5μg/mL.

All inhibitors were diluted in DMSO. The concentration of DMSO in culture never exceeded 0.1% and was typically lower. The specific DMSO vehicle control concentration in each experiment was made to be equivalent to the highest concentration of DMSO in any inhibitor-treated well. Inhibitors were added 5 minutes prior to the addition of stimulating antigen/control. See Table 3.1 for further details on inhibitors and concentrations used.

CRISPR of B1-8 cells

CRISPR gene targeting was achieved by electroporation of ribonucleoprotein complexes containing Cas9 and single guide RNAs (sgRNAs), adapted from a method published for human B cells.[76] Lyophilized modified sgRNAs (Synthego) were designed using Synthego's sgRNA design tool based on the following criteria in order of importance: 1) cut site within coding region of exon, 2) targeted exon early in coding sequence of protein, 3) cut site early within sequence of exon, 4) high on-target score, 5) target sequence not closely related to off-target sequences. Synthego's negative control sgRNA sequence was used as the negative control sgRNA. sgRNAs were resuspended in TE buffer (Synthego) at 80μM. See Table 3.2 for sgRNA sequences.

Igλ-enriched B1-8 cells were cultured for 2-3 days at 4 $*10^5$ cells/well in a 12-well tissue culture plate (BD Falcon) and then washed, resuspended in cRPMI and counted using a Coulter Counter Z2 instrument. After all centrifugation steps, 10μL of DNase I was added to the pellet prior to re-suspension. Cells were washed with D-PBS (Fisher Scientific) and then resuspended in 1M buffer[92] consisting of RNAse-free H_2O (Life technologies), 5mM KCl (Life technologies), 50mM D-Mannitol (Millipore-Sigma), 15mM $MgCl_2$ (Fisher Scientific), and 120mM $NaH_2PO_4/NaHPO_4$ (Fisher Scientific) at 2.5-10 * 10^6 cells/mL. 18-20μL of cells (4.5-20 $*10^4$ cells) were then plated

into 16-well nucleocuvette strips (Lonza). Each well had also previously received 4μL of ribonucleoprotein, which was pre-assembled by gently mixing 2μL 80μM sgRNA with 2μL 40μM Cas9 (UC Berkeley QB3 MacroLab) and incubating at RT for 15-60 minutes. 1μL of 100μM homology-directed repair template (HDRT) with no homology to the mouse or human genome was added to improve editing efficiency. Cells were then electroporated using an Amaxa 4D nucleofector electroporation with the pulse code EN-138. Following electroporation, "rescue" cRPMI was added to the electroporated wells and cells were incubated for 15 minutes. Afterwards, $7 *10^3 – 3 *10^4$ electroporated cells were plated into each well of a previously-prepared culture plate. 2.5-3.5 days following electroporation, cells were stimulated with cognate or control antigen and then analyzed 24 ± 3 hours later by flow cytometry.

Mouse injections (Adoptive transfer, immunization, antibody treatment, and tamoxifen treatment)
Adoptive transfers were performed by intravenous injection of $5 *10^3$ Igλ-enriched B1-8 B cells into the retro-orbital plexus of anesthetized mice. Mice were immunized the following day. All immunizations were performed using NP-CGG (Biosearch Technologies) resuspended at 1mg/mL in D-PBS and mixed 50:50 volumetrically with Alhydrogel (Accurate Chemical and Scientific). Mice were injected subcutaneously with 20μL of this solution (10μg of NP-CGG per injection) in each ear. At endpoint, the facial LNs from each side were pooled for analysis (see figure legends for various timepoints).

Unmodified αIgE (clone R1E4; grown from hybridoma), αIgE with a mutated Fc-receptor binding domain (clone R1E4; Cedarlane), or control rat gamma globulin were diluted in D-PBS to a concentration of 0.3mg/mL and injected intravenously to achieve a final dose of 3.25mg/kg. For

the experiment shown, mouse gamma globulin (Jackson ImmunoResearch) was used as a control whereas in previous experiments that the presented data is representative of rat gamma globulin was used as a control.

Tamoxifen was dissolved at 50mg/mL in corn oil (Sigma-Aldrich) by shaking at 56ºC for several hours. ~100µL/mouse was delivered by intraperitoneal injection to achieve a dose of 200mg/kg.

Production of αIgE clone R1E4

The R1E4 hybridoma was cultured in CELLine bioreactor flasks (Fisher Scientific) in DMEM with Glutamax, 100U/mL Penicillin and 100ug/mL streptomycin, and 55mM β-Mercaptoethanol). The hybridoma was seeded at 10^6 cells/mL in 15 mL 20% FBS in cDMEM, and the nutrient chamber filled with 500-1000 mL 10% FBS in cDMEM. The culture was harvested after seven days and the supernatant purified into PBS by Protein G affinity using a HiTrap Protein G HP affinity column (GE Healthcare), eluted with 0.1M acetic acid (VWR international) pH=3.0 on an AktaPure chromatography system. The eluate was neutralized with $1/10^{th}$ volume of 1.5M NaCl, 1M Tris-HCL pH=8.0 (Fisher Scientific). Fractions containing protein as determined by the A280 absorbance were combined and dialyzed into PBS with 10k MWCO Slide-A-Lyzer dialysis cassettes (Fisher Scientific). The dialysed antibody was concentrated in a 50 MWCO Amicon Ultra Spin column (Fisher Scientific), aliquoted in PBS at 2.5mg/mL, and then frozen at -80ºC until use.

Flow cytometry

For analysis of *in vivo* experiments, cell suspensions were prepared from dLNs as described,[29] counted using a Coulter Counter Z2 instrument, and then plated in triplicate at a density of 3.5 *

10^6 cells per staining well. Cells were then stained with antibodies (Table 3.3) essentially as described,[29] with one notable difference being that sodium azide was excluded from FACS buffer (2% FBS and 1mM EDTA [Fisher Scientific] in PBS) to ensure optimal CD138 staining.[93] All incubations were 20 minutes on ice except for Fc block incubations (10 minutes) and antibody staining of fixed and permeabilized cells (45 minutes to 1 hour). After the final staining centrifugation step was complete, cells from triplicate staining wells were resuspended and pooled using 100µL FACS buffer and then combined with 7500 AccuCount Ultra Rainbow Fluorescent counting beads (Spherotech; hereafter referred to as counting beads) per sample prior to analysis.

Table 3.3: Antibody-fluorochrome conjugates and other reagents used for flow cytometry

Antibody target or reagent designation	**Clone**	**Company**	**Conjugate**	**Dilution**
Active Caspase-3	C92-605	BD Biosciences	V450	1/50-100
			FITC	1/25
			Alexa Fluor 647	1/50-100
B220	RA3-6B2	BD Biosciences	V500	1/100-200
		Life Technologies	Qdot 655	1/100-400 (varies by lot)
			APC	1/150-250
CD38	90	Life Technologies	Alexa Fluor 700	1/100
		BD Biosciences	Brilliant Violet 786	1/200
CD45.1	A20	Biolegend	Brilliant Violet 650	1/150-200
		BD Biosciences	Alexa Fluor 647	1/150-200
			Alexa Fluor 700	1/100
CD45.2	104	Biolegend	FITC	1/100-200
			PerCP-Cy5.5	1/100-200
			Brilliant Violet 785	1/100
		BD Biosciences	PerCP-Cy5.5	1/100-200
			PE-Cy7	1/100-200
CD138	281-2	BD Biosciences	PE	1/200
			Brilliant Violet 711	1/150-200
Antibody target or	**Clone**	**Company**	**Conjugate**	**Dilution**

reagent designation				
Fixable Viability Dye eFluor 780	N/A	Life Technologies	N/A	1/600-1000
IgD	11-26c.2a	Biolegend	Brilliant Violet 510	1/100-1/200
			Brilliant Violet 711	1/200
			FITC	1/200
			PerCP-Cy5.5	1/200
			Alexa Fluor 700	1/100
IgE	RME1	Biolegend	Unconjugated	1/15
			FITC	1/400-500
			PE	1/350-500
	R35-72	BD Biosciences	Unconjugated	1/15
			Brilliant Violet 650	1/150-300
IgG1	A85-1	BD Biosciences	V450	1/300-400
			FITC	1/300-400
$Ig\lambda_1$	R11-153	BD Biosciences	Biotin	1/300-1/400
$Ig\lambda_{1,2,3}$	R26-46	BD Biosciences	FITC	1/150-200
IgM	II/41	Life Technologies	PE-Cy7	1/175-1/500
NP	N/A	Conjugated in-house as described.[33]	APC	1/750 of 0.1mg/mL stock
PNA (peanut agglutinin)	N/A	Vector Laboratories	Biotin	1/1000-2000
			FITC	1/500
p-Syk (pY348)	I120-722	BD Biosciences	Alexa Fluor 488	1/5
p-BLNK (pY84)	J117-1278	BD Biosciences	Alexa Fluor 647	1/5
p-PLCγ2 (pY759)	K86-689.37	BD Biosciences	Alexa Fluor 488	1/5
Streptavidin	N/A	Life Technologies	QDot 605	1/400
		BD Biosciences	Brilliant Violet 711	1/400
TruStain FcX (anti-mouse CD16/32)	93	Biolegend	Unconjugated	1/50

At the endpoint of *in vitro* experiments, supernatants were removed by pipetting, triplicate culture wells (or sextuplicate wells, for some timecourse experiments) were pooled using 100µL FACS buffer per sample, and then the solution of resuspended cells was transferred to a staining plate previously prepared with 7500 counting beads per well. After pelleting and removal of the

supernatant, staining was performed as described above for *in vivo* experiments. Cells were then resuspended in 25µL FACS buffer prior to analysis.

For both *in vivo* and *in vitro* experiments, we used our previously-established intracellular staining technique[29] to sensitively and specifically detect IgE-expressing cells. Briefly, to prevent the detection of IgE captured by non-IgE-expressing cells, surface IgE was blocked with a large excess of unconjugated αIgE (clone RME-1). IgE-expressing cells were then detected after fixation/permeabilization by staining with a low concentration of fluorescently-labelled RME-1.

After staining, cells were collected on an LSRFortessa (BD). Data were analyzed using FlowJo v10. Counting beads were identified by their high SSC and extreme fluorescence and were used to determine the proportion of the cells plated for staining that had been collected on the flow cytometer for each sample. Cells were gated on FSC-W versus FSC-H and then SSC-W versus SSC-H gates to exclude doublets. Except where otherwise specified, cells were also gated as negative for the fixable viability dye eFluor780 and over a broad range of FSC-A to capture resting and blasting lymphocytes. 2D plots were presented as either dot plots or contour plots with outliers shown as dots. In some cases, 'large dots' were used to visualize rare events.

In vivo NP-OVA injection experiments for phosflow and PC depletion assays

Mice were immunized as described above. At D6.33-D6.5, mice were administered 200µg of cognate antigen (NP conjugated to ovalbumin [NP(16)OVA, Biosearch Technologies]) or control antigen (ovalbumin; OVA [Worthington Biochemicals]) in 20µl PBS by subcutaneous injection, such that the injected antigen would drain to the same LN(s) as the initial immunization. To assess

PC depletion, dLNs were analyzed by flow cytometry 16h later. For phosflow analysis of proteins involved in proximal BCR signal transduction, mouse euthanasia was timed so that dLNs could be put in ice-cold PBS with eFluor780 (1/3000) 15-30 min after antigen injection. dLNs were processed into a single cell suspension on ice, combined with an equal volume of 4% PFA, and then incubated for 10 minutes in a 37°C water bath to fix the cells and stop BCR signaling. Fixed cells were washed and then a surface stain was performed as above. Afterwards, cells were incubated with 1.6% PFA for 5 minutes at room temperature and then centrifuged at 1000 × *g*. The supernatant was discarded and then cells were incubated in the residual volume on ice for 5 minutes. Next, cells were permeabilized by adding three consecutive 30µL increments of ice-cold 90% methanol in PBS and mixing with a pipette. Cells were incubated on ice for 30 minutes, then 110µL FACS buffer was added, and cells were incubated for a further 5 minutes. Cells were then washed twice by centrifugation at 1000 × *g*, resuspended in 200µL FACS buffer, and centrifuged again. Washed cells were then incubated with anti-isotype antibodies for 45 minutes on ice. Afterwards, cells were washed twice as before, resuspended in 20µL of FACS buffer containing 1-2% normal mouse serum (Jackson ImmunoResearch) and 1-2% mouse gamma globulin, and incubated at RT for 30 minutes. This step occludes the free arms of the anti-mouse IgG1 antibody, which was used to detect IgG1 PCs, to block subsequent binding to phosflow antibodies of the mouse IgG1 isotype. After 30 minutes of blocking, phosflow antibodies were added and cells were incubated for a further 40 minutes, and then cells were washed prior to analysis. See Table 3.3 for antibodies and dilution factors.

In vitro phosflow experiments

A media swap was performed as described above and then cultured cells were incubated at 37°C

for 5 minutes with 12.5µg/mL goat anti-mouse Igκ F(ab)'2 and eFluor780 (1/1000). Cells were then fixed by addition of PFA to a final concentration of 2% and incubated at 37°C for 10 minutes to stop BCR signaling and fix the cells. The rest of the protocol was performed as described above for *in vivo* phosflow.

Ca^{2+} flux experiments

All Ca^2 flux experiments were performed with cells from mice compound heterozygous for the Verigem and *Igh-J^{tm1Dh}* IgH alleles. This strategy ensured that $mIgE^+$ BCR expression originated from the Verigem allele, such that all IgE^+ cells were $Venus^+$. B cells were purified and cultured as described above for 4.5 days ± 6 hours. Cells were then washed and resuspended in 100µL PBS + 1% FBS. Each time cells were centrifuged, 10µL DNase I (Roche) was added to the pellet prior to re-suspension. Cells were then counted with a Coulter Counter Z2 instrument, diluted to 20 * 10^6 cells/mL, and stained with eFluor780 Fixable Viability Dye (1/1000) and CD138-PE (1/200). Cells were stained for 5-15 minutes at RT or 37°C. Cells were washed, resuspended in cRPMI at 20 * 10^6 cells/mL, and loaded with the Ca^{2+}-sensitive dye Indo-1 at 0.1µM for 20 minutes at 37°C. Finally, cells were washed again and resuspended in cRPMI at 20-100 * 10^6 cells/mL and maintained in a water bath at 37°C prior to flow cytometric analysis. Events were collected on an LSR Fortessa X-20 (BD) for ~10s prior to the addition of anti-BCR antibodies (αIgE clone R1E4 or αIgκ) or control (Goat IgG) at a final concentration of 100µg/mL. After the addition of anti-BCR antibodies, cells were vortexed to mix and returned to the cytometer to observe Ca^{2+} flux.

Cell sorting experiments

Cell sorting experiments were performed using Verigem-homozygous cells cultured for 4.5 days

± 6 hours. Cells were retrieved from culture, washed, and resuspended in Hank's Balanced Salt Solution (HBSS; obtained from UCSF cell culture facility) supplemented with 1% FBS, 0.5% BSA (Sigma-Aldrich), 2mM EDTA and 10mM HEPES, hereafter known as 'sorting media'. Cells were then counted with a Coulter Counter Z2 instrument, diluted to 20M cells/mL, and stained with eFluor780 (1/1000), CD138-PE, and IgD-BV510 for 10-30 minutes at RT. Cells were washed, resuspended in HBSS, and diluted to a final concentration of 30 * 10^6 cells/mL in sorting media. Cells were then sorted on a BD FACS Aria II instrument.

Post-sort media was prepared which consisted of 50% FBS 50% cRPMI. Immediately prior to sorting, post-sort media was passed through a 40μm Falcon cell strainer (Fisher Scientific) into a 5mL polypropylene tube (Fisher Scientific). Cells were sorted with a 70μm nozzle at a frequency of 87,000 droplets/second. Immediately following sorting, the purity of sorted populations was verified by flow cytometry. Sorted cells were plated into previously prepared culture plates at 0.5-2 *10^4 sorted cells/well. Cells were then treated with anti-BCR antibodies or controls (5μg/mL) as well as with or without various inhibitors and controls and maintained in culture for an additional 24 ± 3 hours prior to flow cytometric analysis.

Statistical analysis

To achieve power to discern meaningful differences, experiments were performed with multiple biological replicates and/or multiple times, see figure legends. The number of samples chosen for each comparison was determined based on past similar experiments to gauge the expected magnitude of differences. GraphPad Prism v9 was used for statistical analyses. Data approximated a log-normal distribution and thus were log transformed for statistical tests. Statistical tests were

selected by consulting the GraphPad Statistics Guide according to experimental design. All tests were two-tailed.

Supplementary material

Figure S3.1 presents the flow cytometry gating strategy used to identify IgE, IgG1, and IgM PCs and GC B cells *in vivo*. Figure S3.2 shows the BCR expression and signaling capacity of B cells and PCs of the indicated isotypes *in vitro*. Figure S3.3 contains further characterization related to Figures 3.2 and 3.3, including the effects of 12-hour cognate antigen exposure on PCs as well as the relationship between Igλ_1 expression and NP-binding. Figure S3.4 provides supporting evidence for data in Figure 3.4, including gating schemes, validation, and B cell survival data. Figure S3.5 presents CRISPR experiments using additional guides to support the studies shown in Figure 3.5. Table 3.1 provides the concentrations of inhibitors used in Figure 3.5. Table 3.2 contains the nucleotide sequences of sgRNAs used in Figure 3.5 and Figure S3.5. Table 3.3 details the reagents used for flow cytometry.

Discussion

Here, we reported that IgE PCs had high surface BCR expression that corresponded with the activation of an intracellular signaling cascade in response to antigen exposure. Specifically, BCR stimulation on IgE PCs resulted in the phosphorylation of Syk, BLNK, and PLCγ2 as well as Ca^{2+} flux. This signaling was toxic to IgE PCs, which were depleted proportionally to the strength of BCR stimulation. Consistent with the induction of apoptosis, BCR stimulation resulted in caspase-3 activation in IgE PCs, which could be rescued from cell death by overexpression of a pro-survival *Bcl2* transgene. Through a combination of pharmacological agents and CRISPR gene targeting, we identified Syk, BLNK, and PLCγ2 as key components of the BCR signalosome required for the elimination of IgE PCs after BCR stimulation. In mice, we found that conditional deletion of a single copy of *Syk* in PCs led to a selective increase in the abundance and relative frequency of IgE PCs, indicating that IgE PCs are uniquely constrained by intrinsic BCR signaling *in vivo*. Conversely, ligation of mIgE *in vivo* with cognate antigen or an αIgE monoclonal antibody led to the elimination of IgE PCs.

Overall, our data have revealed that IgE PCs are uniquely sensitive to BCR signaling-induced elimination. Quantitative differences in BCR signal transduction may explain the increased sensitivity of IgE PCs to antigen-induced elimination compared with IgG1 PCs. We found that IgE PCs had higher surface mIg expression than IgG1 PCs, which correlated with enhanced phosphorylation of BCR signalosome components after the ligation of mIgE compared with mIgG1. Our studies showing that IgE PC elimination was dependent on the affinity, avidity, and amount of antigen binding to the BCR further reinforce this concept. Our findings also imply that qualitative differences in BCR signaling promote the elimination of IgE PCs relative to IgM PCs.

Specifically, we found that IgE and IgM PCs had similar surface mIg expression and phosphorylation of proximal BCR signaling proteins, yet IgE PCs were more susceptible to apoptosis induced by BCR stimulation. Furthermore, conditional deletion of *Syk* in PCs *in vivo* led to an increase in IgE PCs but not IgM PCs. The differences in the BCR ligation-induced elimination of IgE and IgM PCs could be related to structural differences between these BCR isotypes. For example, mIgE has an extended cytoplasmic tail (CT), whereas mIgM has a truncated sequence of only three amino acids. The CTs of mIgE and mIgG are thought to prevent recruitment of the inhibitory molecule CD22, which may amplify signaling.[94] In addition, mIgE and mIgG have a conserved tyrosine motif in their CTs that is thought to be important for amplification of BCR signal transduction.[95] The mIgE CT has also been reported to associate with HAX-1, which could play a role in the induction of or protection from apoptosis.[38,96] Arguing against a role for the mIgE CT in promoting IgE PC apoptosis, mice with mutations of the tyrosine motif in the mIgE CT, or truncation of the mIgE CT, have diminished, rather than augmented, IgE responses.[97,98] It is unclear whether this result is due to a role for the mIgE CT in IgE PCs or their activated IgE B cell precursors. Overall, further studies will be needed to elucidate the mechanistic basis for the different functional outcomes of ligation of the IgE BCR versus IgG1 and IgM BCRs in PCs.

Relatedly, we found that BCR ligation has different functional consequences in PCs compared with B cells. Our cell sorting experiments showed that BCR ligation induced robust caspase-3 activation in IgE PCs, followed by their depletion, with more modest effects on IgG1 and IgM PCs. However, BCR ligation did not induce aCas3 in activated B cells of any isotype (IgE, IgG1 or IgM) and instead actually increased their abundance. These outcomes may be related, in part,

to our culture conditions, which included αCD40 and IL-4 to mimic T cell help. Previous studies have provided conflicting data on whether there are differences in the survival of IgE versus IgG1 B cells in cell culture without BCR stimulation,[32,33,35,38,39] which we have reviewed in detail.[1] Our studies reported here are distinct because we specifically investigated the impact of BCR stimulation on cell survival. Overall, our present data indicate that BCR ligation results in signal transduction that is toxic to IgE PCs, but not to IgE B cells.

Our observation that apoptotic PCs lost expression of the marker CD138 also has important implications for the study of apoptosis in the context of IgE responses. Since a large fraction of IgE B cells undergo PC differentiation, apoptotic IgE PCs that have lost CD138 expression could potentially contaminate analyses of IgE B cells. Contamination of dying IgE PCs into IgE B cell flow cytometry gating schemes is especially of concern *in vitro*, where dead cells are not cleared by phagocytes. Therefore, we advise that *in vitro* studies of IgE B cells should take special precautions to exclude dying IgE PCs, which we found have high intracellular IgE staining. Our results further suggest that future studies of PC apoptosis should utilize markers other than CD138 to identify dying PCs.

The studies presented here involving pharmacological inhibitors and CRISPR-Cas9 targeting revealed that Syk, BLNK, and PLCγ2 were essential for the elimination of IgE PCs after BCR stimulation. In contrast, the inhibition of Btk with ibrutinib only partially rescued IgE PCs. This result was unexpected, given the established role of Btk in activating PLCγ2 downstream of BCR stimulation.[99,100] Some residual PLCγ2 phosphorylation was reported in a Btk-deficient B cell line, which may be due to the activity of Syk or Src family kinases.[100–102] Alternatively, these findings

could be explained by redundancy between Btk and other Tec-family kinases for PLCγ2 activation in IgE PCs. A third possibility is that the requirement for PLCγ2 in BCR stimulation-induced IgE PC elimination involves not only its enzymatic effects but also its reported role in stabilizing the assembly of the BCR signalosome.[103] While the partial contribution of Btk requires further investigation, our data establish a crucial role for the BCR signalosome components Syk, BLNK, and PLCγ2 in the elimination of IgE PCs following BCR stimulation.

The above findings regarding the BCR signalosome provide new insights into prior data obtained from mice with *Syk* and *Blnk* mutations. Specifically, we previously observed that when a single copy of *Syk* was conditionally deleted in activated B cells in mice, this resulted in an increase in the abundance of IgE PCs.[33] While this could have reflected signaling mediated by Syk in precursor B cells, here we found that conditional deletion of *Syk* in PCs in mice also led to an increase in the abundance of IgE PCs. Together with our cell culture data showing that Syk inhibition prevented IgE PC apoptosis induced by BCR stimulation, our findings provide evidence that *Syk* heterozygosity directly increases the survival of IgE PCs. In BLNK-deficient mice, IgE PCs accumulated for several weeks, suggesting they were long-lived.[32] While this could have been secondary to enhanced IgE GC B cell responses in these mice, our data here indicate that BLNK-deficiency directly protects IgE PCs from apoptosis after BCR stimulation. Therefore, we propose that the increases in IgE PC responses in mice with perturbations in BCR signal transduction are at least in part due to a direct physiological role for BCR signaling in restraining IgE PC survival.

The idea that BCR signaling in PCs impairs longevity is supported by evidence from mice in which the gene encoding SHP-1, a negative regulator of BCR signaling, was conditionally deleted

following B cell activation. These studies identified several features of SHP-1-deficiency that seem reminiscent of IgE responses, including increased PC apoptosis, an abortive GC response, and a reduction in long-lived PCs.[104,105] One study also identified a role for SHP-1 in PC migration.[104] Interestingly, prior work swapping the mIgE membrane and cytoplasmic domains with those of IgG1 showed that this also affected bone marrow migration.[106] However, in the case of SHP-1 this reportedly affected integrin activity[104] whereas IgE domain swapping reportedly affected migration to CXCL12.[106] Overall, this evidence is consistent with the model that BCR signaling limits IgE PC longevity *in vivo*, and suggests that this could occur through the dual mechanisms of promoting apoptosis and impairing migration to PC survival niches. One outstanding question is whether the effect of BCR ligation varies for long-lived vs short-lived IgE PCs. Here, we exclusively investigated IgE PCs within a few days of their formation. It will be important to determine whether the susceptibility of IgE PCs to BCR signaling-induced death changes as they age and mature.

The major finding reported here, that BCR stimulation induced IgE PC elimination, does not exclude a contribution of antigen-independent BCR signaling to the regulation of IgE PC longevity. Elevated BCR expression on IgE PCs may result in increased antigen-independent mIgE signaling relative to IgE B cells, which could negatively impact the survival of IgE PCs. Consistent with this possibility, a recent study reported a higher proportion of IgE PCs than IgG1 PCs had aCas3 staining in an *in vitro* culture system without antigen.[35] In this study, the authors also noted a reduction in the frequency of $aCas3^{+}$ IgE PCs after CRISPR targeting of *Plcg2* or pharmacological inhibition of Syk. However, this latter finding was not compared to IgG1 PCs. Further exploring how antigen-independent and antigen-dependent BCR signaling govern IgE

responses represents an important area of future inquiry, especially *in vivo* where immunization with antigen makes it difficult to disentangle antigen-dependent and antigen-independent effects.

While in this study we focused on the antigen-induced elimination of IgE PCs in mice, we anticipate that these findings will translate to humans. As in mice, human IgE PCs have elevated surface mIgE expression relative to human IgE B cells.[34] Related observations in IgA and IgM PCs are also consistent between mice and humans, including that these cells express elevated mIg and show evidence of BCR signal transduction following mIg ligation.[48,49] Similar to our finding that αIgE R1E4 depleted IgE PCs, studies of mice in which a human M1' region was inserted into mIgE showed that treatment with a therapeutic anti-M1' antibody led to a reduction in IgE PCs.[107] While the authors of this study attributed this result to effects of the anti-M1' antibody on IgE B cells that were the precursors of IgE PCs, we propose that this therapy could also directly trigger the apoptosis of IgE PCs. Relatedly, our finding that the R1E4 clone of αIgE eliminated IgE PCs *in vivo* raises the possibility that human therapeutic αIgE monoclonal antibodies, such as omalizumab and legilizumab, could similarly ligate mIg on IgE PCs and induce apoptosis. In this regard, we note that the R1E4 clone of αIgE used in our studies only recognizes IgE that is not bound to FcεRI,[87] similar to the omalizumab and legilizumab αIgE therapeutics developed for the treatment of allergic diseases.[108] Interestingly, legilizumab was reported to inhibit IgE production in cell culture,[108] which we propose could be due to the direct elimination of IgE PCs.

Our conclusion that cognate antigen recognition results in IgE PC elimination predicts that the amount of antigen IgE PCs are exposed to may regulate antigen-specific IgE production. Notably, physiological exposures to inhaled aeroallergens in the respiratory tract may be at relatively low

doses compared to those used in mouse models of allergic airway disease. Classic studies found that immunization of rodents with low doses of antigen produced more persistent IgE responses.[109–111] Powerful IgE responses can also be provoked by anti-IgD immunization in mice,[112] which by definition would be unable to ligate mIgE following IgE class switch recombination. Infections with helminth worms are also known to result in dramatic increases in total IgE, yet most of this IgE response is non-specific.[113] In these infections, high doses of antigen exposure could result in the elimination of antigen-specific IgE PCs, favoring the survival of non-antigen-specific IgE PCs. In human food allergy, patients with severe symptoms typically alter their diet to avoid consumption of the foods to which they are allergic. This allergen avoidance may result in enhanced survival of antigen-specific IgE PCs, consistent with the detection of antigen-specific IgE PCs in the blood of patients with peanut allergy.[114] Conversely, regular oral exposure to food allergens early in life, such as peanut, has been reported to promote allergen-specific tolerance.[115] We also note that repeated dosing with increasing amounts of antigen is the key concept underlying allergen immunotherapy. Although such regimens likely have many effects on the immune system, including the induction of antigen-specific IgG4 and impacts on T cells,[116] our results reveal that the administration of cognate antigen can directly eliminate antigen-specific IgE PCs. This represents a new possible mechanism by which allergen immunotherapy may achieve therapeutic benefit. Overall, we propose that the amount of antigen exposure may be an important factor constraining the lifespan of IgE PCs.

Our findings also raise the possibility that genetic variations in molecules involved in BCR signal transduction or apoptosis could affect IgE PC survival. In support of this idea, a wealth of literature links elevated IgE and/or atopy with primary immunodeficiencies or mutations associated with

impairments in antigen receptor signaling pathways,[117] although aberrations of these pathways would likely affect B cells and T cells in addition to PCs. A recent mutagenesis screen in mice determined that several mutations in genes with a role in BCR signaling, including *Syk* and *Plcg2*, led to increased IgE production.[82] This study estimated that over a third of the human population may be heterozygous carriers for atopy risk alleles that affect BCR signaling or class switch recombination. Even in individuals without inherited alleles that affect BCR signaling or apoptosis, it is possible that sporadic somatic mutations could occur in B cells or PCs that could result in enhanced IgE PC survival in the context of antigen exposure. Our studies have shown that the mutation of even one copy of a gene involved in BCR signal transduction, such as *Syk*, can result in an increase in IgE PC abundance. A potentially important source of somatic mutations in IgE PC precursors could be the GC, in which somatic hypermutation of antibody variable genes occasionally leads to off-target somatic mutations in other regions of the genome, as is well-known from studies of lymphomagenesis.[118] We therefore propose that inherited and/or somatic mutations that alter BCR signal transduction or apoptosis could result in enhanced survival of antigen-specific IgE PCs in the context of allergy.

The key conclusion of this study is that antigen-driven BCR signaling eliminates IgE PCs, identifying another important way in which the IgE BCR restricts IgE responses. This work establishes a clear functional role for BCR expression on IgE PCs, which has been poorly understood for any PC isotype. Our findings also raise the possibility of other functional outcomes downstream of BCR activation on IgE PCs or other PC isotypes, such as effects on proliferation, cytoskeletal rearrangement, or metabolism. Overall, we believe that our findings may be important for understanding immune tolerance to allergens, with potential therapeutic implications.

Chapter 4: Conclusion

The regulation of IgE responses by BCR signaling

Our findings represent a significant addition to the growing body of literature investigating the negative regulation of IgE responses by BCR signaling. Prior work encompasses a breadth of studies investigating antigen-driven signaling in naïve B cells or antigen-independent signaling in IgE B cells. To this body of work, we have added our studies of antigen-driven signaling in naïve B cells and IgE PCs, which we have summarized in an overall model in Figure 4.1.

Beginning with naïve B cells, studies agree that PI3K signaling and BCR stimulation both decrease the likelihood of CSR. Mice deficient in PTEN (phosphatase and tensin homolog), which reverses the lipid phosphorylation reaction catalyzed by PI3K, exhibit hyper-phosphorylation of Akt. Akt upregulates BLIMP1 and downmodulates the activity of FOXO family members, whose roles include the regulation of *Aicda* transcription, thereby increasing PC differentiation and reducing CSR.[50,57,59]

Our finding that inhibition of PI3K signaling increases IgE CSR in the absence of a BCR ligand raises the question of what the source of the PI3K signaling being inhibited is. Notably, PI3K can be activated both by antigen-induced BCR signaling and by tonic, BCR-dependent activity, the latter of which is required for B cell survival.[42] It has also been suggested that signaling downstream of CD30 or the IL-4 receptor, can activate PI3K.[119] In the future it would be interesting to examine which source(s) of non-BCR ligation-induced PI3K activity represent(s) the key suppressors of IgE CSR that are targeted by PI3K inhibition.

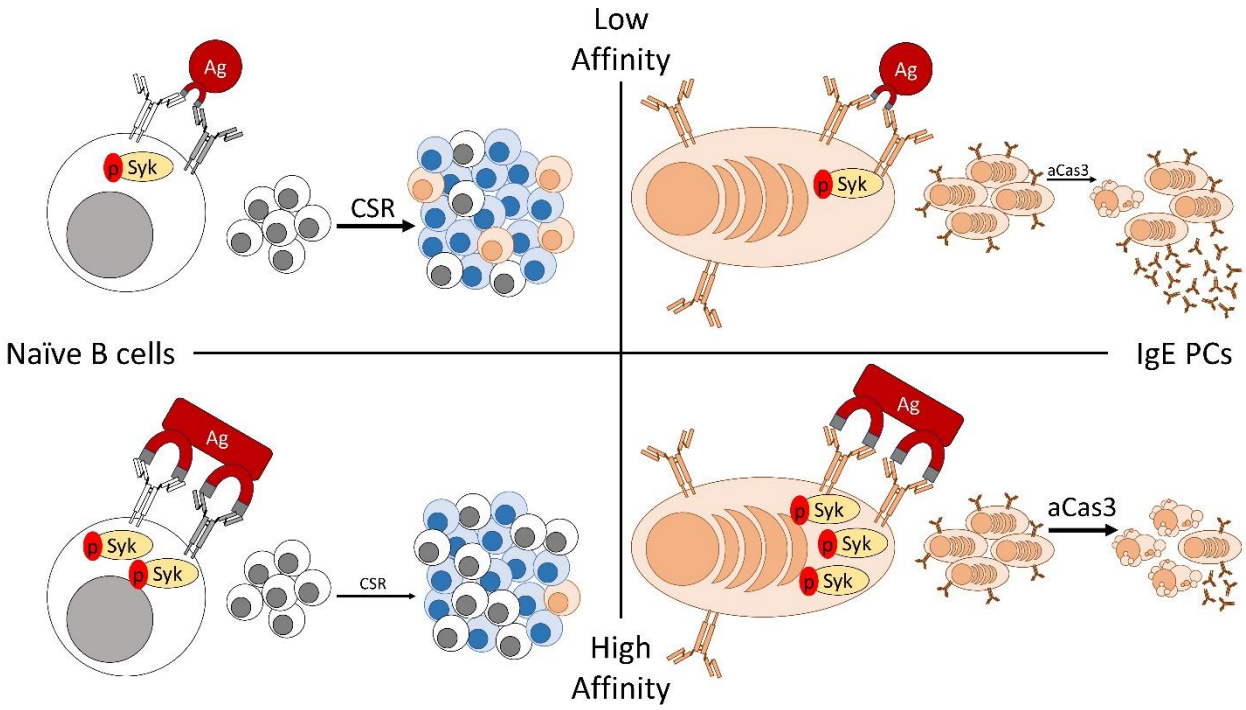

Figure 4.1 The regulation of IgE by antigen-induced BCR signaling. This model is divided into four quadrants. The left half depicts the negative regulation of IgE CSR by BCR stimulation (Chapter 2) while the right depicts the elimination of IgE PCs by BCR stimulation (Chapter 3); the top depicts encounter with a low affinity/avidity antigen while the bottom depicts encounter with a high affinity/avidity antigen. The left side shows that the CSR of naïve B cells to IgE is inhibited by BCR stimulation in a manner corresponding with BCR signal strength. The white-filled cells represent naïve B cells, while the blue-filled cells represent IgG1-switched B cells and the orange-filled cells represent IgE-switched B cells. On the right side it is depicted that the high amount of surface BCR on IgE PCs allows them to capture Ag. Stronger Ag binding results in greater Syk phosphorylation and resultant induction of active caspase-3 (aCas3). This leads to greater IgE PC elimination and ultimately a reduction in secreted IgE.

In our studies the effect of BCR stimulation on CSR in general were relatively modest, while the specific effects on IgE CSR were substantial. Consistent with a selective inhibition of IgE CSR by BCR signaling, immunization with high-affinity antigen reduced the representation of IgE cells in the GC by more than 2-fold and among early PCs by over 5-fold while the proportion of IgG1-switched cells either did not change or increased. Conversely, the weakened BCR signaling in mice with only one copy of Igα increased IgE GC B cells and PCs approximately 2-fold. *In vitro*, we show that IgE CSR can be reduced by about 75% using αBCR antibodies and by well over 90% with just pg/mL quantities of high affinity soluble cognate antigen (50pg/mL of $NIP_{24}BSA$),

with minimal effects on IgG1 CSR at this dose. In combination with other recent work,[54] these results establish the selective effect of BCR stimulation on IgE CSR and, more broadly, reveal how something commonly considered to broadly inhibit CSR can have a more powerful and selective impact on IgE.

While we focused on IgE CSR from naïve B cells, IgE CSR can occur from any upstream isotype at the IgH locus. While emerging evidence on which I am co-first author[120] contests the prevalent notion that sequential switching via IgG1 is important in food allergy,[23,121–125] recent work also provides direct evidence that stimulating the BCR on an IgG1 cell can suppress sequential switching to IgE.[54] This provides another reason to believe that IgG1 to IgE sequential CSR might be limited in a physiologic setting. Many IgG1 cells are present as MBCs or as GC B cells. In a secondary response an IgG1 MBC would be recalled by sensing antigen through its BCR, activating a BCR signal that would likely reduce its odds of further CSR to IgE. Meanwhile, within the GC are both T_{FH} and antigen-laden follicular dendritic cells (FDCs). These would provide sources of IL-21 and BCR stimulation, respectively, which we have shown here synergize to radically suppress IgE CSR. That said, the nature and role of BCR signaling within the GC remains an area of active inquiry[126–130] and it is unclear if the altered state of GC B cells might alter the inhibition of CSR normally driven by BCR ligation. Furthermore, GC B cells also express high levels of Bcl6, which has been described to inhibit IgE.[70,131] Therefore, further *in vivo* study is needed to confirm the role of BCR stimulation not only in suppressing direct CSR to IgE but also in impairing sequential class-switching to IgE via IgG1.

Once IgE CSR occurs, expression of the IgE BCR in an activated B cell initiates antigen-independent signaling that is sufficient to induce PC differentiation.[32,33] Our findings in Chapter 3 of this dissertation provide the first evidence that, following PC differentiation, the direct regulation of IgE responses by BCR signaling continues in IgE PCs. Our key finding was that IgE PCs responded to cognate antigen encounter with robust activation of BCR signaling pathways followed by cell death (Figure 4.1). While we focused on antigen-driven signaling, the high mIgE expression on IgE PCs may result in stronger antigen-independent signaling relative to IgE B cells that might also predispose IgE PCs towards cell death. Following BCR ligation, we identified a clear requirement for the BCR signalosome (e.g. BLNK, PLCγ2) and the kinases that activate it (e.g. Syk, Btk) in the elimination of IgE PCs. Demonstrating the importance of BCR signaling to constraining IgE PC longevity, BLNK-deficient mice have sustained titers of IgE following immunization.[32] However, whether this is due to defective antigen-induced BCR signaling in IgE PCs or impaired tonic signaling in either IgE B cells or PCs remains to be determined.

It is interesting to observe how the importance of some molecules overlaps between the inhibition of IgE CSR, the antigen-independent signaling of the IgE BCR, and the antigen-dependent elimination of IgE PCs. This overlap may serve to explain how even heterozygous impairments in some signaling proteins (e.g. Syk), which normally would not be expected to produce a phenotype, can result in substantial increases in IgE. While homozygous mutations in BCR signaling proteins are difficult to study due to effects on B cell development and viability (even BLNK deficiency, discussed above, has serious effects on B cell development and circulating mature B cell numbers), we posit that the substantial dysregulation of IgE seen in heterozygous mutants for BCR signaling pathway components belies a much greater total contribution of BCR signaling to IgE regulation.

Overall, the data presented here, in combination with prior work, establish a picture whereby BCR signaling limits the fraction of the immune response that undergoes IgE CSR, and then shepherds those cells that do switch to IgE towards a PC fate doomed to rapid apoptosis. It will be interesting to investigate in future work whether these IgE-inhibitory mechanisms are intact in allergic individuals, or if dysregulation at various steps within this pathway could partly explain the emergence of their allergic pathology.

References

1. Wade-Vallance, A. K. & Allen, C. D. C. Intrinsic and extrinsic regulation of IgE B cell responses. *Curr Opin Immunol* **72**, 221–229 (2021).

2. Wade-Vallance, A. K. *et al.* B cell receptor ligation induces IgE plasma cell elimination. *J Exp Med* **220**, e20220964 (2023).

3. Platts-Mills, T. A. E., Heymann, P. W., Commins, S. P. & Woodfolk, J. A. The discovery of IgE 50 years later. *Ann. Allergy, Asthma Immunol.* **116**, 179–182 (2016).

4. Geha, R. S., Jabara, H. H. & Brodeur, S. R. The regulation of immunoglobulin E class-switch recombination. *Nat Rev Immunol* **3**, 721–732 (2003).

5. Finkelman, F. D. *et al.* Lymphokine Control of in Vivo Immunoglobulin Isotype Selection. *Annu. Rev. Immunol.* **8**, 303–333 (1990).

6. Coffman, R. L. Origins of the TH1-TH2 model: a personal perspective. *Nat. Immunol.* **7**, 539–541 (2006).

7. Crotty, S. T Follicular Helper Cell Biology: A Decade of Discovery and Diseases. *Immunity* **50**, 1132–1148 (2019).

8. Reinhardt, R. L., Liang, H.-E. & Locksley, R. M. Cytokine-secreting follicular T cells shape the antibody repertoire. *Nat Immunol* **10**, 385–393 (2009).

9. King, I. L. & Mohrs, M. IL-4–producing CD4+ T cells in reactive lymph nodes during helminth infection are T follicular helper cells. *J. Exp. Med.* **206**, 1001–1007 (2009).

10. Harada, Y. *et al.* The 3′ Enhancer CNS2 Is a Critical Regulator of Interleukin-4-Mediated Humoral Immunity in Follicular Helper T Cells. *Immunity* **36**, 188–200 (2012).

11. Liang, H.-E. *et al.* Divergent expression patterns of IL-4 and IL-13 define unique functions in allergic immunity. *Nat Immunol* **13**, 58–66 (2012).

12. Kobayashi, T., Iijima, K., Dent, A. L. & Kita, H. Follicular helper T cells mediate IgE antibody response to airborne allergens. *J Allergy Clin Immun* **139**, 300-313.e7 (2017).

13. Yang, Z., Wu, C.-A. M., Targ, S. & Allen, C. D. C. IL-21 is a broad negative regulator of IgE class switch recombination in mouse and human B cells. *J Exp Medicine* **217**, (2020).

14. Ozaki, K. *et al.* A Critical Role for IL-21 in Regulating Immunoglobulin Production. *Science* **298**, 1630–1634 (2002).

15. Kotlarz, D., Zitara, N., Milner, J. D. & Klein, C. Human IL-21 and IL-21R deficiencies. *Curr Opin Pediatr* **26**, 704–712 (2014).

16. Minegishi, Y. *et al.* Dominant-negative mutations in the DNA-binding domain of STAT3 cause hyper-IgE syndrome. *Nature* **448**, 1058–1062 (2007).

17. Berglund, L. J. *et al.* IL-21 signalling via STAT3 primes human naïve B cells to respond to IL-2 to enhance their differentiation into plasmablasts. *Blood* **122**, 3940–3950 (2013).

18. Gowthaman, U. *et al.* Identification of a T follicular helper cell subset that drives anaphylactic IgE. *Science* eaaw6433 (2019) doi:10.1126/science.aaw6433.

19. Clement, R. L. *et al.* Follicular regulatory T cells control humoral and allergic immunity by restraining early B cell responses. *Nat Immunol* 1–12 (2019) doi:10.1038/s41590-019-0472-4.

20. Kim, C. J. *et al.* The Transcription Factor Ets1 Suppresses T Follicular Helper Type 2 Cell Differentiation to Halt the Onset of Systemic Lupus Erythematosus. *Immunity* **49**, 1034-1048.e8 (2018).

21. Lehrer, S. B. *et al.* Enhancement of murine IgE antibody detection by IgG removal. *J. Immunol. Methods* **284**, 1–6 (2004).

22. Erazo, A. *et al.* Unique Maturation Program of the IgE Response In Vivo. *Immunity* **26**, 191–203 (2007).

23. Xiong, H., Dolpady, J., Wabl, M., Lafaille, M. A. C. de & Lafaille, J. J. Sequential class switching is required for the generation of high affinity IgE antibodies. *J Exp Medicine* **209**, 353–364 (2012).

24. Wing, J. B., Ise, W., Kurosaki, T. & Sakaguchi, S. Regulatory T Cells Control Antigen-Specific Expansion of Tfh Cell Number and Humoral Immune Responses via the Coreceptor CTLA-4. *Immunity* **41**, 1013–1025 (2014).

25. Lafaille, M. A. C. de *et al.* Adaptive Foxp3+ Regulatory T Cell-Dependent and -Independent Control of Allergic Inflammation. *Immunity* **29**, 114–126 (2008).

26. Xie, M. M. *et al.* T follicular regulatory cells and IL-10 promote food antigen-specific IgE. *J Clin Invest* **130**, 3820–3832 (2020).

27. Gonzalez-Figueroa, P. *et al.* Follicular regulatory T cells produce neuritin to regulate B cells. *Cell* **184**, 1775-1789.e19 (2021).

28. Cañete, P. F. *et al.* Regulatory roles of IL-10–producing human follicular T cells. (2017) doi:10.1084/jem.20190493.

29. Yang, Z., Sullivan, B. M. & Allen, C. D. C. Fluorescent In Vivo Detection Reveals that IgE+ B Cells Are Restrained by an Intrinsic Cell Fate Predisposition. *Immunity* **36**, 857–872 (2012).

30. Talay, O. *et al.* IgE+ memory B cells and plasma cells generated through a germinal-center pathway. *Nat Immunol* **13**, 396–404 (2012).

31. He, J.-S. *et al.* The distinctive germinal center phase of IgE+ B lymphocytes limits their contribution to the classical memory response. *J Exp Medicine* **210**, 2755–2771 (2013).

32. Haniuda, K., Fukao, S., Kodama, T., Hasegawa, H. & Kitamura, D. Autonomous membrane IgE signaling prevents IgE-memory formation. *Nat Immunol* **17**, 1109–1117 (2016).

33. Yang, Z. *et al.* Regulation of B cell fate by chronic activity of the IgE B cell receptor. *Elife* **5**, e21238 (2016).

34. Ramadani, F. *et al.* Ontogeny of human IgE-expressing B cells and plasma cells. *Allergy* **72**, 66–76 (2016).

35. Newman, R. & Tolar, P. Chronic calcium signaling in IgE+ B cells limits plasma cell differentiation and survival. *Immunity* (2021) doi:10.1016/j.immuni.2021.11.006.

36. Shinnakasu, R. & Kurosaki, T. Regulation of memory B and plasma cell differentiation. *Curr. Opin. Immunol.* **45**, 126–131 (2017).

37. Tong, P. *et al.* IgH isotype-specific B cell receptor expression influences B cell fate. *Proc National Acad Sci* **114**, E8411–E8420 (2017).

38. Laffleur, B. *et al.* Self-Restrained B Cells Arise following Membrane IgE Expression. *Cell Reports* **10**, 900–909 (2015).

39. Ramadani, F., Bowen, H., Gould, H. J. & Fear, D. J. Transcriptional Analysis of the Human IgE-Expressing Plasma Cell Differentiation Pathway. *Front Immunol* **10**, 402 (2019).

40. Tsubata, T., Wu, J. & Honjo, T. B-cell apoptosis induced by antigen receptor crosslinking is blocked by a T-cell signal through CD40. *Nature* **364**, 645–648 (1993).

41. Finkelman, F. D., Holmes, J. M., Dukhanina, O. I. & Morris, S. C. Cross-linking of membrane immunoglobulin D, in the absence of T cell help, kills mature B cells in vivo. *J Exp Medicine* **181**, 515–525 (1995).

42. Srinivasan, L. *et al.* PI3 Kinase Signals BCR-Dependent Mature B Cell Survival. *Cell* **139**, 573–586 (2009).

43. Mayer, C. T. *et al.* The microanatomic segregation of selection by apoptosis in the germinal center. *Sci New York N Y* **358**, eaao2602 (2017).

44. Karnowski, A., Achatz-Straussberger, G., Klockenbusch, C., Achatz, G. & Lamers, M. C. Inefficient processing of mRNA for the membraneform of IgE is a genetic mechanism to limit recruitment of IgE-secreting cells. *Eur J Immunol* **36**, 1917–1925 (2006).

45. Venkitaraman, A. R., Williams, G. T., Dariavach, P. & Neuberger, M. S. The B-cell antigen receptor of the five immunoglobulin classes. *Nature* **352**, 777–781 (1991).

46. Vanshylla, K., Opazo, F., Gronke, K., Wienands, J. & Engels, N. The extracellular membrane-proximal domain of membrane-bound IgE restricts B cell activation by limiting B cell antigen receptor surface expression. *Eur J Immunol* **48**, 441–453 (2017).

47. Goodnow, C. C. *et al.* Altered immunoglobulin expression and functional silencing of self-reactive B lymphocytes in transgenic mice. *Nature* **334**, 676–682 (1988).

48. Blanc, P. *et al.* Mature IgM-expressing plasma cells sense antigen and develop competence for cytokine production upon antigenic challenge. *Nat Commun* **7**, 13600 (2016).

49. Pinto, D. *et al.* A functional BCR in human IgA and IgM plasma cells. *Blood* **121**, 4110–4 (2013).

50. Omori, S. A. *et al.* Regulation of Class-Switch Recombination and Plasma Cell Differentiation by Phosphatidylinositol 3-Kinase Signaling. *Immunity* **25**, 545–557 (2006).

51. Hauser, J. *et al.* B-cell receptor activation inhibits AID expression through calmodulin inhibition of E-proteins. *P Natl Acad Sci Usa* **105**, 1267–72 (2008).

52. Jabara, H. H. *et al.* B-cell receptor cross-linking delays activation-induced cytidine deaminase induction and inhibits class-switch recombination to IgE. *J Allergy Clin Immun* **121**, 191-196.e2 (2008).

53. Heltemes-Harris, L. M., Gearhart, P. J., Ghosh, P. & Longo, D. L. Activation-induced deaminase-mediated class switch recombination is blocked by anti-IgM signaling in a phosphatidylinositol 3-kinase-dependent fashion. *Mol Immunol* **45**, 1799–1806 (2008).

54. Udoye, C. C. *et al.* B-cell receptor physical properties affect relative IgG1 and IgE responses in mouse egg allergy. *Mucosal Immunol* 1–14 (2022) doi:10.1038/s41385-022-00567-y.

55. Baba, Y. & Kurosaki, T. Role of Calcium Signaling in B Cell Biology - Book Chapter - Current topics in Microbiology and Immunology. *Curr Top Microbiol* **393**, 143–174 (2015).

56. Zhang, T. *et al.* Genetic or pharmaceutical blockade of p110δ phosphoinositide 3-kinase enhances IgE production. *J Allergy Clin Immun* **122**, 811-819.e2 (2008).

57. Wang, J. *et al.* PTEN-Regulated AID Transcription in Germinal Center B Cells Is Essential for the Class-Switch Recombination and IgG Antibody Responses. *Front Immunol* **9**, 371 (2018).

58. Suzuki, A. *et al.* Critical Roles of Pten in B Cell Homeostasis and Immunoglobulin Class Switch Recombination. *J Exp Medicine* **197**, 657–667 (2003).

59. Chen, Z. *et al.* Imbalanced PTEN and PI3K Signaling Impairs Class Switch Recombination. *J Immunol* **195**, 5461–5471 (2015).

60. Chan, T. D. *et al.* Antigen Affinity Controls Rapid T-Dependent Antibody Production by Driving the Expansion Rather than the Differentiation or Extrafollicular Migration of Early Plasmablasts. *J Immunol* **183**, 3139–3149 (2009).

61. Paus, D. *et al.* Antigen recognition strength regulates the choice between extrafollicular plasma cell and germinal center B cell differentiation. *J Exp Medicine* **203**, 1081–1091 (2006).

62. Sonoda, E. *et al.* B Cell Development under the Condition of Allelic Inclusion. *Immunity* **6**, 225–233 (1997).

63. Hasbold, J., Lyons, A. B., Kehry, M. R. & Hodgkin, P. D. Cell division number regulates IgG1 and IgE switching of B cells following stimulation by CD40 ligand and IL-4. *Eur. J. Immunol.* **28**, 1040–1051 (1998).

64. Zhang, T., Makondo, K. J. & Marshall, A. J. p110δ phosphoinositide 3-kinase represses IgE switch by potentiating BCL6 expression. *J Immunol Baltim Md 1950* **188**, 3700–8 (2012).

65. Hauser, J., Grundström, C., Kumar, R. & Grundström, T. Regulated localization of an AID complex with E2A, PAX5 and IRF4 at the Igh locus. *Mol Immunol* **80**, 78–90 (2016).

66. Depoil, D. *et al.* CD19 is essential for B cell activation by promoting B cell receptor–antigen microcluster formation in response to membrane-bound ligand. *Nat Immunol* **9**, 63–72 (2007).

67. Fujimoto, M., Bradney, A. P., Poe, J. C., Steeber, D. A. & Tedder, T. F. Modulation of B Lymphocyte Antigen Receptor Signal Transduction by a CD19/CD22 Regulatory Loop. *Immunity* **11**, 191–200 (1999).

68. Fearon, D. T. & Carroll, M. C. Regulation of B Lymphocyte Responses to Foreign and Self-Antigens by the CD19/CD21 Complex. *Annu. Rev. Immunol.* **18**, 393–422 (2000).

69. Limon, J. J. & Fruman, D. A. Akt and mTOR in B Cell Activation and Differentiation. *Front Immunol* **3**, 228 (2012).

70. Tong, P. & Wesemann, D. R. Molecular Mechanisms of IgE Class Switch Recombination. *Curr Top Microbiol* **388**, 21–37 (2015).

71. Lu, H. Y. *et al.* Germline CBM-opathies: From immunodeficiency to atopy. *J Allergy Clin Immun* **143**, 1661–1673 (2019).

72. Saijo, K. *et al.* Protein Kinase C β Controls Nuclear Factor κB Activation in B Cells Through Selective Regulation of the IκB Kinase α. *J. Exp. Med.* **195**, 1647–1652 (2002).

73. Rickert, R. C., Jellusova, J. & Miletic, A. V. Signaling by the tumor necrosis factor receptor superfamily in B-cell biology and disease. *Immunol Rev* **244**, 115–33 (2011).

74. Cutrina-Pons, A., Sa, A. D., Fear, D. J., Gould, H. J. & Ramadani, F. Inhibition of PI3K p110δ activity reduces IgE production in IL-4 and anti-CD40 stimulated human B cell cultures. *Immunology* **170**, 483–494 (2023).

75. Rickert, R. C., Roes, J. & Rajewsky, K. B lymphocyte-specific, Cre-mediated mutagenesis in mice. *Nucleic Acids Res* **25**, 1317–1318 (1997).

76. Wu, C.-A. M. *et al.* Genetic engineering in primary human B cells with CRISPR-Cas9 ribonucleoproteins. *J Immunol Methods* **457**, 33–40 (2018).

77. Müller, U. *et al.* A Gene-Dosage Effect for Interleukin-4 Receptor α-Chain Expression Has an Impact on Th2-Mediated Allergic Inflammation during Bronchopulmonary Mycosis. *J. Infect. Dis.* **198**, 1714–1721 (2008).

78. Bürgis, S. & Gessner, A. Unexpected Phenotype of STAT6 Heterozygous Mice Implies Distinct STAT6 Dosage Requirements for Different IL-4 Functions. *Int. Arch. Allergy Immunol.* **143**, 263–268 (2007).

79. Robinson, M. J. *et al.* IL-4 Haploinsufficiency Specifically Impairs IgE Responses against Allergens in Mice. *J. Immunol.* **198**, 1815–1822 (2017).

80. Allen, C. D. C. Features of B Cell Responses Relevant to Allergic Disease. *J. Immunol.* **208**, 257–266 (2022).

81. Jiménez-Saiz, R. *et al.* Human BCR analysis of single-sorted, putative IgE+ memory B cells in food allergy. *J Allergy Clin Immun* (2019) doi:10.1016/j.jaci.2019.04.001.

82. SoRelle, J. A. *et al.* Dominant atopy risk mutations identified by mouse forward genetic analysis. *Allergy* **76**, 1095–1108 (2021).

83. Shih, T.-A. Y., Meffre, E., Roederer, M. & Nussenzweig, M. C. Role of BCR affinity in T cell–dependent antibody responses in vivo. *Nat Immunol* **3**, ni803 (2002).

84. Noviski, M. *et al.* Optimal Development of Mature B Cells Requires Recognition of Endogenous Antigens. *J Immunol Baltim Md 1950* **203**, 418–428 (2019).

85. Robinson, M. J. *et al.* Long-lived plasma cells accumulate in the bone marrow at a constant rate from early in an immune response. *Sci. Immunol.* **7**, eabm8389 (2022).

86. Saijo, K. *et al.* Essential role of Src-family protein tyrosine kinases in NF-κB activation during B cell development. *Nat Immunol* **4**, 274–279 (2003).

87. Keegan, A. D., Fratazzi, C., Shopes, B., Baird, B. & Conrad, D. H. Characterization of new rat anti-mouse IgE monoclonals and their use along with chimeric IgE to further define the site that interacts with FcεRII and FcεRI. *Mol Immunol* **28**, 1149–1154 (1991).

88. Ota, T., Aoki-Ota, M., Duong, B. H. & Nemazee, D. Suppression of IgE B Cells and IgE Binding to FcεRI by Gene Therapy with Single-Chain Anti-IgE. *J Immunol* **182**, 8110–8117 (2009).

89. Strasser, A. *et al.* Enforced BCL2 expression in B-lymphoid cells prolongs antibody responses and elicits autoimmune disease. *Proc. Natl. Acad. Sci.* **88**, 8661–8665 (1991).

90. Chen, J. *et al.* Immunoglobulin gene rearrangement in B cell deficient mice generated by targeted deletion of the J H locus. *Int Immunol* **5**, 647–656 (1993).

91. Sullivan, B. M. *et al.* Genetic analysis of basophil function in vivo. *Nat. Immunol.* **12**, 527–535 (2011).

92. Chicaybam, L., Sodre, A. L., Curzio, B. A. & Bonamino, M. H. An Efficient Low Cost Method for Gene Transfer to T Lymphocytes. *PLoS ONE* **8**, e60298 (2013).

93. Wilmore, J. R., Jones, D. D. & Allman, D. Protocol for improved resolution of plasma cell subpopulations by flow cytometry. *Eur. J. Immunol.* **47**, 1386–1388 (2017).

94. Sato, M., Adachi, T. & Tsubata, T. Augmentation of Signaling through BCR Containing IgE but not That Containing IgA Due to Lack of CD22-Mediated Signal Regulation. *J Immunol* **178**, 2901–2907 (2007).

95. Engels, N. *et al.* Recruitment of the cytoplasmic adaptor Grb2 to surface IgG and IgE provides antigen receptor–intrinsic costimulation to class-switched B cells. *Nat Immunol* **10**, 1018–1025 (2009).

96. Oberndorfer, I. *et al.* HS1-Associated Protein X-1 Interacts with Membrane-Bound IgE: Impact on Receptor-Mediated Internalization. *J. Immunol.* **177**, 1139–1145 (2006).

97. Achatz, G., Nitschke, L. & Lamers, M. C. Effect of Transmembrane and Cytoplasmic Domains of IgE on the IgE Response. *Science* **276**, 409–411 (1997).

98. Schmitt, M. E. R. *et al.* The B cell antigen receptor of IgE-switched plasma cells regulates memory IgE responses. *J Allergy Clin Immunol* (2020) doi:10.1016/j.jaci.2020.02.015.

99. Watanabe, D. *et al.* Four Tyrosine Residues in Phospholipase C-γ2, Identified as Btk-dependent Phosphorylation Sites, Are Required for B Cell Antigen Receptor-coupled Calcium Signaling*. *J. Biol. Chem.* **276**, 38595–38601 (2001).

100. Rodriguez, R. *et al.* Tyrosine Residues in Phospholipase Cγ2 Essential for the Enzyme Function in B-cell Signaling*. *J. Biol. Chem.* **276**, 47982–47992 (2001).

101. Takata, M. & Kurosaki, T. A role for Bruton's tyrosine kinase in B cell antigen receptor-mediated activation of phospholipase C-gamma 2. *J Exp Medicine* **184**, 31–40 (1996).

102. Özdener, F., Dangelmaier, C., Ashby, B., Kunapuli, S. P. & Daniel, J. L. Activation of Phospholipase Cγ2 by Tyrosine Phosphorylation. *Mol. Pharmacol.* **62**, 672–679 (2002).

103. Wang, J., Sohn, H., Sun, G., Milner, J. D. & Pierce, S. K. The autoinhibitory C-terminal SH2 domain of phospholipase C–γ2 stabilizes B cell receptor signalosome assembly. *Sci. Signal.* **7**, ra89 (2014).

104. Li, Y.-F., Xu, S., Ou, X. & Lam, K.-P. Shp1 signalling is required to establish the long-lived bone marrow plasma cell pool. *Nat Commun* **5**, 4273 (2014).

105. Yam-Puc, J. C. *et al.* Enhanced BCR signaling inflicts early plasmablast and germinal center B cell death. *Iscience* **24**, 102038 (2021).

106. Achatz-Straussberger, G. *et al.* Migration of antibody secreting cells towards CXCL12 depends on the isotype that forms the BCR. *Eur J Immunol* **38**, 3167–3177 (2008).

107. Brightbill, H. D. *et al.* Antibodies specific for a segment of human membrane IgE deplete IgE-producing B cells in humanized mice. *J Clin Invest* **120**, 2218–2229 (2010).

108. Gasser, P. *et al.* The mechanistic and functional profile of the therapeutic anti-IgE antibody ligelizumab differs from omalizumab. *Nat. Commun.* **11**, 165 (2020).

109. Vaz, E. M., Vaz, N. M. & Levine, B. B. Persistent formation of reagins in mice injected with low doses of ovalbuminl. *Immunology* **21**, 11–5 (1971).

110. HOLT, P. G. & McMENAMIN, C. Defence against allergic sensitization in the healthy lung: the role of inhalation tolerance. *Clin. Exp. Allergy* **19**, 255–262 (1989).

111. Prouvost-Danon, A., Mouton, D., Abadie, A., Mevel, J. -C. & Biozzi, G. Genetic regulation of IgE and agglutinating antibody synthesis in lines of mice selected for high and low immune responsiveness. *Eur. J. Immunol.* **7**, 342–348 (1977).

112. Finkelman, F. D., Snapper, C. M., Mountz, J. D. & Katona, I. M. Polyclonal activation of the murine immune system by a goat antibody to mouse IgD. IX. Induction of a polyclonal IgE response. *J Immunol Baltim Md 1950* **138**, 2826–30 (1987).

113. Jarrett, E., Mackenzie, S. & Bennich, H. Parasite-induced 'nonspecific' IgE does not protect against allergic reactions. *Nature* **283**, 302–303 (1980).

114. Croote, D., Darmanis, S., Nadeau, K. C. & Quake, S. R. High-affinity allergen-specific human antibodies cloned from single IgE B cell transcriptomes. *Science* **362**, 1306–1309 (2018).

115. Toit, G. du *et al.* Allergen specificity of early peanut consumption and effect on development of allergic disease in the Learning Early About Peanut Allergy study cohort. *J. Allergy Clin. Immunol.* **141**, 1343–1353 (2018).

116. Akdis, C. A. & Akdis, M. Mechanisms of allergen-specific immunotherapy. *J Allergy Clin Immun* **127**, 18–27 (2011).

117. Sokol, K. & Milner, J. D. The overlap between allergy and immunodeficiency. *Curr Opin Pediatr* **30**, 848–854 (2018).

118. Cyster, J. G. & Allen, C. D. C. B Cell Responses: Cell Interaction Dynamics and Decisions. *Cell* **177**, 524–540 (2019).

119. Bilancio, A. *et al.* Key role of the p110δ isoform of PI3K in B-cell antigen and IL-4 receptor signaling: comparative analysis of genetic and pharmacologic interference with p110δ function in B cells. *Blood* **107**, 642–650 (2006).

120. Koenig, J. F. E. *et al.* A Distinct Phenotype of Polarized Memory B cell holds IgE Memory. *Biorxiv* 2023.01.25.525495 (2023) doi:10.1101/2023.01.25.525495.

121. He, J.-S. *et al.* IgG1 memory B cells keep the memory of IgE responses. *Nat Commun* **8**, 641 (2017).

122. Jiménez-Saiz, R. *et al.* IgG1+ B-cell immunity predates IgE responses in epicutaneous sensitization to foods. *Allergy* **74**, 165–175 (2019).

123. Hoof, I. *et al.* Allergen-specific IgG+ memory B cells are temporally linked to IgE memory responses. *J Allergy Clin Immun* **146**, 180–191 (2020).

124. Yoshida, K. *et al.* Immunoglobulin switch circular DNA in the mouse infected with Nippostrongylus brasiliensis: evidence for successive class switching from mu to epsilon via gamma 1. *Proc National Acad Sci* **87**, 7829–7833 (1990).

125. Mandler, R., Finkelman, F. D., Levine, A. D. & Snapper, C. M. IL-4 induction of IgE class switching by lipopolysaccharide-activated murine B cells occurs predominantly through sequential switching. *J Immunol Baltim Md 1950* **150**, 407–18 (1993).

126. Luo, W. *et al.* The AKT kinase signaling network is rewired by PTEN to control proximal BCR signaling in germinal center B cells. *Nat Immunol* **20**, 736–746 (2019).

127. Luo, W., Weisel, F. & Shlomchik, M. J. B Cell Receptor and CD40 Signaling Are Rewired for Synergistic Induction of the c-Myc Transcription Factor in Germinal Center B Cells. *Immunity* **48**, 313-326.e5 (2018).

128. Sundling, C. *et al.* Positive selection of IgG+ over IgM+ B cells in the germinal center reaction. *Immunity* **54**, 988-1001.e5 (2021).

129. Kräutler, N. J. *et al.* Differentiation of germinal center B cells into plasma cells is initiated by high-affinity antigen and completed by Tfh cells. *J Exp Med* **214**, jem.20161533 (2017).

130. Chen, S. T., Oliveira, T. Y., Gazumyan, A., Cipolla, M. & Nussenzweig, M. C. B cell receptor signaling in germinal centers prolongs survival and primes B cells for selection. *Immunity* **56**, 547-561.e7 (2023).

131. Kitayama, D. *et al.* A role for Bcl6 in sequential class switch recombination to IgE in B cells stimulated with IL-4 and IL-21. *Mol Immunol* **45**, 1337–1345 (2008).

Publishing Agreement

It is the policy of the University to encourage open access and broad distribution of all theses, dissertations, and manuscripts. The Graduate Division will facilitate the distribution of UCSF theses, dissertations, and manuscripts to the UCSF Library for open access and distribution. UCSF will make such theses, dissertations, and manuscripts accessible to the public and will take reasonable steps to preserve these works in perpetuity.

I hereby grant the non-exclusive, perpetual right to The Regents of the University of California to reproduce, publicly display, distribute, preserve, and publish copies of my thesis, dissertation, or manuscript in any form or media, now existing or later derived, including access online for teaching, research, and public service purposes.

DocuSigned by:
BEC994089E3948E...
Author Signature

12/12/2023
Date